

**ESD analysis for PLANCK and HERSCHEL satellites**

**H-P-1-ASPI-AN-0268**

**Product Code : 000000**

<b>Rédigé par/ Written by</b>	<b>Responsabilité-Service-Société Responsibility-Office -Company</b>	<b>Date</b>	<b>Signature</b>
C.BERTHOU / N.REAU / P.COUZIN		15/7/04	
<b>Vérifié par/ Verified by</b>			
Hervé ZUGAJ	EMC/ESD/radiation responsible		
Patrice COUZIN	Electrical Architect	20/07/04	
Pascal RIDEAU	System Engineering Manager	20/07/04	
C. MASSE	Product Assurance Manager	20/07/04	
<b>Approbation/ Approved</b>			
J. J. JUILLET	Project Manager	20.07.04	

Data management : G. SERRA

**Entité Emettrice** : Alcatel Space - Cannes  
(détentrice de l'original) :

# ESD analysis for PLANCK and HERSCHEL satellites

REFERENCE : H-P-1-ASPI-AN-0268

DATE : 15/07/2004

ISSUE : Issue 2.0 Page : 2/83

HERSCHEL/PLANCK		DISTRIBUTION RECORD	
DOCUMENT NUMBER : H-P-1-ASPI-AN-0268		Issue 2.0 Rev. : 0.0 Date: 15/07/04	
EXTERNAL DISTRIBUTION		INTERNAL DISTRIBUTION	
ESA		HP team	X
ASTRIUM			
ALENIA			
CONTRAVES			
TICRA			
TECNOLOGICA			
		Clf Documentation	Orig.

ENREGISTREMENT DES EVOLUTIONS / CHANGE RECORDS

ISSUE	DATE	§ : DESCRIPTION DES EVOLUTIONS § : CHANGE RECORD	REDACTEUR AUTHOR
01	22/03/2004	First Issue	N.Reau / C.Berthou P.Couzin
1.1	15/07/2004	CDR update : <ul style="list-style-type: none"><li>- Kapton has been implemented on the back side of the Herschel telescope</li><li>- 30% Kapton has been considered on Planck Solar Array</li></ul>	

## TABLE OF CONTENTS

1. INTRODUCTION.....	7
1.1 PURPOSE OF THIS DOCUMENT.....	7
1.2 APPLICABLE AND REFERENCE DOCUMENTS.....	7
1.2.1 Applicable documents.....	7
1.2.2 Reference documents.....	7
1.3 ACRONYMS.....	8
2. THE ELECTROSTATIC ENVIRONMENTS.....	9
2.1 THE EARTH'S MAGNETOSPHERE.....	9
2.2 HERSCHEL-PLANCK ELECTROSTATIC ENVIRONMENT.....	10
2.2.1 The ionosphere.....	12
2.2.2 The plasmasphere.....	13
2.3 ELECTROSTATIC ENVIRONMENT AROUND THE GEOSTATIONARY ORBIT.....	13
2.3.1 External charging.....	13
2.3.2 Internal chargingx.....	14
2.4 THE INTERPLANETARY MEDIUM.....	15
2.5 THE ENVIRONMENT AT THE 2 <sup>ND</sup> LAGRANGE POINT.....	15
3. ELECTROSTATIC DESIGN RULES.....	16
3.1 GENERAL DESIGN RULES.....	16
3.2 DESIGN RULES TO PREVENT FROM EXTERNAL CHARGING.....	17
3.2.1 Grounding of conductive materials.....	17
3.2.2 Choice of materials directly space exposed.....	17
3.2.3 Wiring and cable shielding.....	19
3.2.4 Solar Array.....	19
4. HERSCHEL NASCAP ANALYSIS.....	22
4.1 TRADE-OFF.....	22
4.1.1 Introduction.....	22
4.1.2 Simulation parameters.....	23
4.1.3 Results.....	27
4.1.4 Synthesis.....	66
4.2 CDR BASELINE.....	67
4.2.1 Simulations parameters and configuration.....	67
4.2.2 Results.....	69
5. PLANCK NASCAP ANALYSIS.....	72
5.1 TRADE-OFF.....	72
5.1.1 Introduction.....	72
5.1.2 Simulation parameters.....	72
5.1.3 Results.....	75
5.1.4 Synthesis.....	81
5.2 CDR BASELINE.....	82
5.2.1 Simulations parameters and configuration.....	82
6. CONCLUSION.....	83

## LIST OF FIGURES

FIGURE 1. MATERIALS OF HERSCHEL NASCAP MODEL (CONFIGURATION 1) .....	28
FIGURE 2. MATERIALS OF HERSCHEL NASCAP MODEL (CONFIGURATION 1) .....	28
FIGURE 3. DISTRIBUTION OF DIFFERENTIAL POTENTIALS.....	29
FIGURE 4. DISTRIBUTION OF DIFFERENTIAL POTENTIALS.....	30
FIGURE 5. DISTRIBUTION OF DIFFERENTIAL POTENTIALS.....	31
FIGURE 6. DISTRIBUTION OF DIFFERENTIAL POTENTIALS.....	32
FIGURE 7. DISTRIBUTION OF DIFFERENTIAL POTENTIALS.....	33
FIGURE 8. DISTRIBUTION OF DIFFERENTIAL POTENTIALS.....	34
FIGURE 9. EVOLUTION OF ABSOLUTE POTENTIALS DURING CHARGING .....	34
FIGURE 10. DISTRIBUTION OF DIFFERENTIAL POTENTIALS.....	35
FIGURE 11. DISTRIBUTION OF DIFFERENTIAL POTENTIALS.....	36
FIGURE 12. EVOLUTION OF ABSOLUTE POTENTIALS DURING CHARGING .....	36
FIGURE 13. MATERIALS OF HERSCHEL NASCAP MODEL (CONFIGURATIONS 2, 3, 4) .....	37
FIGURE 14. MATERIALS OF HERSCHEL NASCAP MODEL (CONFIGURATIONS 2, 3, 4) .....	38
FIGURE 15. DISTRIBUTION OF DIFFERENTIAL POTENTIALS.....	39
FIGURE 16. DISTRIBUTION OF DIFFERENTIAL POTENTIALS.....	40
FIGURE 17. DISTRIBUTION OF DIFFERENTIAL POTENTIALS.....	41
FIGURE 18. DISTRIBUTION OF DIFFERENTIAL POTENTIALS.....	42
FIGURE 19. DISTRIBUTION OF DIFFERENTIAL POTENTIALS.....	43
FIGURE 20. DISTRIBUTION OF DIFFERENTIAL POTENTIALS.....	44
FIGURE 21. EVOLUTION OF ABSOLUTE POTENTIALS DURING CHARGING .....	44
FIGURE 22. DISTRIBUTION OF DIFFERENTIAL POTENTIALS.....	45
FIGURE 23. DISTRIBUTION OF DIFFERENTIAL POTENTIALS.....	46
FIGURE 24. EVOLUTION OF ABSOLUTE POTENTIALS DURING CHARGING .....	46
FIGURE 25. MATERIALS OF HERSCHEL NASCAP MODEL (CONFIGURATION 2 WITH ITO).....	47
FIGURE 26. MATERIALS OF HERSCHEL NASCAP MODEL (CONFIGURATION 2 WITH ITO).....	47
FIGURE 27. DISTRIBUTION OF DIFFERENTIAL POTENTIALS.....	48
FIGURE 28. DISTRIBUTION OF DIFFERENTIAL POTENTIALS.....	49
FIGURE 29. EVOLUTION OF ABSOLUTE POTENTIALS DURING CHARGING .....	49
FIGURE 30. DISTRIBUTION OF DIFFERENTIAL POTENTIALS.....	50
FIGURE 31. DISTRIBUTION OF DIFFERENTIAL POTENTIALS.....	51
FIGURE 32. DISTRIBUTION OF DIFFERENTIAL POTENTIALS.....	52
FIGURE 33. DISTRIBUTION OF DIFFERENTIAL POTENTIALS.....	53
FIGURE 34. DISTRIBUTION OF DIFFERENTIAL POTENTIALS.....	54
FIGURE 35. DISTRIBUTION OF DIFFERENTIAL POTENTIALS.....	55
FIGURE 36. EVOLUTION OF ABSOLUTE POTENTIALS DURING CHARGING .....	55
FIGURE 37. DISTRIBUTION OF DIFFERENTIAL POTENTIALS.....	56
FIGURE 38. DISTRIBUTION OF DIFFERENTIAL POTENTIALS.....	57
FIGURE 39. EVOLUTION OF ABSOLUTE POTENTIALS DURING CHARGING .....	57
FIGURE 40. DISTRIBUTION OF DIFFERENTIAL POTENTIALS.....	58
FIGURE 41. DISTRIBUTION OF DIFFERENTIAL POTENTIALS.....	59
FIGURE 42. DISTRIBUTION OF DIFFERENTIAL POTENTIALS.....	60
FIGURE 43. DISTRIBUTION OF DIFFERENTIAL POTENTIALS.....	61
FIGURE 44. DISTRIBUTION OF DIFFERENTIAL POTENTIALS.....	62
FIGURE 45. DISTRIBUTION OF DIFFERENTIAL POTENTIALS.....	63
FIGURE 46. EVOLUTION OF ABSOLUTE POTENTIALS DURING CHARGING .....	63
FIGURE 47. DISTRIBUTION OF DIFFERENTIAL POTENTIALS.....	64

FIGURE 48. DISTRIBUTION OF DIFFERENTIAL POTENTIALS.....	65
FIGURE 49. EVOLUTION OF ABSOLUTE POTENTIALS DURING CHARGING .....	65
FIGURE 50. MATERIALS OF HERSCHEL NASCAP BASELINE MODEL.....	68
FIGURE 51. MATERIALS OF HERSCHEL NASCAP BASELINE MODEL.....	68
FIGURE 52. MATERIALS OF HERSCHEL NASCAP BASELINE MODEL.....	69

## LIST OF TABLES AND FIGURES

TABLE 1.: MAIN RESULTS OF NASCAP CALCULATIONS : HERSCHEL.....	66
TABLE 2. MAIN RESULTS OF NASCAP CALCULATIONS : PLANCK.....	81

## 1. INTRODUCTION

### 1.1 Purpose of this document

This document presents :

- the Herschel/Planck electrostatic environments
- the electrostatic design rules (both to prevent electrostatic charging and ESD detrimental effects)
- the electrostatic charging analyses for Planck and Herschel satellites

Around the geostationary orbit (from 20000 km up to some hundreds km above the geostationary altitude), external spacecraft charging has been well known for some twenty years. External charging occurs during geomagnetic storms that take place in the Earth geomagnetic tail. In the last seventies, the NASA Charging Analyzer Program (NASCAP) has been developed to predict surface satellite absolute and differential potentials for all suitable mission conditions. Some design rules have been established to prevent S/C external charging [1] or, if charging is not avoidable, to limit the effects of resulting electrostatic discharges. Far from the Earth, the space plasma is known to be harmless to spacecraft charging.

### 1.2 Applicable and reference documents

#### 1.2.1 Applicable documents

- AD01.1 Herschel/Planck System Requirements Specification (SRS)  
SCI-PT-RS-05991
- AD05.1 General Design and Interface Requirements  
H-P-1-ASPI-SP-0027
- AD05.2 Environment and Test Requirements  
H-P-1-ASPI-SP-0030
- AD05.4 EMC Specification  
H-P-1-ASPI-SP-0037

#### 1.2.2 Reference documents

- [1] "Design Guidelines for Assessing and Controlling Spacecraft Charging Effects" NASA Technical Paper 2361 (Authors : C. Purvis, H. Garrett, A. Whittlesey, N. Stevens)
- [2] "Avoiding Problems caused by Spacecraft On-orbit Internal Charging Effects " NASA Technical Handbook 4002 (Authors : A. Whittlesey and Al)
- [3] "Natural Orbital environment Guidelines for Use in Aerospace Vehicle Development" NASA TM4527, 1994
- [4] "L2 natural environment summary" by Nancy J. Lindsey, Lockheed Martin, 1998

- [5] "Structure polarisée dans un plasma ionosphérique: nature, seuil et dimensionnement des décharges" rapport ONERA DERTS RF4533.11/août 1997
- [6] "Effects of active spacecraft potential control on cluster plasma observations – first results" K. Torkar and AI, Space Research Institute, Austrian Academy of science, Proc. 7<sup>th</sup> Spacecraft charging technology conference, April 2001, ESTEC, Noordwijk
- [7] "Characteristics of the plasma environment for the SMART-1 mission" Laakso and Foing, ESA Space Science Department, 7<sup>th</sup> Spacecraft charging technology conference, April 2001, ESTEC, Noordwijk
- [8] "The Messenger Spacecraft charging analysis" Katz I., SAIC, Proc. 7<sup>th</sup> Spacecraft charging technology conference, April 2001, ESTEC, Noordwijk
- [9] "Solar array triggered arc phenomena studies and modeling (EMAGS)" study performed by the ONERA-DESP Toulouse under ESA contract N°13607/99/NL/SB
- [10] "Les anomalies sur les générateurs solaires induites par l'environnement électrisant" Atelier CNES, Toulouse, 29-30 nov. 2000
- [11] ESABASE/CHARGING Users Manual, ESA document number TS101/RT/16.85, dated 17/6/85
- [12] NASCAP Programmer's Reference Manual, S-Cubed document no. SSS-R-84-6638, March 1984
- [13] IMPLEMENTATION OF NASCAP UNDER VAX/VMS, S-Cubed document, dated February 1987

## 1.3 Acronyms

EMC :	Electromagnetic Compatibility
ESD :	Electrostatic Discharge
ESA :	European Space Agency
GEO :	Geostationary orbit
IVG :	Inverted Voltage Gradient
MLI :	Multi-Layer Insulating
NASCAP :	NASA Charging Analyzer Program
NVG :	Normal Voltage Gradient
OSR :	Optical Solar Reflector
PPLM :	Planck payload Module
S/A :	Solar Array
S/C :	Spacecraft
SEE :	Secondary Electron Emission
SVM :	SerVice Module
CVV :	Cryostat Vacuum Vessel



## 2. THE ELECTROSTATIC ENVIRONMENTS

### 2.1 The Earth's magnetosphere

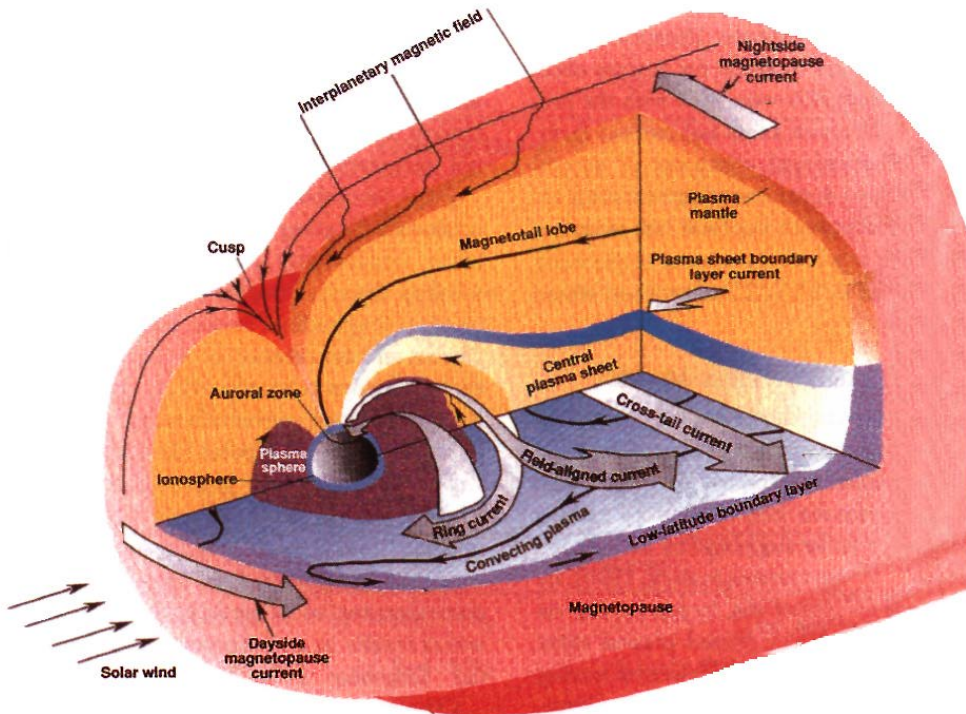


Figure 1.: The Earth magnetosphere

The Earth is a huge magnet, and its magnetic influence extends far into space.

The global morphology of the Earth's magnetosphere is fairly well understood now. It is pictured below. In this view, we are looking from the side and down on the equatorial plane. The edge of magnetosphere, called magnetopause is clearly visible. It is a moving frontier, submitted to the solar wind pressure. The magnetopause is generally located at  $10 R_E$  ( $R_E =$  Earth Radius) on the day side, but it can sometimes go down below the geosynchronous orbit ( $6.6 R_E$ ). Just inside the magnetopause is a thin layer called the mantle. The magnetic field lines from the dayside of the magnetosphere are drawn over the poles into to night side to form a long stretched tail (around  $500 R_E$ ). In the process, they form the northern and southern lobes, which are separated from each other by a very interesting region, called the plasma sheet. In the plasma sheet, by some process not yet fully understood, the magnetic energy of the lobes is converted to plasma kinetic energy during violent geomagnetic storms. The electrons are injected toward the Earth and eastwards close to the geosynchronous altitude, directly affecting telecommunication satellites.

Close to the poles, two cusps open to space let the solar and space particles entered into the Earth's atmosphere : this phenomenon is called aurora.

# ESD analysis for PLANCK and HERSCHEL satellites

REFERENCE : H-P-1-ASPI-AN-0268

DATE : 15/07/2004

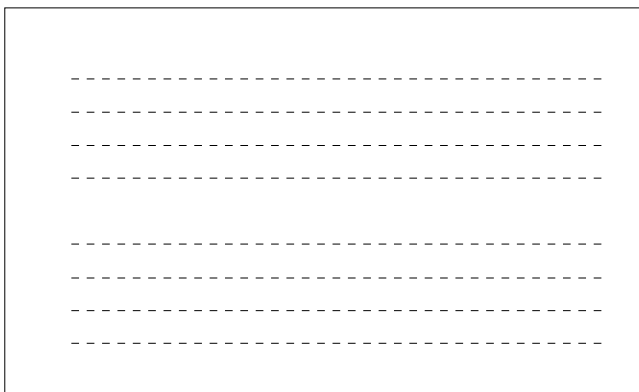
ISSUE : Issue 2.0 Page : 10/83

In the internal magnetosphere (under  $10 R_E$ ), the particles are trapped by the Earth's magnetic field : They form the Van Allen radiation belts. This region is highly dynamic.

## 2.2 Herschel-Planck electrostatic environment

Herschel and Planck satellites will be injected towards the L2 Lagrange point following two particular trajectories.

Earth rotating coordinate system



Earth rotating coordinate system

During this transfer, the satellites will encounter various regimes of plasma :

- the Earth ionosphere (at low altitude) : low-energy and dense plasma
- the plasmasphere : low-energy and low-density plasma
- the internal magnetosphere : low-density but "high"-energy plasma (during stormy days)
- the mantle : low-energy and low-density plasma
- the magnetopause : low-energy and low-density plasma
- the magnetosheath : low-energy and low-density plasma
- the bow shock : low-energy and low-density plasma
- the interplanetary medium (the solar wind) around the L2 Lagrange point

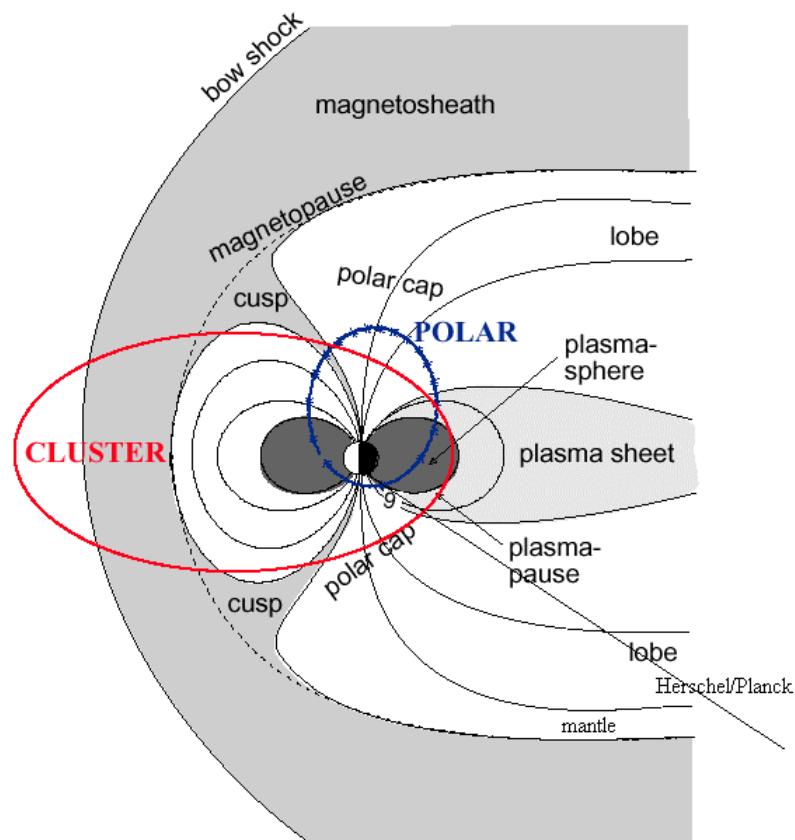


Figure 3. : various satellite trajectories in the magnetosphere

## 2.2.1 The ionosphere

After the injection, the satellites will encounter a low energy but high density plasma whose constitution depends from the altitude and the longitude.

The lowest region in altitude is the ionosphere. The ionosphere is the ionized plasma at the top of the atmosphere. Its constitution is rather complex and needs dozens of pages to be fully described [3]. It is generally divided into layers D, E and F1 at low altitudes ( $< \approx 150$  km) and F2 at higher altitude. F2 layer (between 250 and 400 km altitude) is permanent and is the densest (between  $10^{+5}$  e-/cm<sup>3</sup> and  $10^{+6}$  e-/cm<sup>3</sup>). Immediately above the F2 peak, density falls off nearly exponentially with height.

The cold and dense ionospheric plasma is not an aggressive environment by its own. The electron energy (less than 1 eV) is too low to be able to penetrate into the 1<sup>st</sup> micron of dielectrics and then to induce differential potentials. But, as the plasma is dense, it will impose its potential to all the satellite external dielectric surfaces, such as coverglasses, paints and oxides.

The dielectric « grounding » by a plasma can also be at the origin of solar array discharge : the coverglass is close to « 0 V » but the solar cell can be at solar array operational voltage (for example 100 V). The Solar Array design shall take into account this phenomenon and dedicated plasma tests shall be performed if the operational voltage is above 40 V and if the available current is above 3 A. This is not the case for Herschel and Planck. The operational voltage is 28 V and the maximum current is less than 3 A per section.

A dense and cold plasma induces some current collection by metallic and polarized surfaces directly space-exposed like solar cells. A power loss on the solar array is the direct consequence of this phenomenon. Fortunately, below 100 V the power loss is very negligible.

As a conclusion, no electrostatic effect in the ionosphere is expected for Herschel and Planck satellites.

## 2.2.2 The plasmasphere

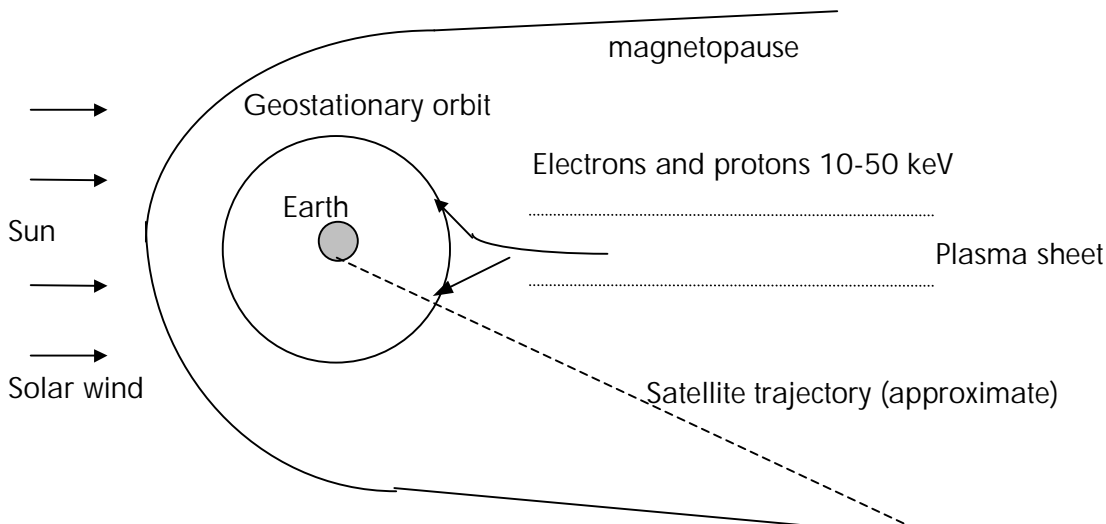
Above the ionosphere, the plasmasphere is a region of cold and less dense plasma originating in the ionosphere and trapped by the Earth magnetic field. This region is harmless for spacecraft charging. Ion and electron energies are between 0.5 and 1 eV and densities are roughly between 10 and 1000 particles/cm<sup>3</sup>. The frontier between the plasmasphere and the internal magnetosphere where the geostationary orbit is located is called the plasmopause. This frontier is highly movable: it can be located between 3 L-shell and 7 L-shell (L-shell= magnetic equatorial distance from the center of the Earth, in Earth radius; the geostationary orbit is located at 6.6 L-shell).

Once the satellite has crossed the plasmopause, it may come across geomagnetic storms. Due to the presence of energetical particles, spacecraft charging may occur and ESD may have to be considered.

## 2.3 Electrostatic environment around the geostationary orbit

### 2.3.1 External charging

Herschel and Planck satellites will move inside the Earth's internal magnetosphere towards the Earth magnetotail. In this region, low-energy electrons and protons that are harmless to satellite charging usually constitute the space plasma. But, injections of electrons and protons of some energy range able to cause spacecraft charging occur occasionally around midnight: these events are known as geomagnetic storms.



A geomagnetic storm can modify a satellite potential down to negative thousands of Volt, especially if the satellite is not sunlit.

The charging phenomenon takes place in two stages.

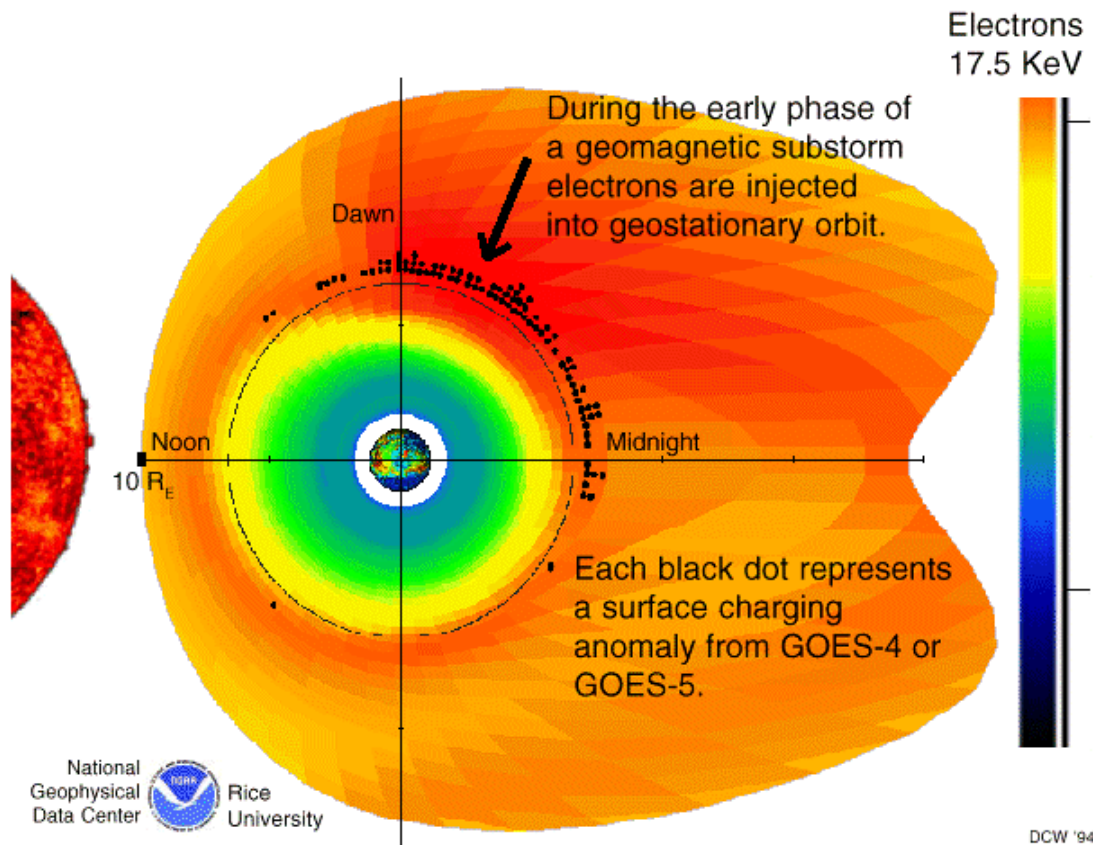
The first stage, called absolute charging, is devoted to a uniform potential difference between spacecraft and space. Photoemission and incoming geomagnetic storm electron fluxes are the driving parameters of this phenomenon which can occur very quickly (the time scale may be as short as a few milliseconds).

The second stage is called differential charging. The difference of electrostatic properties of materials covering the spacecraft and also the electric fields surrounding the satellite cause the surface potentials to become different from the metallic substrate potential. The phenomenon time scale is different : more than 1000 seconds are often necessary to reach the equilibrium state.

In general, shaded dielectrics have potentials more negative than the spacecraft structure. This fact has fortunately a limited effect because dielectrics can withstand high negative internal electric field without damage. This situation is called "Normal Voltage Gradient".

On the contrary, sunlit dielectrics have potentials less negative than the spacecraft structure. This situation is called "Inverted Voltage Gradient". Unfortunately, they can only withstand a limited difference of potentials (+500 V) before a discharge occurs. For this reason, it is important to know the spacecraft potential map to identify the sensitive dielectric areas and take all precautions to prevent a discharge to occur.

NASA, in a guideline [1], have defined a worse case environment.



## 2.3.2 Internal charging

After a geomagnetic storm, the injected electrons can be strongly accelerated by some complex internal processes: they may reach high-energy values (up to 2 MeV) and stay during some few days in the electronic Van Allen belt (the geostationary orbit is located inside the Van Allen belt). If the spacecraft stays more than a few hours inside the electronic Van Allen belt, these electrons can be at the origin of internal charging or deep dielectric charging of satellites because they have sufficient energy to penetrate inside the satellite and be deposited inside a good dielectric or in some floating metallic part (if any) [2]. One has considered here that given the low probability of the phenomenon combined with the very small time

Herschel and Planck will spent inside the Van Allen belts, the internal charging phenomenon to be neglected, ie. no special design rules will be applied to encompass it.

This statement is especially valid for the Herschel satellite and its external overshielded cryo-harness ( refer to HEPLM CDR Panel report SCI-PT-28442 §5-EMC/ESD design and Analysis). It should be noticed that this configuration is identical to the ISO cryostat one which has shown no malfunction after 2 years spent in a much more "aggressive" orbit (1000km-70000km around the Earth) wrt charging environment.

## 2.4 The interplanetary medium

When leaving the Earth's magnetosphere, the satellite shall cross the magnetopause, which is the frontier between the magnetosphere and the interplanetary medium.

This environment is currently observed by the ESA Cluster satellites [6], [7]. It is harmless as far as external spacecraft charging is concerned (low energy and low density plasma). Generally, the satellite potential is below 20 V.

The interplanetary medium has been observed at the 1<sup>st</sup> Lagrange location where the satellites WIND or ACE analyze the solar wind.

The solar wind is constituted from charged particles literally exploding continuously from two regions of the solar corona :

- from the coronal holes for the "fast wind" (700 km/s in average)
- from the "neutral coronal wave" for the "slow wind" (350 km/s in average)

The solar wind is driven away from the sun to the planets and reaches the interstellar medium by thermal pressure from the solar corona. Its density and speed can vary greatly over a short time period : from 1 to 30 particles/cm<sup>3</sup> and from 300 km/s to 900 km/s. The density decreases when far from the sun. The ion and electron energy is basically inferior to 1000 eV. It might induce some moderate charging, especially if the solar array is cold and not well sunlit, which is not at all the case of Herschel and Planck : some tens of Volt of differential charging could then be expected [8].

## 2.5 The environment at the 2<sup>nd</sup> Lagrange point

The plasma found at L2 and the orbits around L2 is that contained in the solar wind, far from the Sun. Specifically, this plasma will have the following characteristics at L2 and the orbits around it [4]:

- Composition = 95 % H<sup>+</sup>, 5% He<sup>++</sup> with equivalent electrons
- Density = 1-10 particles/cm<sup>3</sup>
- Velocity ≈ 450 km/s
- Energy (ions) ≈ 10 eV
- Energy (electrons) ≈ 50 eV

This environment may eventually induce some limited differential potentials : some tens of Volt [8] can eventually be expected on the solar array. This difference of potentials is too tenuous to be at the origin of a discharge.

## 3. ELECTROSTATIC DESIGN RULES

### 3.1 General design rules

To prevent from detrimental effects of spacecraft charging - or discharges - the following rules shall be applied on Herschel and Planck satellites, according to AD01.1 :

1. "Spacecraft design and materials selected shall be such as to ensure that no parts of the spacecraft are charged to high potentials." from AD01.1 (SENV 140) and AD05.1 (ENVR 189)

2. "All spacecraft surfaces exposed to the plasma environment shall be conductive and grounded to the spacecraft structure. Agreed exceptions are : solar arrays" from AD01.1 (SENV 145) and AD05.1 (ENVR 190).

3. "The exposed harness dielectric charging shall be taken into account and appropriate design provisions shall be taken." from AD01.1 (SENV 150) and AD05.1 (GDEL 282)

"Braided overshields with greater than 85% coverage shall be required on all cabling outside the satellite." from AD05.1 (GDEL-195)

"Each overshield shall be grounded to structure prior entering the spacecraft or any external closed Faraday chamber." from AD05.1 (GDEL-210)

4. From AD01.1 (SENV 155) "The spacecraft design and component selection shall take these effects into account and shall ensure that these effects do not cause a degraded performance or hazardous situations, which could lead to a loss of mission.

The spacecraft shall withstand without being disturbed, the following design goal :

- for Conducted Electrostatic discharge (current injected anywhere in the structure) :
  - I<sub>max</sub> : 50 A (TBC)
  - Risetime : < 5 ns (10-90%)
  - Duration : 30 ns (at half amplitude)
  - Rate : 10 Hz
- for Radiated Electrostatic discharge (spark gap at 30 cm distance) :
  - Energy : 15 mJ
  - Voltage : 10 kV
  - Rate : 10 Hz"

The points 1 and 2 are related to the prevention of electrostatic charging by the use of selected space-exposed materials. Satellite potentials can be estimated through the help of a dedicated software (NASCAP).

The point 3 implies the prevention of electrostatic discharge on the cables.

The point 4 objective is to prevent any detrimental effect of an electrostatic discharge by the qualification of each equipment through ESD tests specified within the EMC Specification. The tests are made at unit and system levels. Radiated and conducted discharges are specified which involve all the identified coupling mechanisms.



## 3.2 Design rules to prevent from external charging

To meet SENV-140 and SENV-145 requirements, the following precautions are taken.

### 3.2.1 Grounding of conductive materials

Any external conductive area shall be connected to the ground whatever its size.

Bonding requirements, electrical continuity and controls are defined for each element in the document AD05.1 (section 6.2). Electrical grounding and bonding is requested : (GDEL-015)

- to prevent hazard from high potentials
- to prevent build up and accumulation of electrostatic charges
- to avoid differential charge build up that could result in an electrostatic discharge
- to reduce electromagnetic interference due to electric field or other forms of mutual coupling
- to protect from high voltage arcing
- to provide an Electrical Ground Reference Network used as an equipotential surface reference plane.

"All radiation shields, circuit traces and conductors with a surface greater than 3 cm<sup>2</sup> shall be electrically grounded unless it can be demonstrated that their resistance w.r.t structure is < 10 Mohms." From AD05.1 GDEL-190.

### 3.2.2 Choice of materials directly space exposed

Materials directly space exposed shall be ESD – conductive (except for the solar array coverglasses).

"Use of non conductive material > 0.5 cm<sup>2</sup> shall be justified." from AD05.1 (GDEL-100)

"No dielectric part of disconnected electrical conductors shall be exposed to space." from AD05.1 (GDEL-185)

"Material used as blanketing > 0.5 cm<sup>2</sup> shall be metallized or conductively coated on at least one side of each blanket layer." (GDEL-095)

A material is considered to be conductive in an ESD sense if:

Bulk resistivity < 1.10<sup>+9</sup> ohm.m

OR Surface resistivity < 1.10<sup>+9</sup> ohm/square

These values are often encountered in the space community [1]. Black kapton (used as external sheet of MLI), Chemglaze Z307 paint are compliant to this requirement.

A material can be considered compliant to this requirement if :

- its bulk resistivity  $\rho$  is inferior to 1.10<sup>+9</sup> ohm.m, if measured by :
  - ASTM D257-99 methodology
  - or ASTM D4496 if the material is expected to be moderately conductive that means  $1 < \rho < 1.10^{+5}$  ohm.m
- its bulk resistivity  $\rho$  is inferior to 1.10<sup>+11</sup> ohm.m, if measured :
  - under electron gun irradiation
  - the temperature range shall be the one expected during the transfer of the satellite from 15000 km to 70000 km altitude.
  - under vacuum (about 10<sup>-6</sup> mbar)
  - after a few hours of outgassing under vacuum

OR :

- its surface resistivity  $R_s$  is inferior to  $1.10+9$  ohm/square, if measured by ASTM D257-99 methodology
- its surface resistivity  $R_s$  is inferior to  $1.10+11$  ohm/square, if measured
  - under electron gun irradiation
  - the temperature range shall be the one expected during the transfer from 15000 km to 70000 km
  - under vacuum (about  $10^{-6}$  mbar)
  - after a few hours of outgassing under vacuum

Electron gun irradiation is known to decrease the resistivity ought to the implementation of charges along the dielectric thickness.

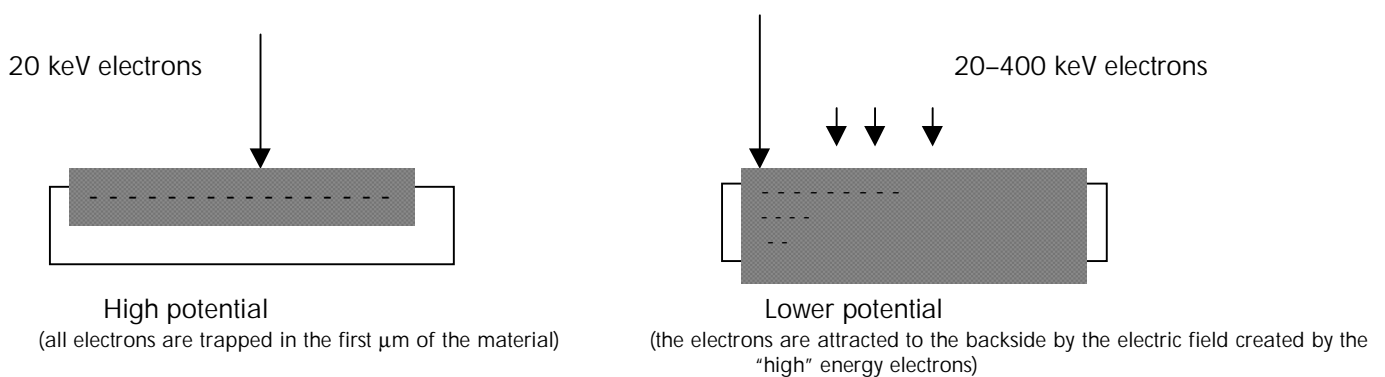
Other methodologies to measure high values of resistivity shall be submitted to Alcatel Space, prior to the usage of the dielectric.

In a first step, the material can be submitted to a mono-energetical electronic irradiation (20 or 30 keV, flux  $1 \text{ nA/cm}^2$ , secondary vacuum, outgassing delay and adequate temperature).

During the test, the potentials shall be monitored and the ESD transient (if any) be recorded.

If the material does not charge during the test, its behavior in space will be very satisfactory. For example, PSG120FD and SG120FD do not charge during the test whereas they are not "ESD conductive" in usual conditions : these paints become conductive under irradiation.

If high negative potentials are recorded, the material sample shall be tested in multi-energetical electronic irradiation (SIRENE 2 facility in ONERA Toulouse), representative to what may occur at the geostationary orbit during a geomagnetic storm. Indeed, a mono-energetical electronic irradiation is much more severe to what happens in space. During a geomagnetic storm, a small quantity of "high" energy electrons exists. This flux enables the implementation of electrons along the dielectric thickness. These electrons modify the internal electric field : the electrons trapped in the first micrometers move towards the backside of the sample. The surface potentials are highly modified due to this phenomenon called "radiation-induced conductivity".



The yellow MLI (with an external layer of yellow kapton  $25 \mu\text{m}$  thick) has been tested under mono-energy (electron beam 30 keV) and multi-energy irradiation (SIRENE facility in ONERA, representative of the energy-spectrum range of a severe geomagnetic substorm). During the tests, no discharge event was observed. The comparison of the two results (around  $-3000 \text{ V}$  for mono-energy irradiation and around  $-300 \text{ V}$  for multi-energy irradiation) shows the significant effect of the radiation-induced conductivity to reduce the differential charging.

The Thalès CMX OSR ( $150 \mu\text{m}$ ) has been tested in the same multi-energy irradiation facility (SIRENE). No discharge event occurs. The Thalès CMX OSR charges to a very limited potential (about  $-200 \text{ V}$ ) at room

temperature. This very low level of potential should prevent any charging in space to a level where a discharge can occur, if the OSR are not cold.

### 3.2.3 Wiring and cable shielding

Despite all the precautions taken to prevent the satellite charging, you can have some unexpected discharge due to a local particular configuration.

In order to eliminate the electromagnetic effects of the discharge, the following precautions have been decided.

"All wiring and cable exiting the satellite Faraday cage shall carry an ESD over-shielding." AD01.5 GDEL-195 and GDEL 535

"Each overshield shall be grounded to the structure prior entering the spacecraft or any external closed Faraday cage" AD01.5 GDEL-205

"All electronic components external to a closed Faraday chamber shall be shielded" AD01.5 GDEL-210

Wires coming from outside the spacecraft are filtered and then separated from other cables (segregation of cabling to prevent coupling into the interior of the satellite).

### 3.2.4 Solar Array

At GEO location, positive differential potentials usually predicted on coverglasses are so high that primary discharges on solar array cannot be avoided.

The effect of the discharge on the S/A is not visible if :

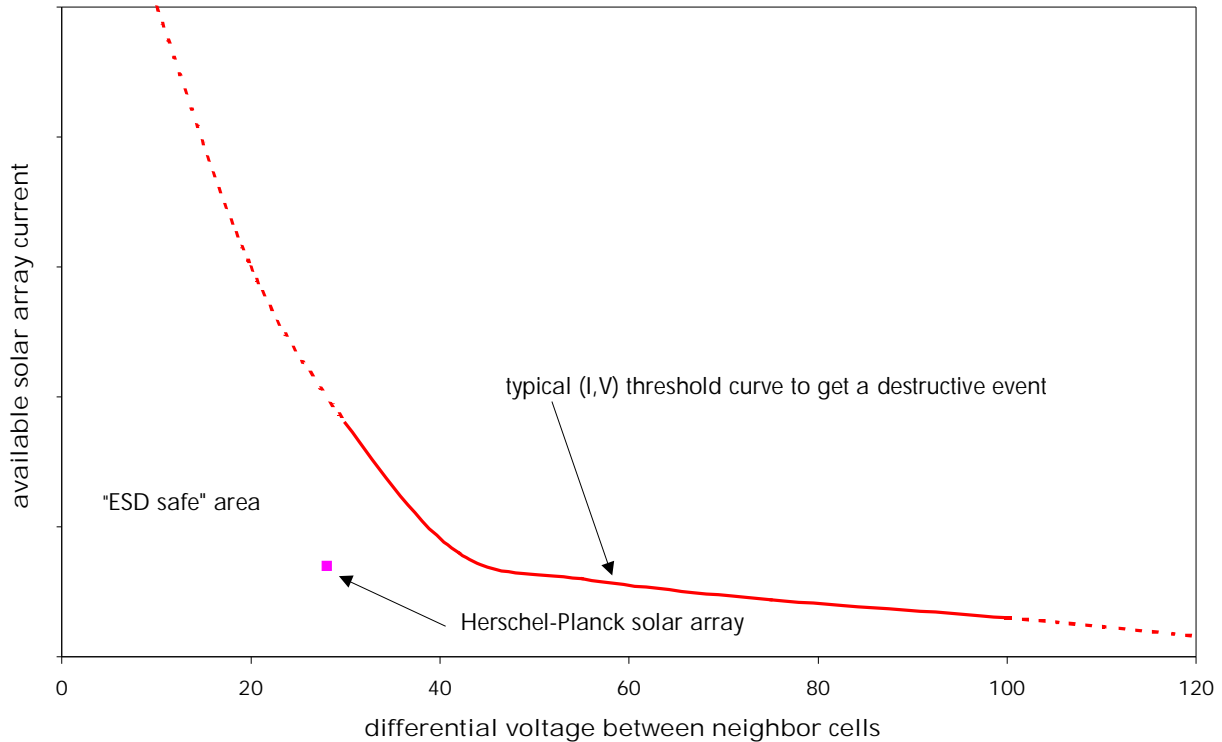
- the differential voltage between 2 adjacent solar cells is inferior to a threshold
- AND the available current to sustain a discharge is inferior to a threshold.

The critical thresholds (I,V) depend from the nature of materials (solar cells, coverglasses) and the geometry (the size of the gap between cells).

Herschel and Planck solar arrays and power system are characterized by :

- power bus voltage : 28 V (Solar array max voltage : 30V)
- string current : 0.5 A
- section current : 3.5 A

With such a low voltage, and relatively low section current, no discharge has ever been observed.



Recent studies [9] [10] have demonstrated the solar array discharge mechanism. For information, the main stages of a solar array discharge mechanism are described below.

Causes of ESD triggered on a solar array is the existence of a positive differential potential (also named Inverted Voltage Gradient IVG) formed between the spacecraft chassis and the coverglass.

When the differential potential increases to a critical value (close to 500 V) and when the spacecraft chassis is of some thousand Volt negative, the local electric field extracts electrons from solar cell or interconnects towards the coverglass.

Impact of these electrons on coverglass allow a secondary electrons emission which tends to increase the differential potential between coverglass and solar cell, and consequently, amplifies the existing electric field emission until the onset of a spontaneous arc called "primary arc".

The primary arc creates a plasma plume that may fill the inter-cells gap and expands over the top of the solar array. Plasma density close to the arc site is very dense and remains sufficiently high some few meters above to discharges at least a solar panel. The energy stored in the network of coverglass capacitance is delivered.

The power bus voltage and the solar array layout fix the differential voltage ( $\Delta V$ ) on adjacent cells separated by only the inter-cell gap.

If  $\Delta V$  between the cell supporting the arc site and the closest adjacent cell is greater than a threshold ( $V_{thres}$ ), electrons emitted from the arc site can also travel the following current loop through a so called "secondary arc":

arc site  $\rightarrow$  inter-cell gap  $\rightarrow$  adjacent cell  $\rightarrow$  back to the arc site  
 (through dense plasma) (through solar array circuit)

The secondary arc is self-extinguish if the current flowing through the inter-cell gap is smaller than an extinguish threshold ( $I_{exting}$ ), or if the voltage  $\Delta V$  is reduced to a value smaller than an extinguish level ( $V_{exting}$ ) with  $V_{exting} < V_{thres}$ .

# ESD analysis for PLANCK and HERSCHEL satellites

REFERENCE : H-P-1-ASPI-AN-0268

DATE : 15/07/2004

ISSUE : Issue 2.0 Page : 21/83

---

If the current flowing through the secondary arc is mainly due to the cover-glass capacitance discharge, extinction duration is close to two hundred micro-seconds. Experience shows that no single trigger arc has caused measurable damage to solar array.

On the other hand, if  $\Delta V$  is maintained at sufficient value ( $\Delta V > V_{\text{exting}}$ ), and if the functional current available in the solar array circuit ( $I_{\text{circuit}}$ ) is greater than  $I_{\text{exting}}$ , the secondary arc can be sustained until the Kapton pyrolyses. In this case, the final state is a short circuit (few ohms) between adjacent cells and possibly between cells and solar array panel.

## 4. HERSCHEL NASCAP ANALYSIS

### 4.1 TRADE-OFF

#### 4.1.1 Introduction

This part presents the electrostatic charging analyses for Herschel satellite using the NASCAP software. Several thermal or powerwise design driving configurations have been analyzed in order to quantify their impact from a charging point of view :

- the use of CMO as coverglass on the solar cells (sunshield) instead of CMX
- the use of grounded/not grounded OSR on the sunshade
- the use of high resistivity CVV painting

The NASCAP software does not take into account the discharges occurring in the orbit but only the charging phenomenon. So, the predicted absolute potential values (especially for solar array) can be overestimated because natural discharges may occur with rather low differential charging (+500 V). NASCAP allows quantifying the sensitivity of the spacecraft to the electrostatic charging.

The simulations are carried out considering a worse case for the charging environment and a very simplified geometry of Herschel spacecraft in transfer orbit.

The section 4.1.2. describes the parameters used for NASCAP analysis, charging environment, spacecraft geometry and the property of surface materials (pessimistic values have been considered to ensure the worse charging prediction).

The section 4.1.3. presents the results of analysis for the 4 different calculation configurations (anti-static paint and non conductive paint with different resistivity).

A synthesis 4.1.4. summarizes the main results of this study.

These results shall be used as inputs to the trade-off between the different configurations.

## 4.1.2 Simulation parameters

### 4.1.2.1 Environment

The following charging environment for electrons and protons is a worse case in geostationary orbit recommended by NASA [1]. In practice, such severe environments would probably be encountered very rarely in a satellite lifetime. The particle flux is modeled as a single Maxwellian function that is summarized in the following Table 1.

	Electrons	Protons
Density	1.12 cm <sup>-3</sup>	0.236 cm <sup>-3</sup>
Temperature	12 keV	29.5 keV

Table 1 : Charging environment description

### 4.1.2.2 Configurations

4 spacecraft configurations have been studied, corresponding to trade off run in order to support the selection of the solar cells coverglass type, of the CVV painting and of the OSR grounding scheme on the Sunshade :

- with an anti-static paint on the CVV with a resistivity of 1.E+08 Ω.m (configuration 1)
- with a non conductive paint on the CVV with a resistivity of 1.E+13 Ω.m (configuration 2)
- with a non conductive paint on the CVV with a resistivity of 1.E+14 Ω.m (configuration 3)
- with a non conductive paint on the CVV with a resistivity of 1.E+15 Ω.m (configuration 4)

For each configurations, different analyses have been performed :

- with non conductive OSR not grounded :
  - ê with CMO on the cells (conductivity of 1.E-13 Ω<sup>-1</sup>.m<sup>-1</sup> at 83°C)
  - ê with CMX on the cells (conductivity of 1.9E-12 Ω<sup>-1</sup>.m<sup>-1</sup> at 83°C)
- with non conductive OSR grounded :
  - ê with CMO on the cells (conductivity of 1.E-13 Ω<sup>-1</sup>.m<sup>-1</sup> at 83°C)
  - ê with CMX on the cells (conductivity of 1.9E-12 Ω<sup>-1</sup>.m<sup>-1</sup> at 83°C)

For the configuration 2 (non conductive paint with a resistivity of 1.E+13 Ω.m), a specific analysis with conductive OSR (OSR with ITO) and with CMO on solar cells has been performed.

Again, these configurations correspond to the main (as far as charging are concerned) design alternatives.

The satellite is always sunlit perpendicularly to the solar array.

# ESD analysis for PLANCK and HERSCHEL satellites

REFERENCE : H-P-1-ASPI-AN-0268

DATE : 15/07/2004

ISSUE : Issue 2.0 Page : 24/83

---

The duration of simulation is 1300 s. This duration does not always allow achieving a total equilibrium of the potentials but is largely sufficient to establish the probability of discharges on the solar array. If longer simulations were required, the stability of NASCAP algorithm is not guaranteed.



## 4.1.2.3 Satellite geometry

The model used in NASCAP represents the Herschel geometry that is simplified. This simplification is due to the calculation box of NASCAP (32x16x16 cells) and due to the elements of geometry used in the NASCAP tool which are simple.

The NASCAP tool obliges to choose only one elementary mesh that is 0.4 meter. These inaccuracies about the geometrical representation are inherent to the NASCAP modeling.

With this elementary mesh size, the surfaces of the NASCAP model are as closed as possible to the real spacecraft surfaces. The ratio between the real surface and the model surface for all elements is less than 20 %.

Some examples are mentioned in the following list:

- |             |                                     |                                      |
|-------------|-------------------------------------|--------------------------------------|
| • SVM       | real surface = 9.11 m <sup>2</sup>  | model surface = 9.49 m <sup>2</sup>  |
| • Sunshield | real surface = 10.66 m <sup>2</sup> | model surface = 9.60 m <sup>2</sup>  |
| • Sunshade  | real surface = 14.44 m <sup>2</sup> | model surface = 14.08 m <sup>2</sup> |
| • CVV       | real surface = 15.37 m <sup>2</sup> | model surface = 18.34 m <sup>2</sup> |
| • Telescope | real surface = 8.98 m <sup>2</sup>  | model surface = 9.60 m <sup>2</sup>  |

## 4.1.2.4 Spacecraft surface materials

The external materials, used on Herschel satellite, are detailed below and are shown on figures 1, 2 for configuration 1 and, figures 13, 14, 25, 26 for configurations 2, 3 and 4.

The material names of NASCAP are written in brackets.

- [EQSO] represents the coverglass which covers the sunshield, always exposed to the sun. The coverglass resistivity is the driving parameter of the calculation and is very sensitive to the temperature. Herschel sunshield is "hot" (T<sub>min</sub>=83°C). 2 coverglass types are analysed : CMO and CMX MgF2 with both 100 µm thickness [8] [9] [10]. In the case of cells are recovered by CMX MgF2, the coverglass conductivity is assumed to be 1.9E-12 Ω<sup>-1</sup>.m<sup>-1</sup> at 83°C. In the use of CMO, the coverglass resistivity is rather high (1.E+13 Ω.m).
- [OSR] which covers the sunshade represents the non conductive OSR with CMX (100 µm thickness) and with a conductivity of 1.7E-18 Ω<sup>-1</sup>.m<sup>-1</sup> at -50°C [11]. 2 analyses have been performed for each type of coverglass (CMO and CMX) : OSR grounded and OSR not grounded.
- [ITOC] represents the OSR with ITO (50 µm thickness). This material covers the sunshade (configuration 2).
- [BLAC] represents the black kapton MLI (back side of the SVM).
- [APAIN] represents an anti-static paint (thickness 20 µm) that covers the CVV (configuration 1). The paint resistivity is assumed to be 1.E+08 Ω.m.
- [NPAIN] represents a non conductive paint (thickness 20 µm) that could cover the CVV (configurations 2, 3 and 4). The paint conductivity is assumed to be :
  - ê 1.E-13 Ω<sup>-1</sup>.m<sup>-1</sup> (configuration 2)
  - ê 1.E-14 Ω<sup>-1</sup>.m<sup>-1</sup> (configuration 3)
  - ê 1.E-15 Ω<sup>-1</sup>.m<sup>-1</sup> (configuration 4)
- [ALUM] represents aluminum (telescope, back side of the sunshield and sunshade, back side of the CVV).

# ESD analysis for PLANCK and HERSCHEL satellites

REFERENCE : H-P-1-ASPI-AN-0268

DATE : 15/07/2004

ISSUE : Issue 2.0 Page : 26/83

---

The characteristics of the paint (anti-static paint and non conductive paint) are the same as the ones used in ESD Planck analysis.

The electrical properties of the materials are extracted from the literature as from the NASCAP reference manual and from measurements performed at the ONERA-DESP.

As the black paint for the CVV is not yet selected, its electrostatic parameters are unknown. They have been replaced by the values extracted from NASCAP reference "CPAI" [12], except for the resistivity.

## 4.1.3 Results

In this section, two kinds of potentials are presented which are explained below :

- 'delta' is defined as being the differential potential between the dielectric material and the underlying conductor
- 'potential' is defined as being the absolute potential. Indeed, a spacecraft material reaches a potential that is referred to the absolute potential of space, considered as being equal to zero.

The orientation of Herschel satellite – sunshield sunshade in sunlit / satellite body in shadow – is a worse case for the satellite charging phenomenon. Indeed, sunlit dielectrics (as coverglass) are known to create a large differential charging area while sunlit conductive materials are wholesome to charging. The large satellite body in shadow collects many electrons and re-emits a few. This can lead to a fast decrease of the satellite absolute potential. A largely negative satellite absolute potential is not dangerous by its own, but unfortunately, the most negative absolute potential leads to the worst differential charging on the S/A.

Different configurations have been analysed in order to determine if the use of CMO on the solar cells and if not grounded OSR are acceptable with regards to ESD risks.

## 4.1.3.1 Herschel satellite charging with anti-static paint (configuration 1)

The anti-static paint resistivity that covers the CVV is assumed to be  $1.E+08 \Omega.m$ .

The Figures 1 and 2 show the satellite surface materials used for the calculations.

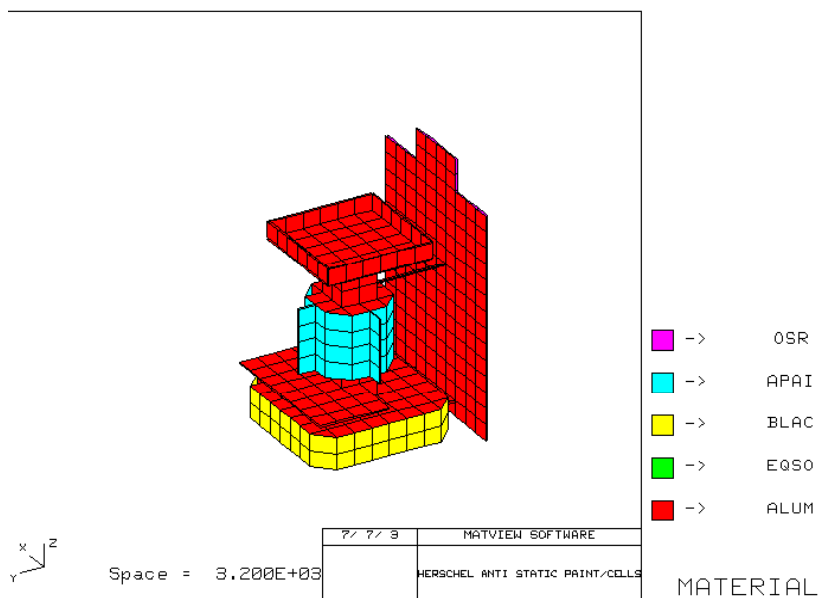


Figure 1. Materials of Herschel Nascap model (configuration 1)

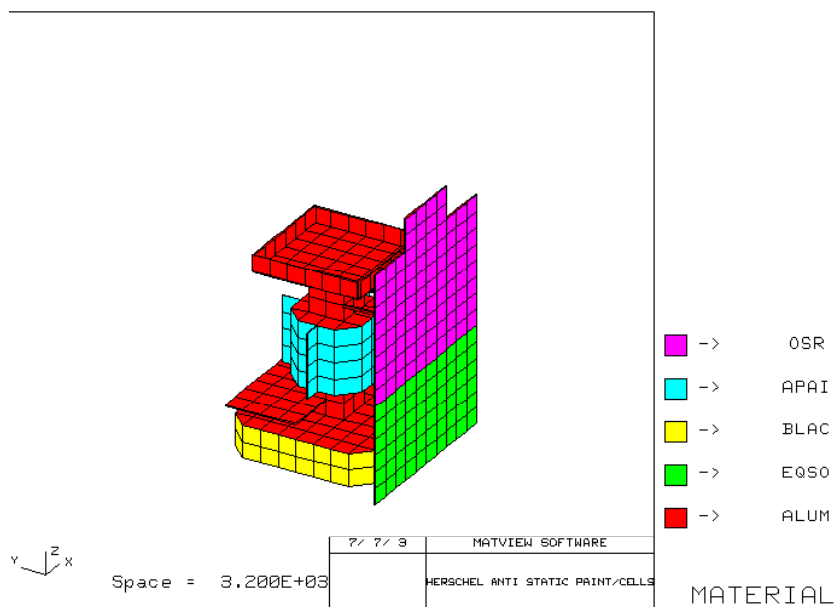


Figure 2. Materials of Herschel Nascap model (configuration 1)

### 4.1.3.1.1 CMO on the cells and non conductive OSR not grounded

The Figures 3 and 4 show the differential potentials of Herschel spacecraft surfaces after 1300 s of charging.

The main results of NASCAP simulations are following :

- The final absolute potential of the structure is -10390 V.
- Ought to the anti-static paint, no negative differential potential exists.
- The positive differential potential reaches +3670 V on the OSR and reaches the maximum value +4770 V on the sunshield (CMO cells).

This value is highly above the threshold of primary discharge on solar array (+500 V). This high level of differential charging is due to the high resistivity of CMO coverglass (1.E+13 Ω.m at T=83°C).

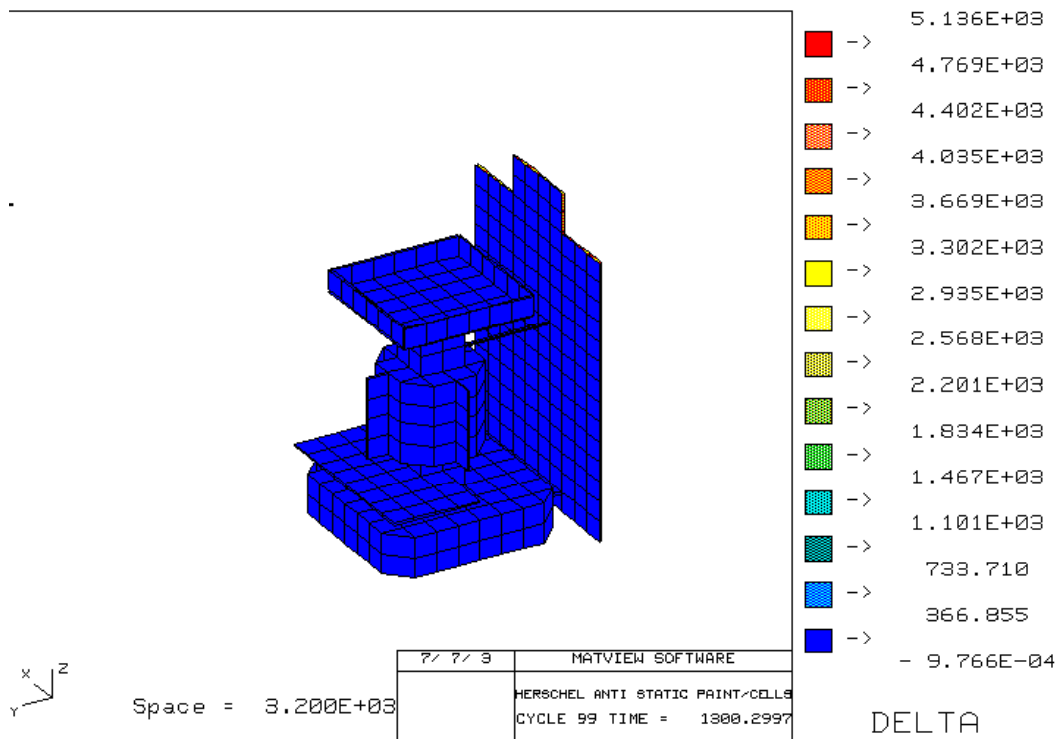


Figure 3. Distribution of differential potentials

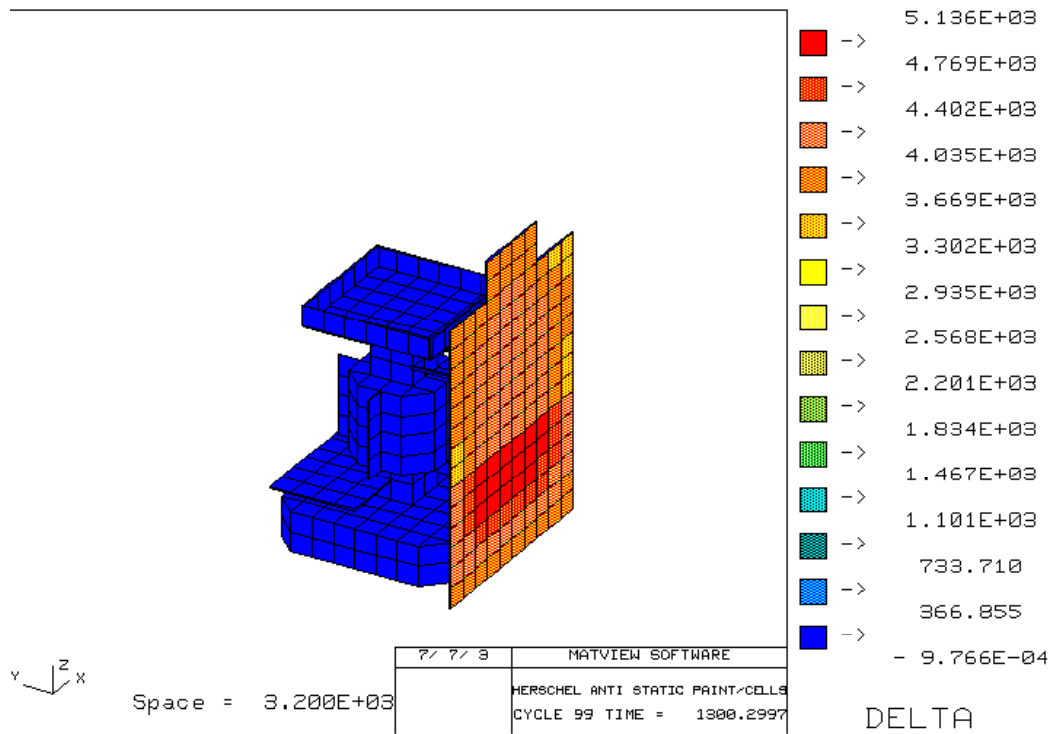


Figure 4. Distribution of differential potentials

## 4.1.3.1.2 CMX on the cells and non conductive OSR not grounded

The Figures 5 and 6 show the differential potentials of Herschel spacecraft surfaces after 1300 s of charging.

The main results of NASCAP simulations are following :

- The final absolute potential of the structure is -2280 V.
- Ought to the anti-static paint, no negative differential potential exists.
- The positive differential potential reaches +3900 V on the OSR and +1530 V on the sunshield (CMX cells).

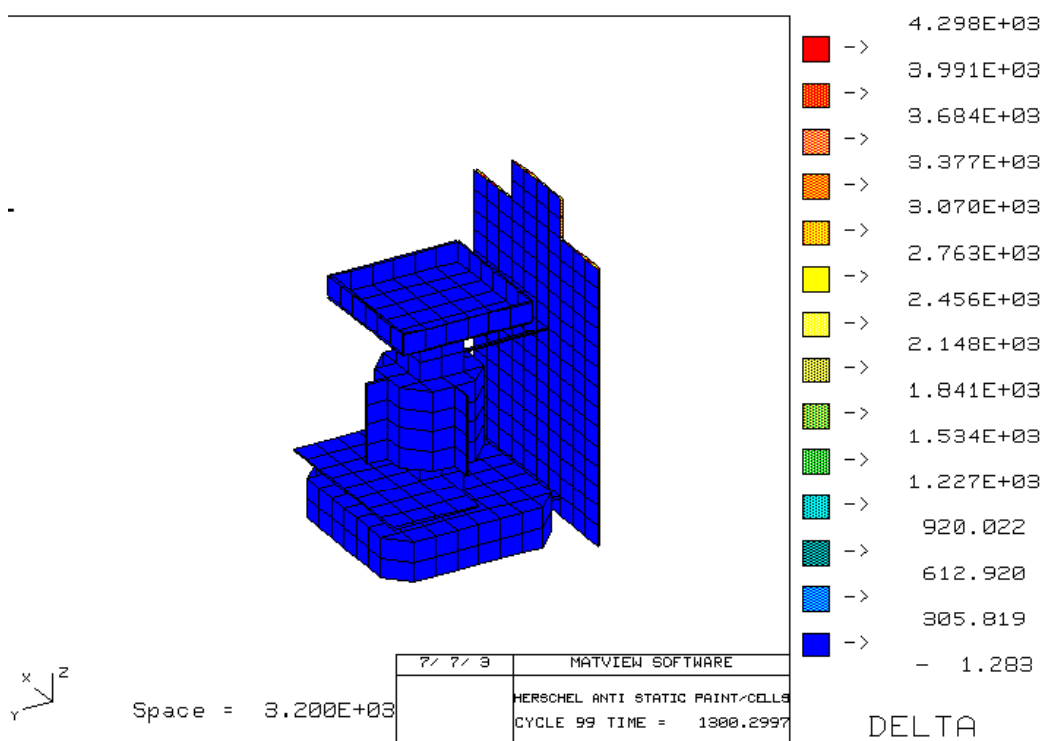


Figure 5. Distribution of differential potentials

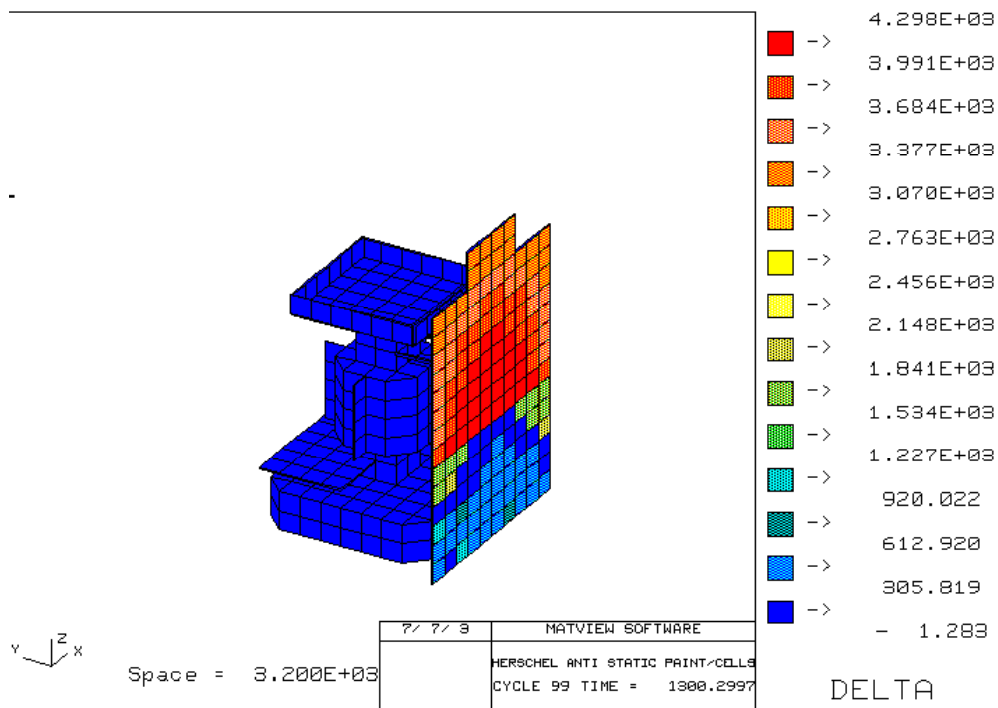


Figure 6. Distribution of differential potentials



### 4.1.3.1.3 CMO on the cells and non conductive OSR grounded

The Figures 7 and 8 show the differential potentials of Herschel spacecraft surfaces after 1300 s of charging.

The Figure 9 presents the evolution of the absolute potentials of some Herschel representative cells during charging.

The main results of NASCAP simulations are following :

- The final absolute potential of the structure is -10420 V.
- Ought to the anti-static paint, no negative differential potential exists.
- The positive differential potential reaches +4820 V on the OSR and +4300 V on the sunshield (CMO cells).

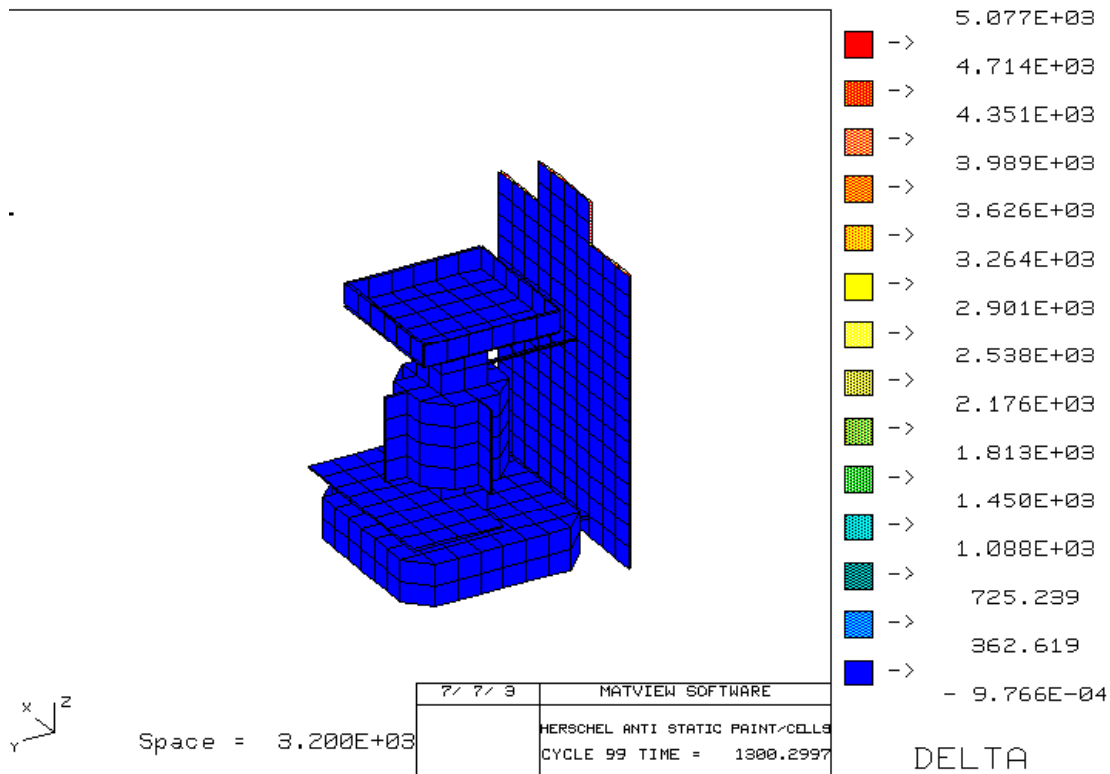


Figure 7. Distribution of differential potentials

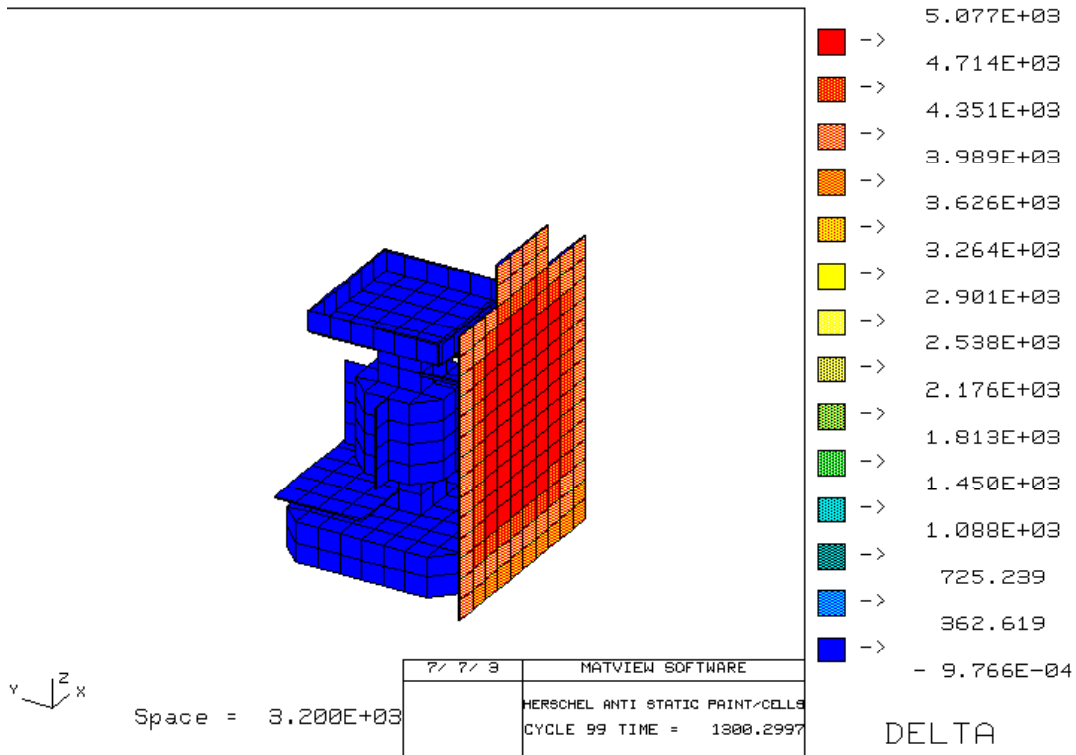


Figure 8. Distribution of differential potentials

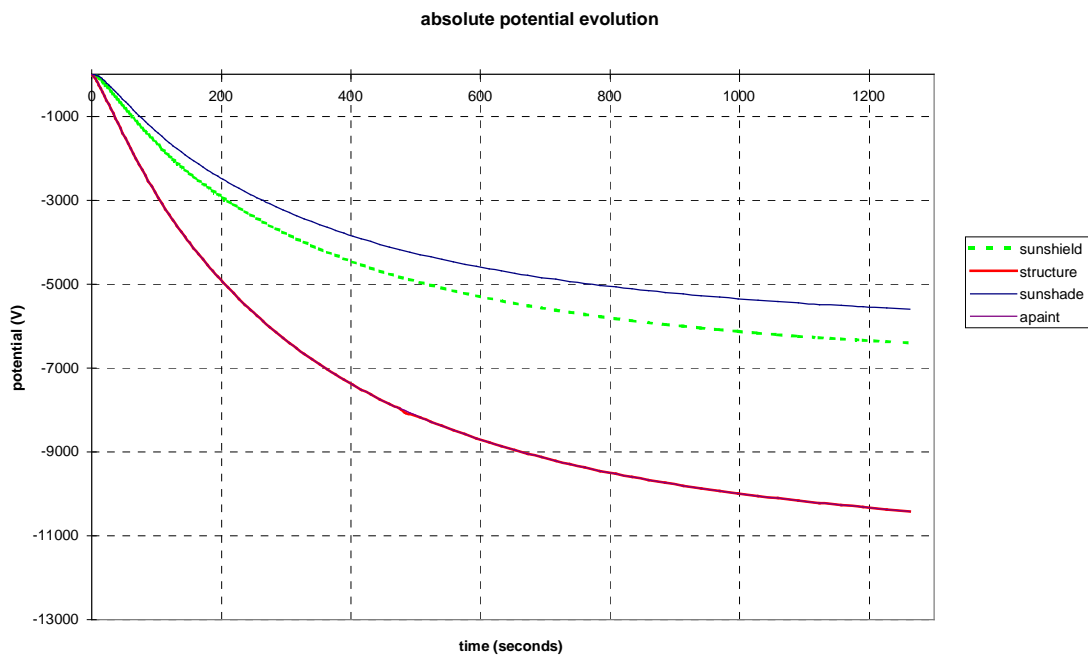


Figure 9. Evolution of absolute potentials during charging

### 4.1.3.1.4 CMX on the cells and non conductive OSR grounded

The Figures 10 and 11 show the differential potentials of Herschel spacecraft surfaces after 1300 s of charging.

The Figure 12 presents the evolution of the absolute potentials of some Herschel representative cells during charging.

The main results of NASCAP simulations are following :

- The final absolute potential of the structure is -1650 V. The equilibrium is reached since 300 s of simulation.
- Ought to the anti-static paint, no negative differential potential exists.
- The positive differential potential reaches +760 V on the OSR and +680 V on the sunshield (CMX cells).

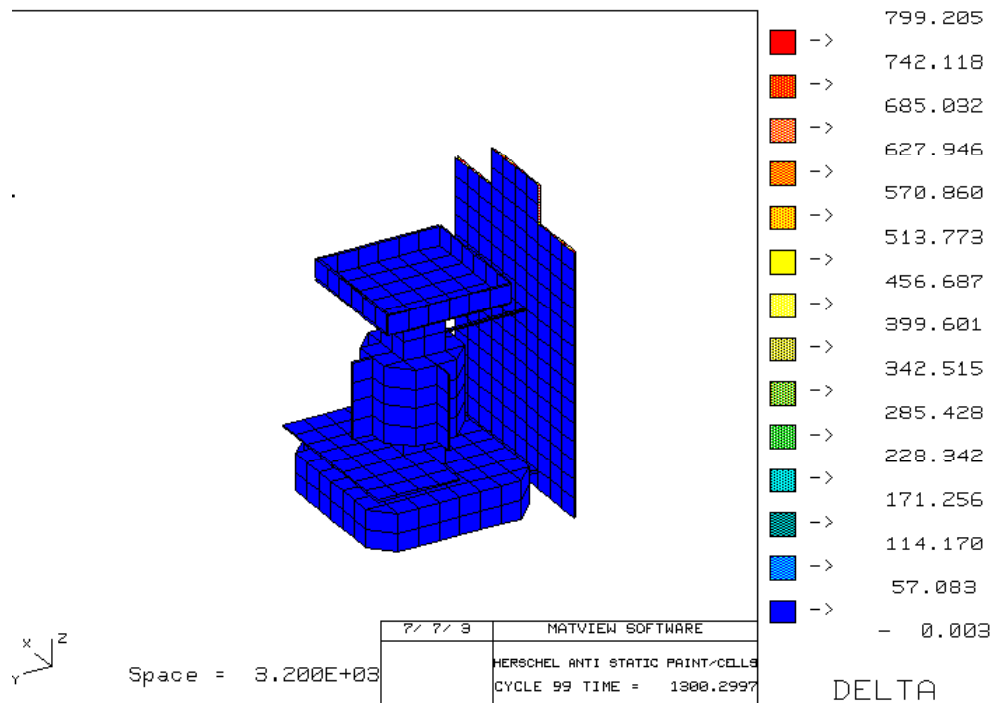


Figure 10. Distribution of differential potentials

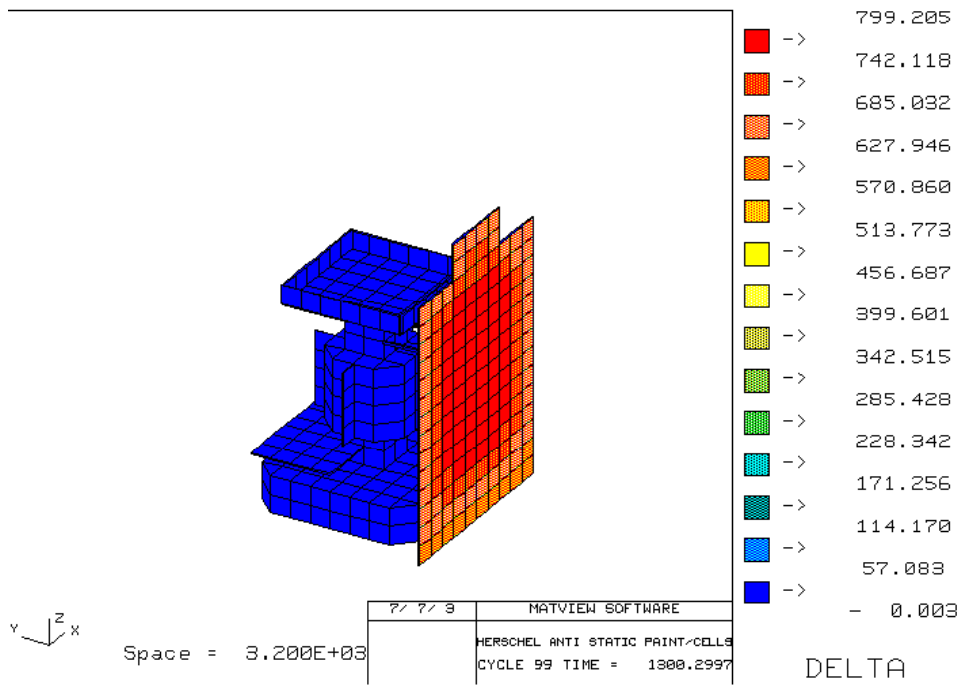


Figure 11. Distribution of differential potentials

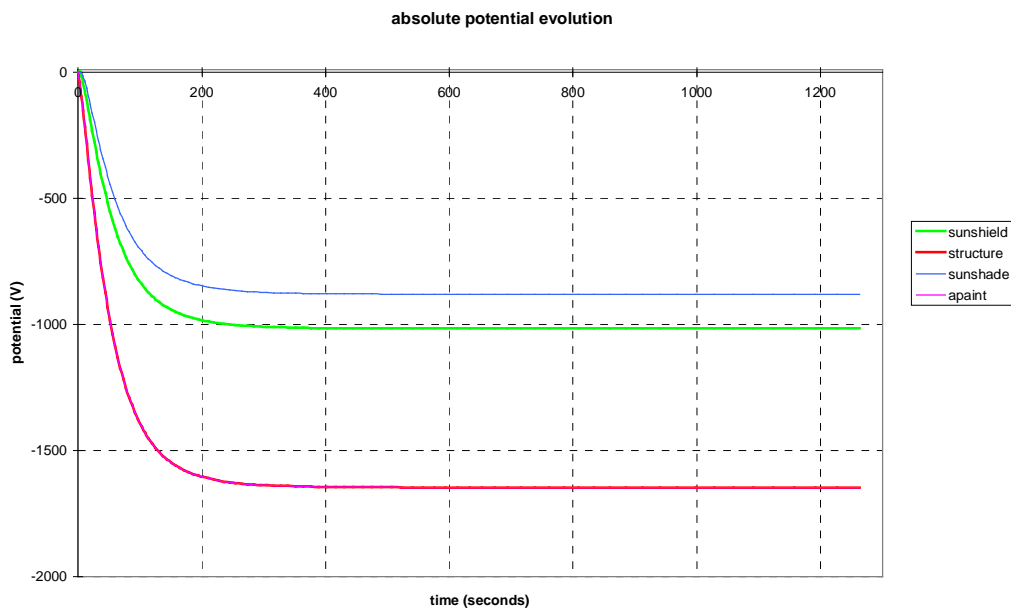


Figure 12. Evolution of absolute potentials during charging

## 4.1.3.2 Herschel satellite charging with non conductive paint (configurations 2, 3, 4)

The non conductive paint resistivity that covers the CVV is assumed to be :

- 1.E+13  $\Omega$ .m in configuration 2
- 1.E+14  $\Omega$ .m in configuration 3
- 1.E+15  $\Omega$ .m in configuration 4

The Figures 13 and 14 show the satellite surface materials used for the calculations.

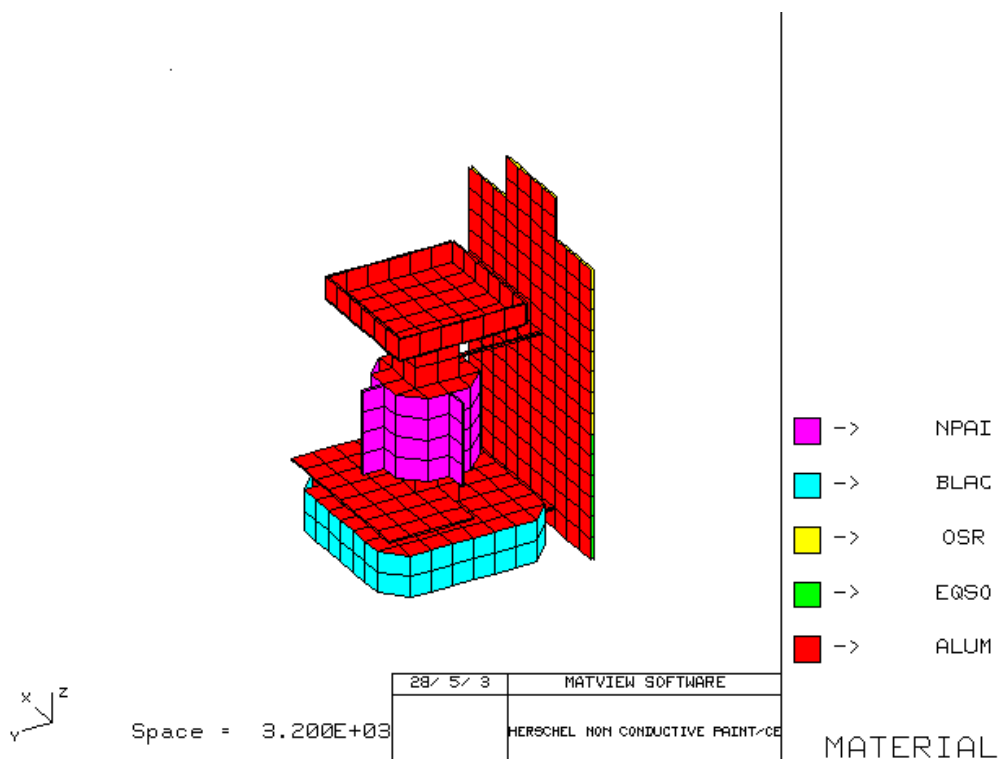


Figure 13. Materials of Herschel Nascap model (configurations 2, 3, 4)

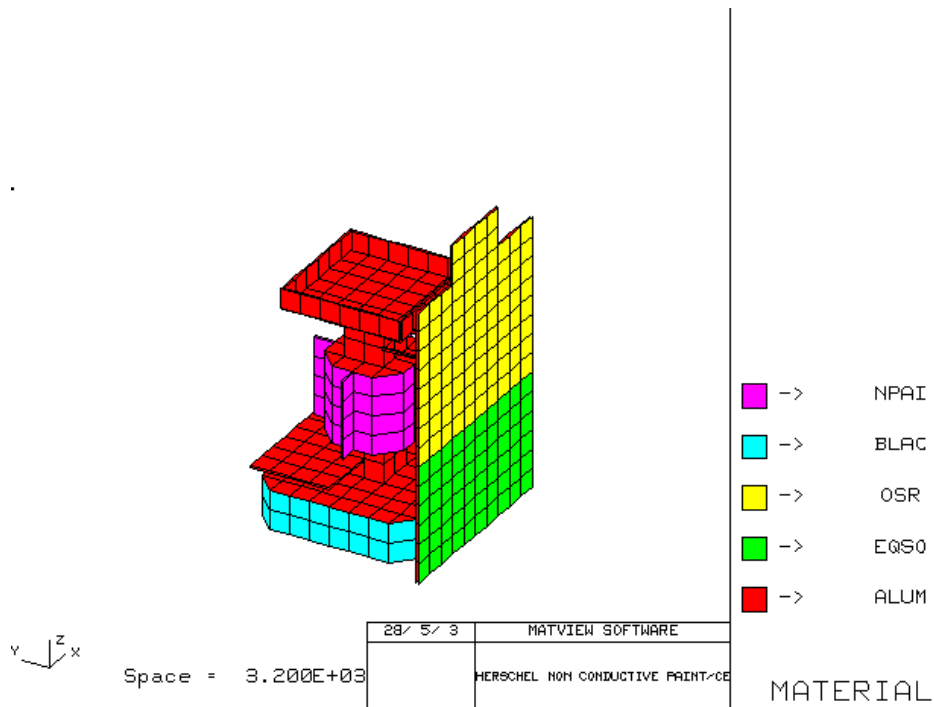


Figure 14. Materials of Herschel Nascap model (configurations 2, 3, 4)

## 4.1.3.2.1 Non conductive paint with a resistivity of $1.E+13$ W.m (configuration 2)

### 4.1.3.2.1.1 CMO on the cells and non conductive OSR not grounded

The Figures 15 and 16 show the differential potentials of Herschel spacecraft surfaces after 1300 s of charging.

The main results of NASCAP simulations are following :

- The final absolute potential of the structure is -10530 V. The equilibrium is reached since 800s of simulation.
- Negative differential potentials exist on the non conductive paint, -110 V. This situation called Normal Voltage Gradient (NVG) is not dangerous until a difference of -1500 V occurs. Moreover, It is not possible to quantify exactly the level of negative differential charging. Indeed, this level depends on the secondary electron emission parameters that are unknown on the eventually selected paints. If the paint is selected, ground tests should be performed.
- The positive differential potential reaches +4000 V on the OSR (not grounded) and reaches the maximum value +5200 V on the sunshield (CMO cells).

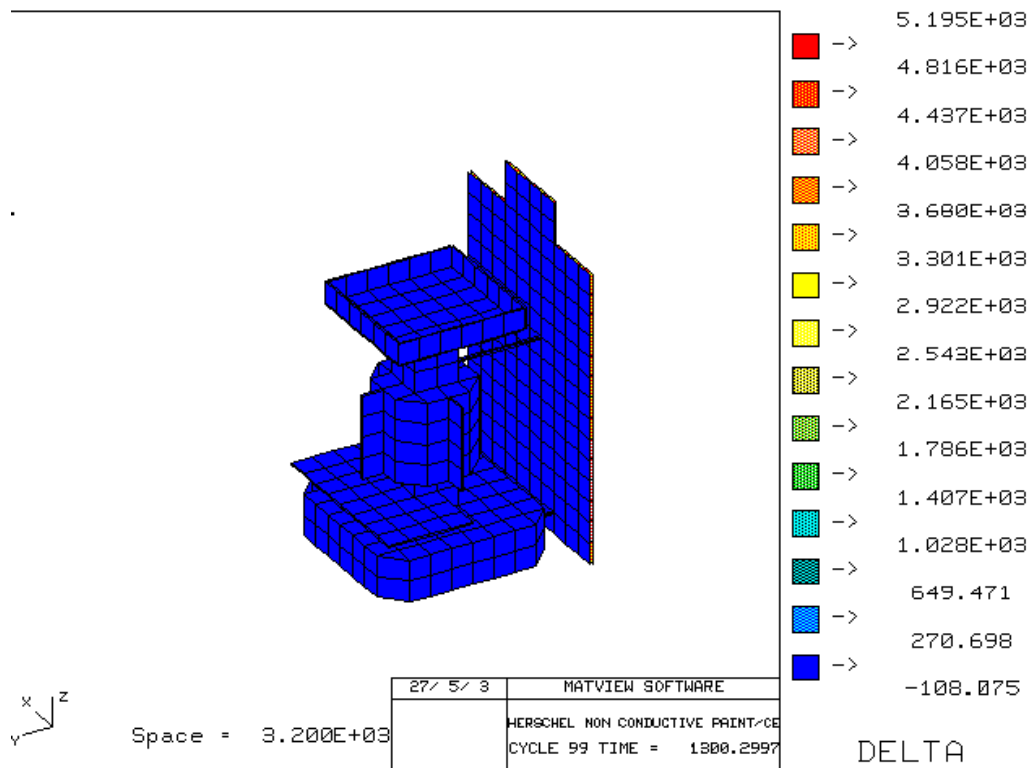


Figure 15. Distribution of differential potentials

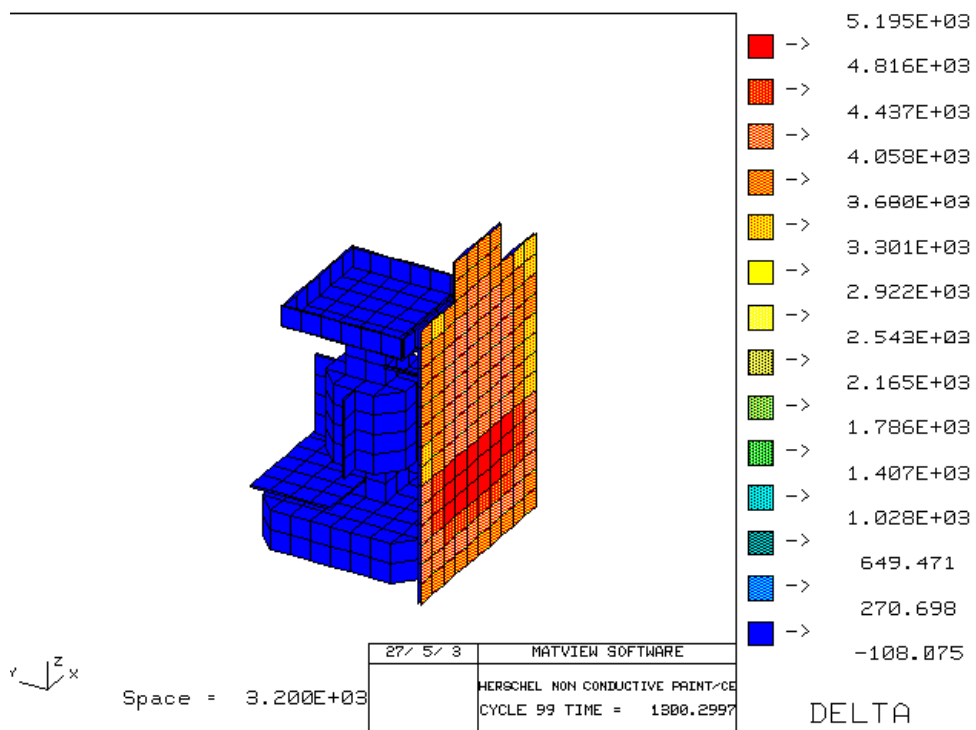


Figure 16. Distribution of differential potentials



## 4.1.3.2.1.2 CMX on the cells and non conductive OSR not grounded

The Figures 17 and 18 show the differential potentials of Herschel spacecraft surfaces after 1300 s of charging.

The main results of NASCAP simulations are following :

- The final absolute potential of the structure is -2200 V.
- Negative differential potentials exist on the non conductive paint, -400 V.
- The positive differential potential reaches +3900 V on the OSR (not grounded) +600 V on the sunshield (CMX cells).

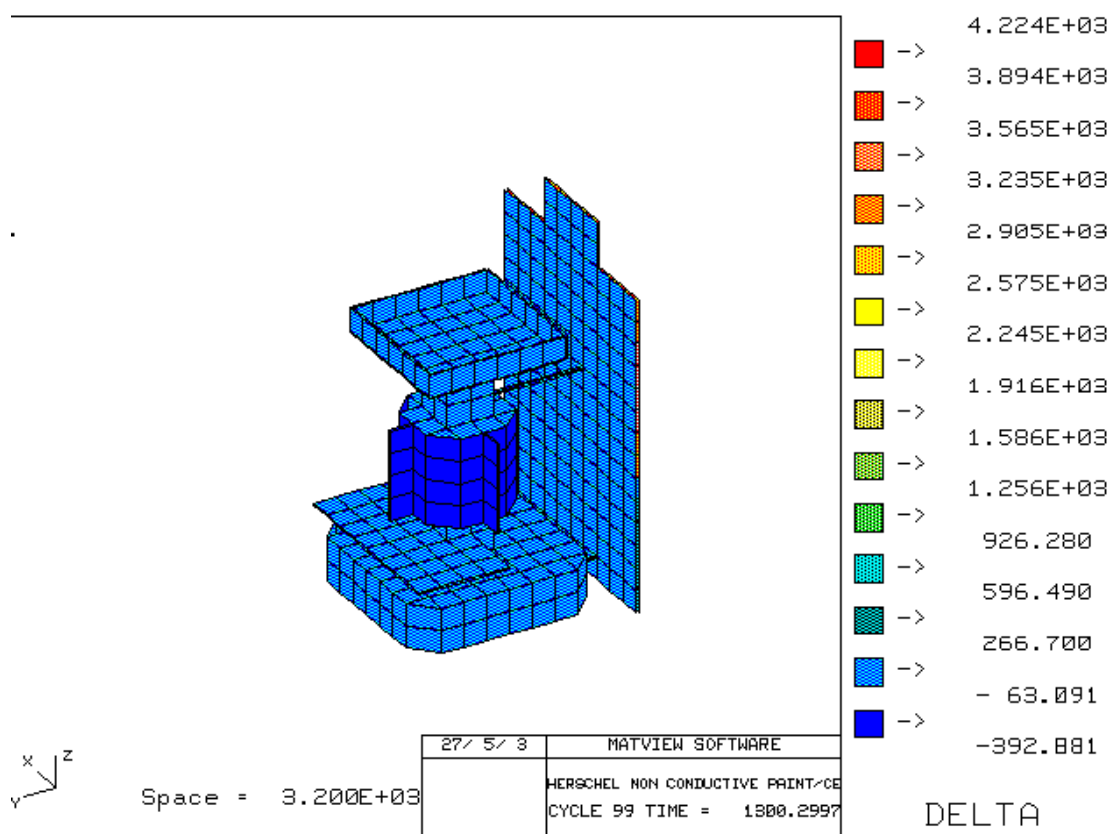


Figure 17. Distribution of differential potentials

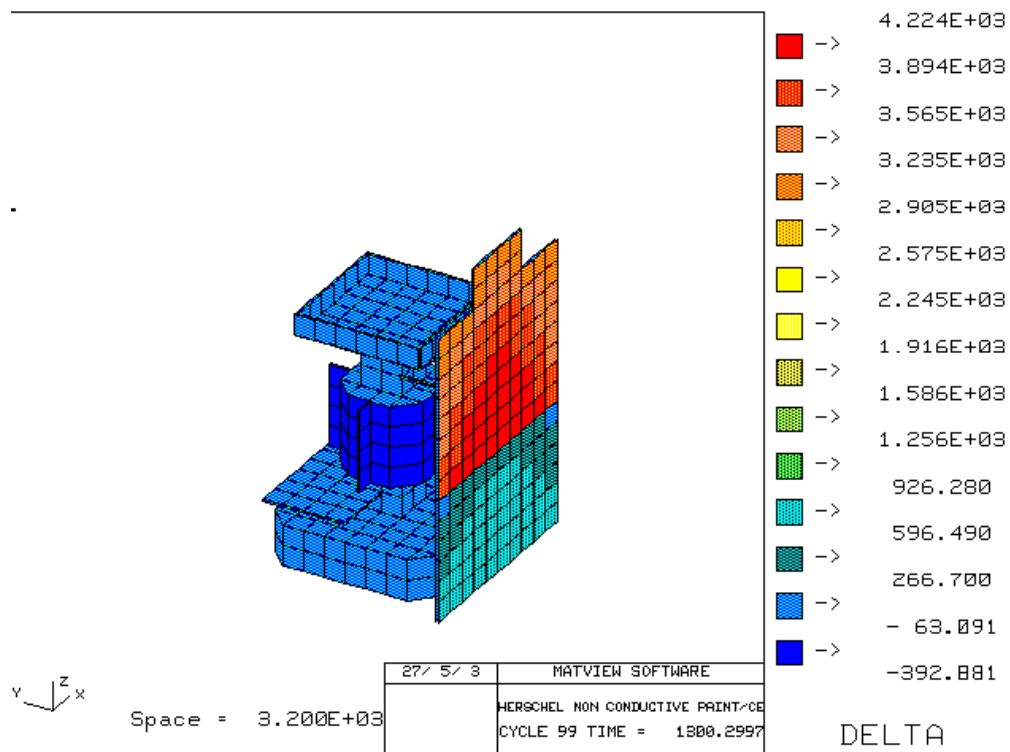


Figure 18. Distribution of differential potentials

### 4.1.3.2.1.3 CMO on the cells and non conductive OSR grounded

The Figures 19 and 20 show the differential potentials of Herschel spacecraft surfaces after 1300s of charging.

The Figure 21 presents the evolution of the absolute potentials of some Herschel representative cells during charging.

The main results of NASCAP simulations are following :

- The final absolute potential of the structure is -10660 V. The equilibrium is reached since 800s of simulation.
- Negative differential potentials exist on the non conductive paint, -110 V.
- The positive differential potential reaches +4900 V on the OSR and +4400 V on the sunshield (CMO cells).

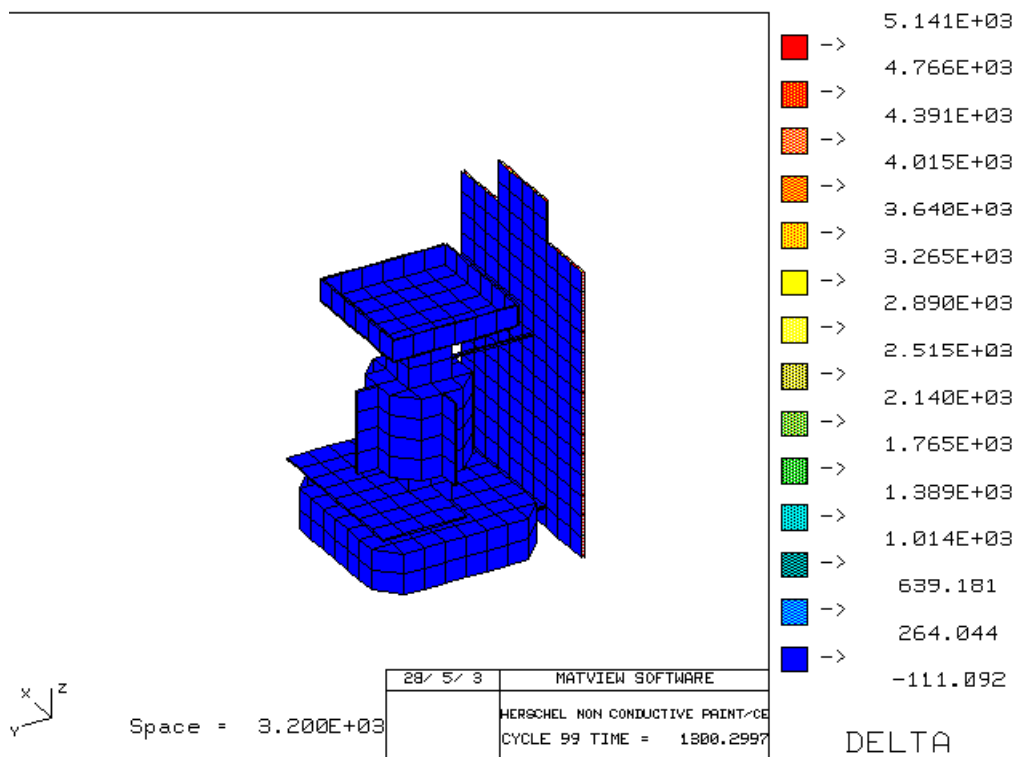


Figure 19. Distribution of differential potentials

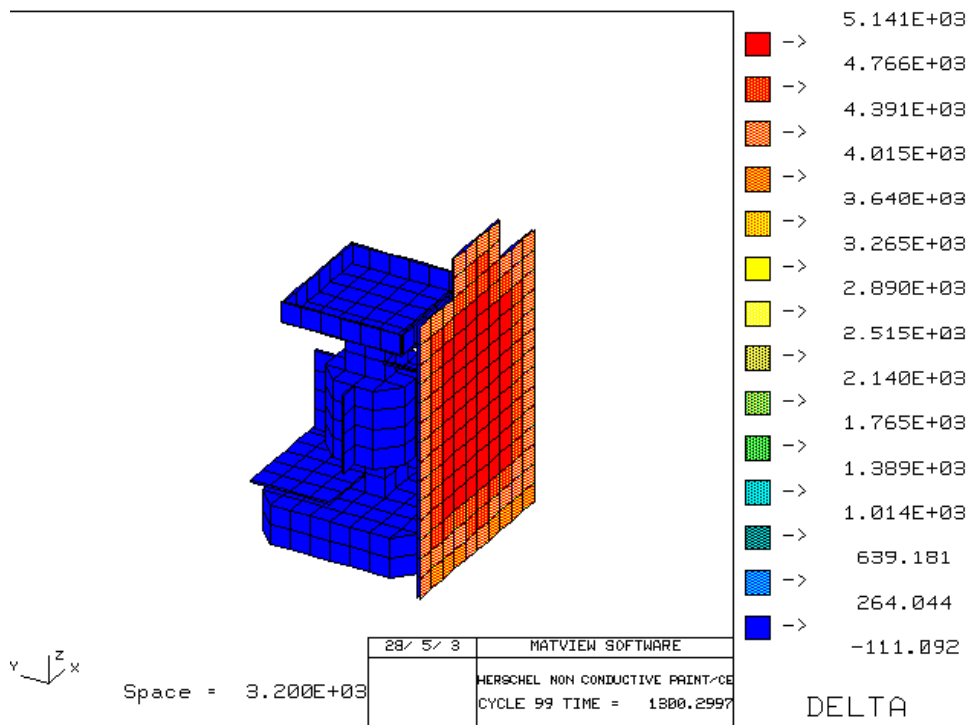


Figure 20. Distribution of differential potentials

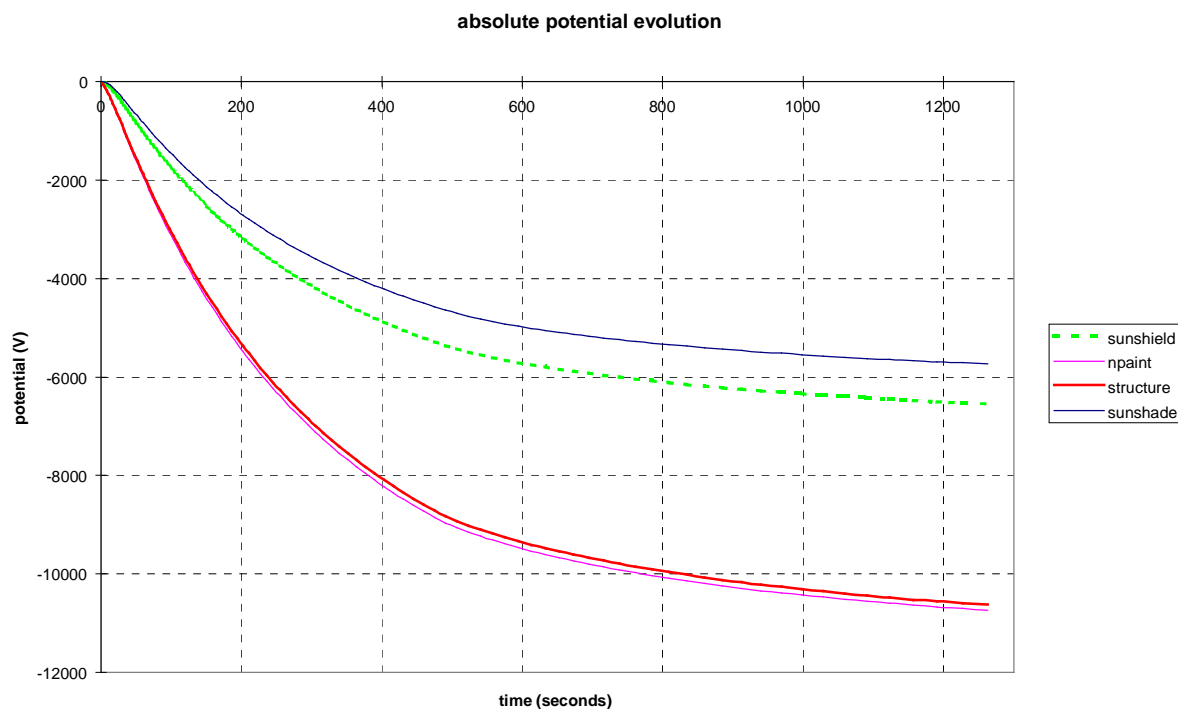


Figure 21. Evolution of absolute potentials during charging

### 4.1.3.2.1.4 CMX on the cells and non conductive OSR grounded

The Figures 22 and 23 show the differential potentials of Herschel spacecraft surfaces after 1300 s of charging.

The Figure 24 presents the evolution of the absolute potentials of some Herschel representative cells during charging.

The main results of NASCAP simulations are following :

- The final absolute potential of the structure is -1650 V. The equilibrium is reached since 300s of simulation.
- Negative differential potentials exist on the non conductive paint, -270 V.
- The positive differential potential reaches +760 V on the OSR +680 V on the sunshield (CMX cells).

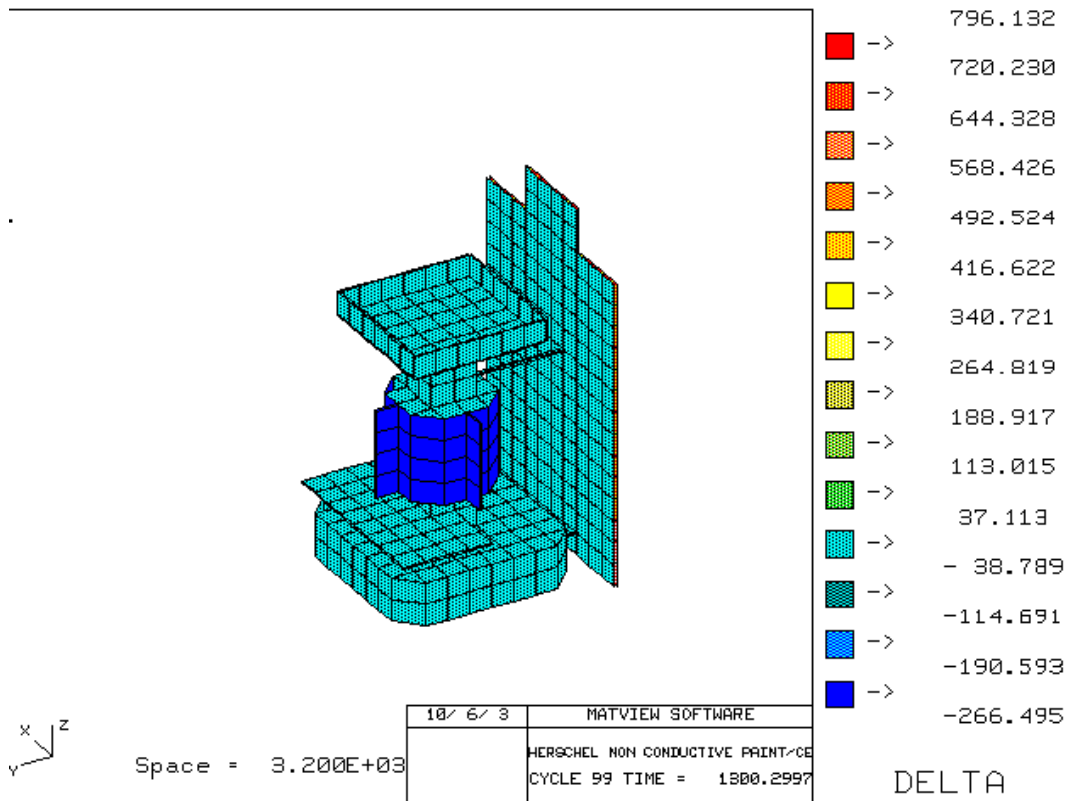


Figure 22. Distribution of differential potentials

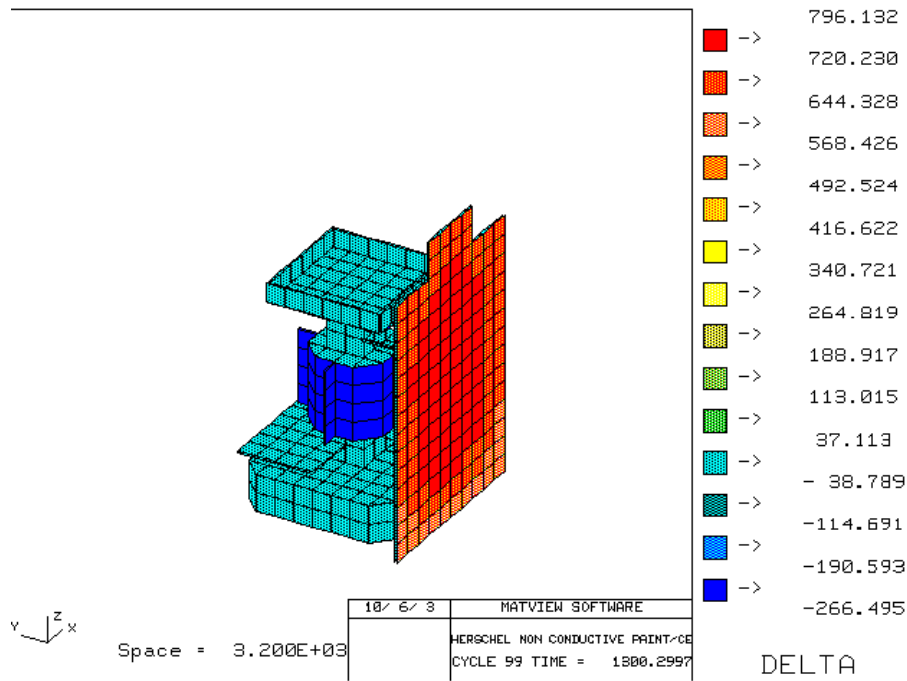


Figure 23. Distribution of differential potentials

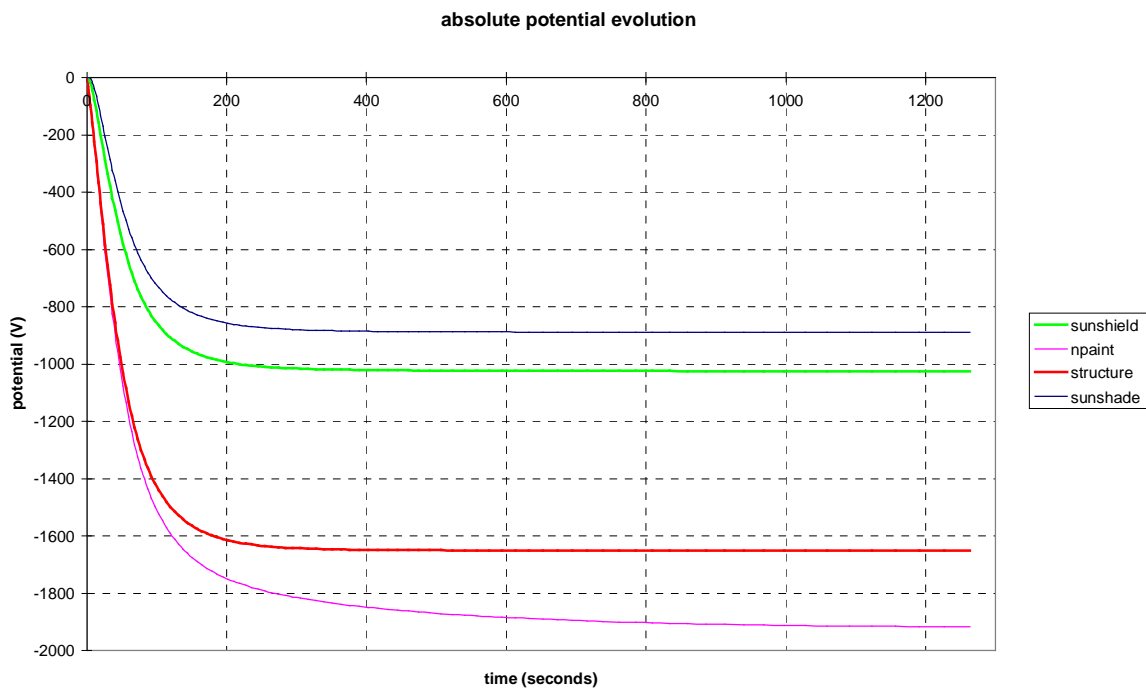


Figure 24. Evolution of absolute potentials during charging

## 4.1.3.2.1.5 CMO on the cells and OSR with ITO

The Figures 25 and 26 show the satellite surface materials used for the calculations.

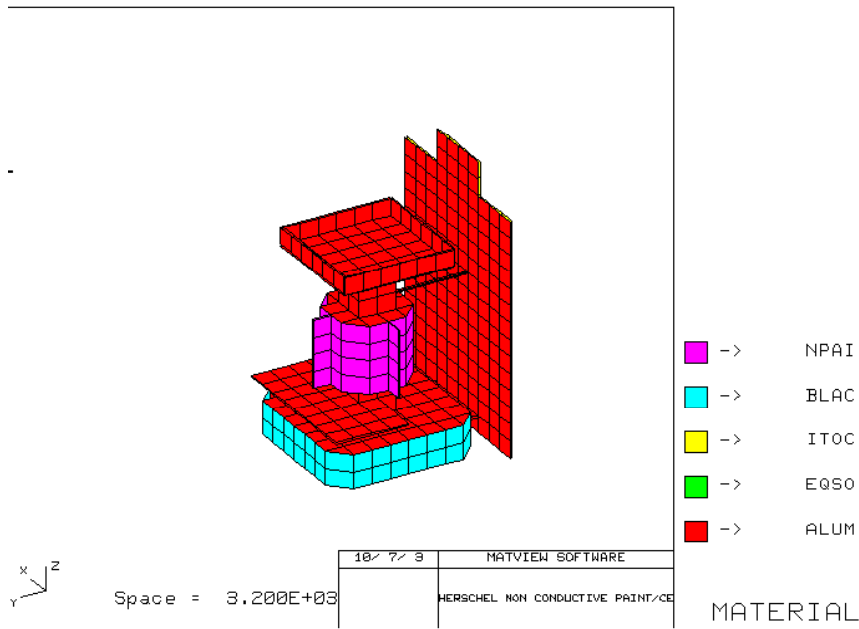


Figure 25. Materials of Herschel Nascap model (configuration 2 with ITO)

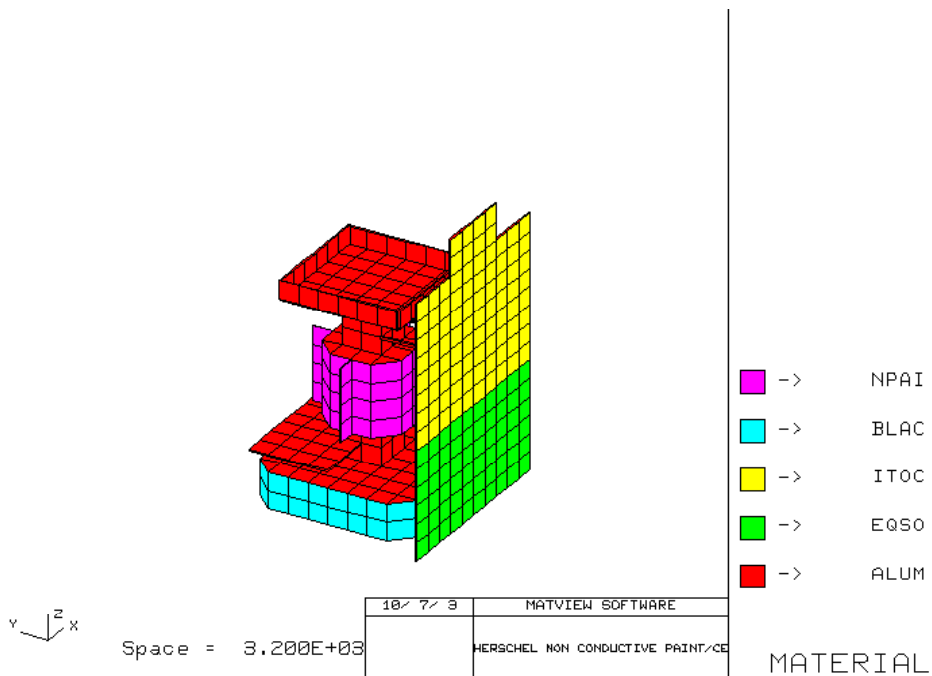


Figure 26. Materials of Herschel Nascap model (configuration 2 with ITO)

The Figures 27 and 28 show the differential potentials of Herschel spacecraft surfaces after 1300 s of charging.

The Figure 29 presents the evolution of the absolute potentials of some Herschel representative cells during charging.

The main results of NASCAP simulations are following :

- The final absolute potential of the structure is -15.5 V.
- Negative differential potentials exist on the non conductive paint, -310 V.
- The positive differential potential reaches +10 V on the sunshield (CMO cells).

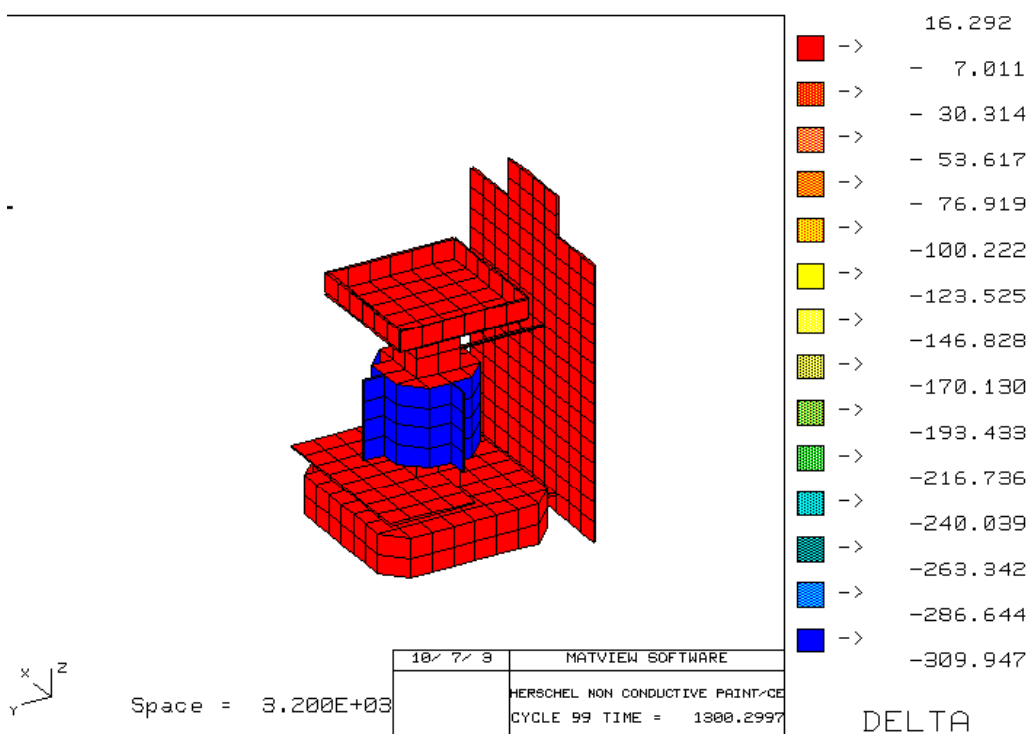


Figure 27. Distribution of differential potentials



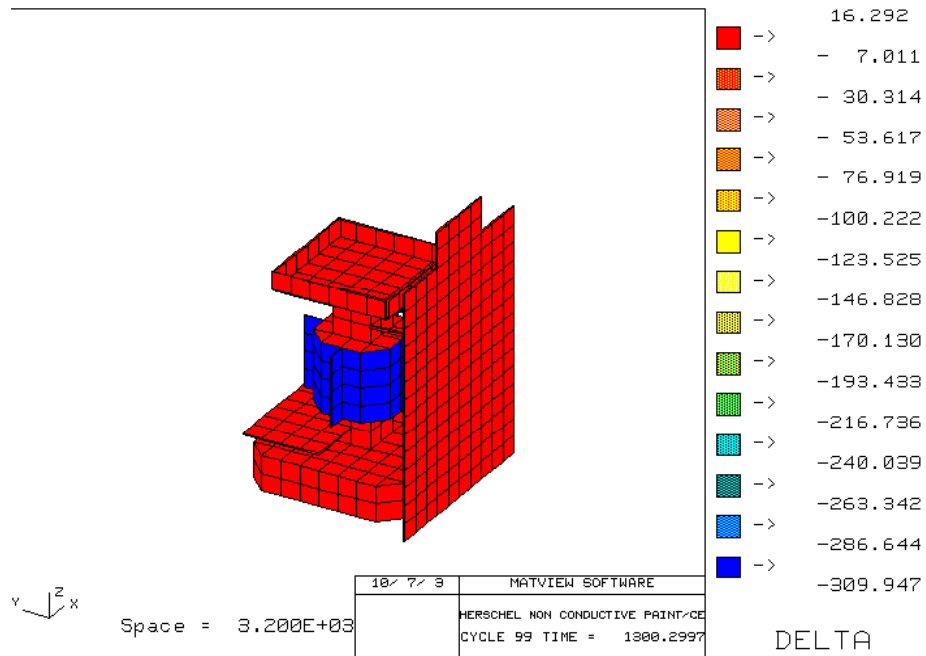


Figure 28. Distribution of differential potentials

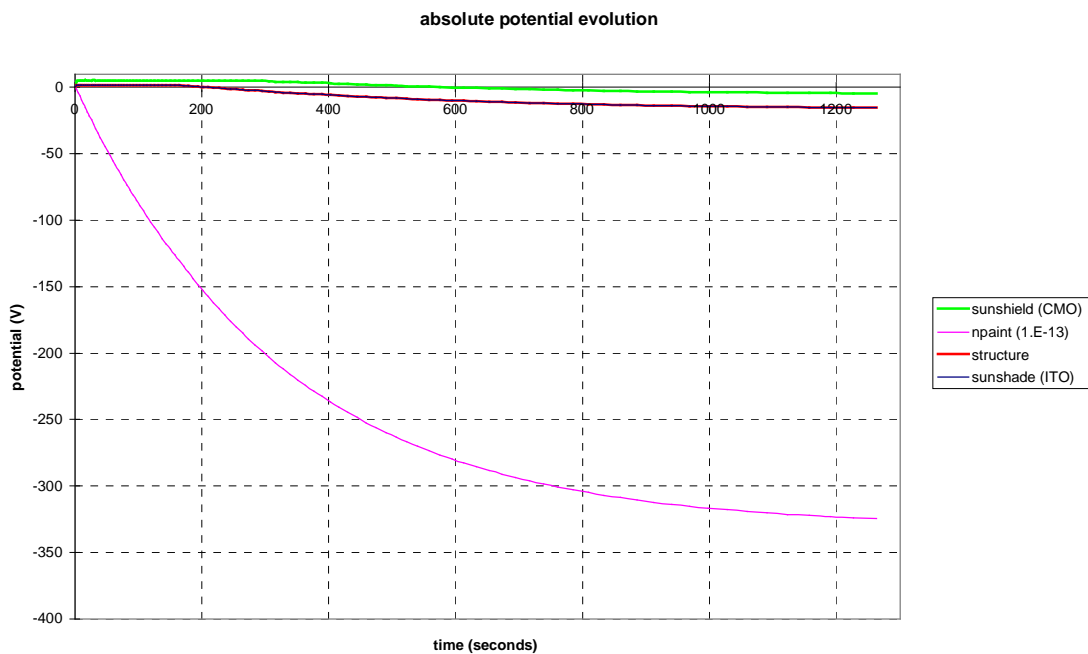


Figure 29. Evolution of absolute potentials during charging

## 4.1.3.2.2 Non conductive paint with a resistivity of $1.E+14$ W.m (configuration 3)

### 4.1.3.2.2.1 CMO on the cells and non conductive OSR not grounded

The Figures 30 and 31 show the differential potentials of Herschel spacecraft surfaces after 1300 s of charging.

The main results of NASCAP simulations are following :

- The final absolute potential of the structure is -10660 V.
- Negative differential potentials exist on the non conductive paint, -410 V.
- The positive differential potential reaches +4000 V on the OSR (not grounded) and reaches the maximum value +5240 V on the sunshield (CMO cells).

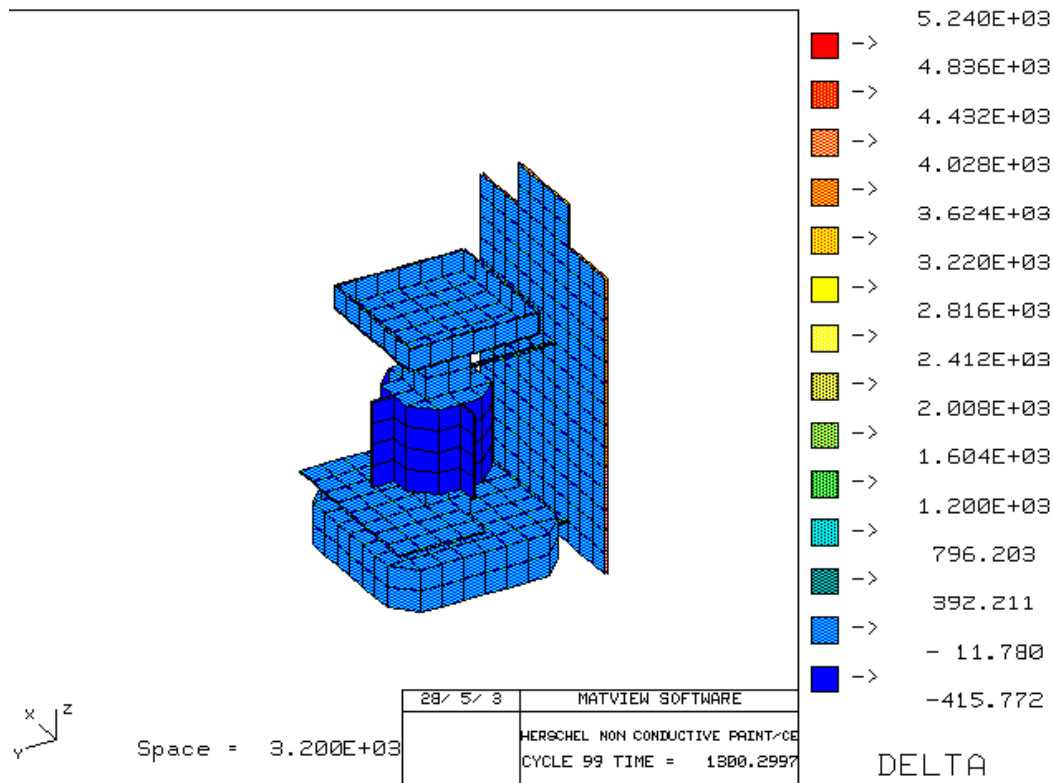


Figure 30. Distribution of differential potentials

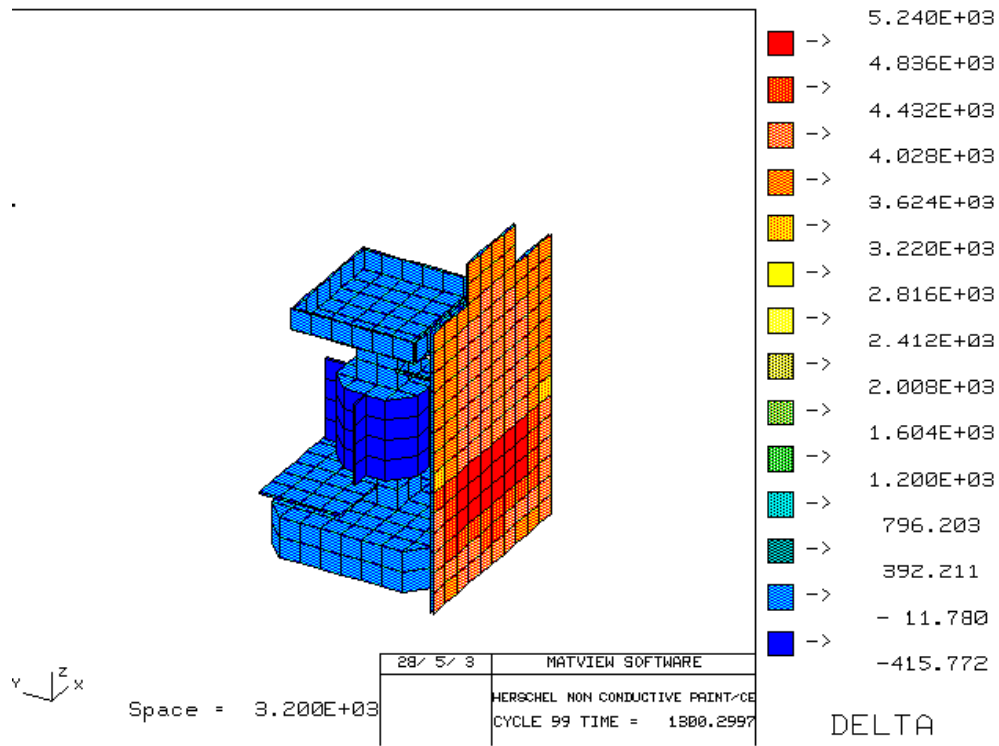


Figure 31. Distribution of differential potentials

## 4.1.3.2.2.2 CMX on the cells and non conductiveOSR not grounded

The Figures 32 and 33 show the differential potentials of Herschel spacecraft surfaces after 1300 s of charging.

The main results of NASCAP simulations are following :

- The final absolute potential of the structure is -2320 V.
- Negative differential potentials exist on the non conductive paint, -1230 V.
- The positive differential potential reaches +3800 V on the OSR (not grounded) and +1100 V on the sunshield (CMX cells).

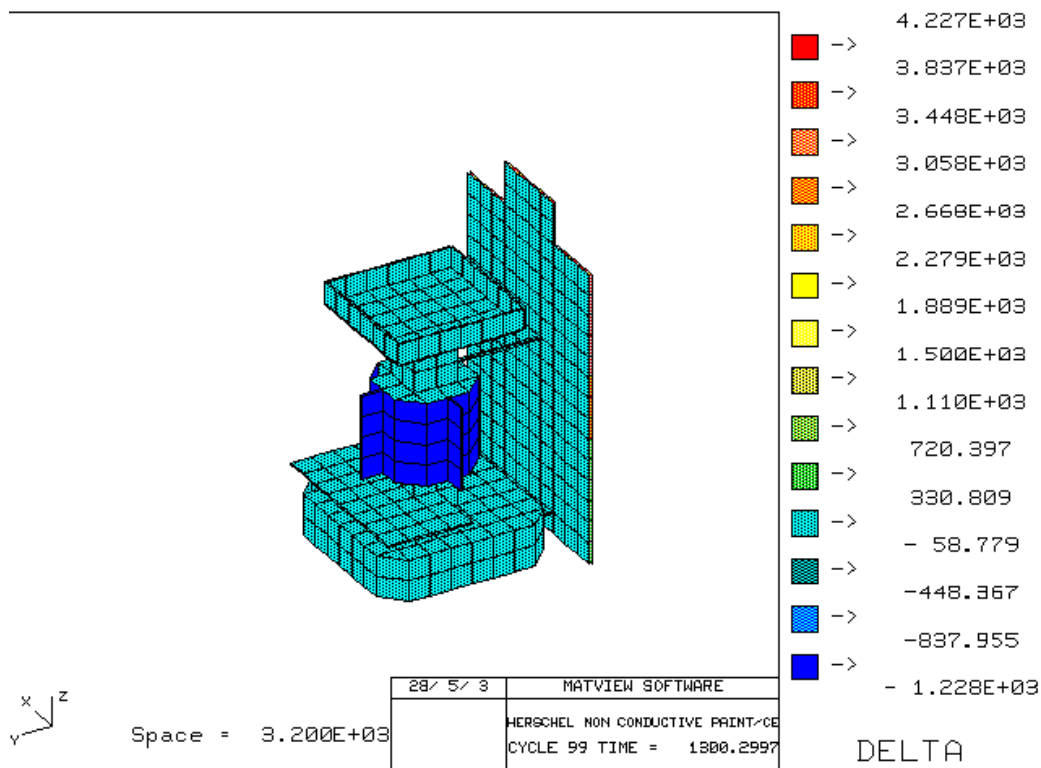


Figure 32. Distribution of differential potentials

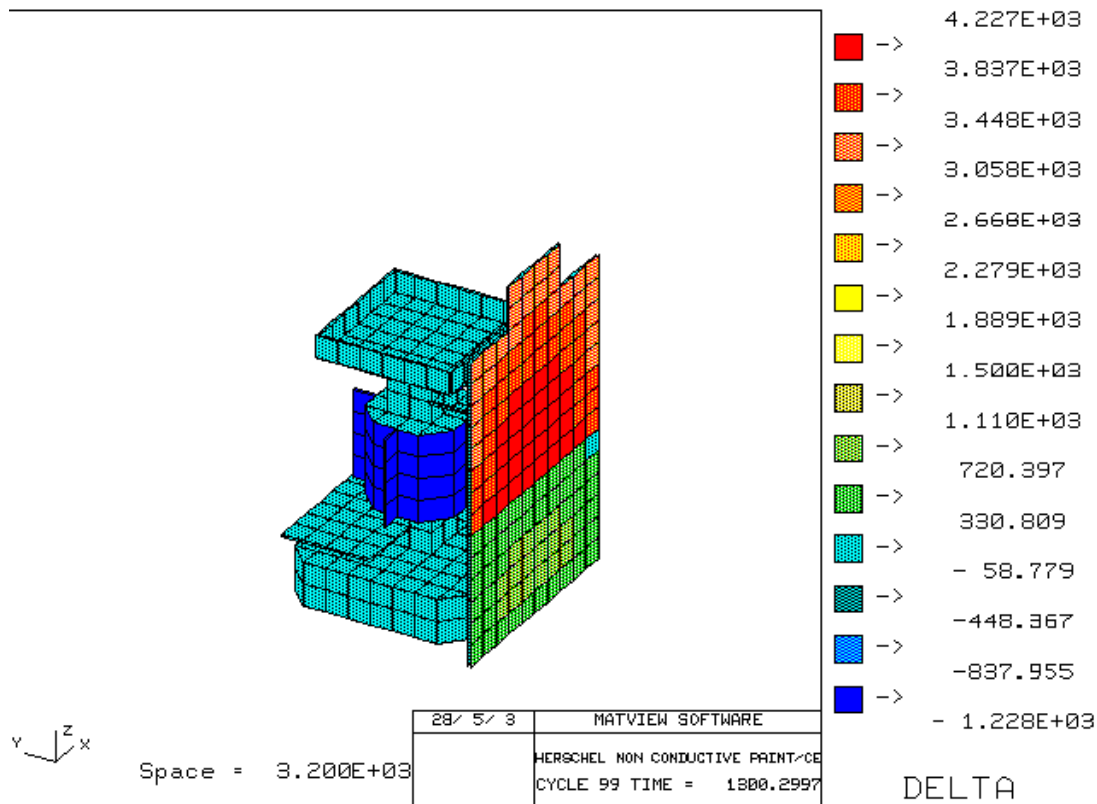


Figure 33. Distribution of differential potentials

### 4.1.3.2.2.3 CMO on the cells and non conductive OSR grounded

The Figures 34 and 35 show the differential potentials of Herschel spacecraft surfaces after 1300 s of charging.

The Figure 36 presents the evolution of the absolute potentials of some Herschel representative cells during charging.

The main results of NASCAP simulations are following :

- The final absolute potential of the structure is -11100 V.
- Negative differential potentials exist on the non conductive paint, -450 V.
- The positive differential potential reaches +5100 V on the OSR and +4600 V on the sunshield (CMO cells).

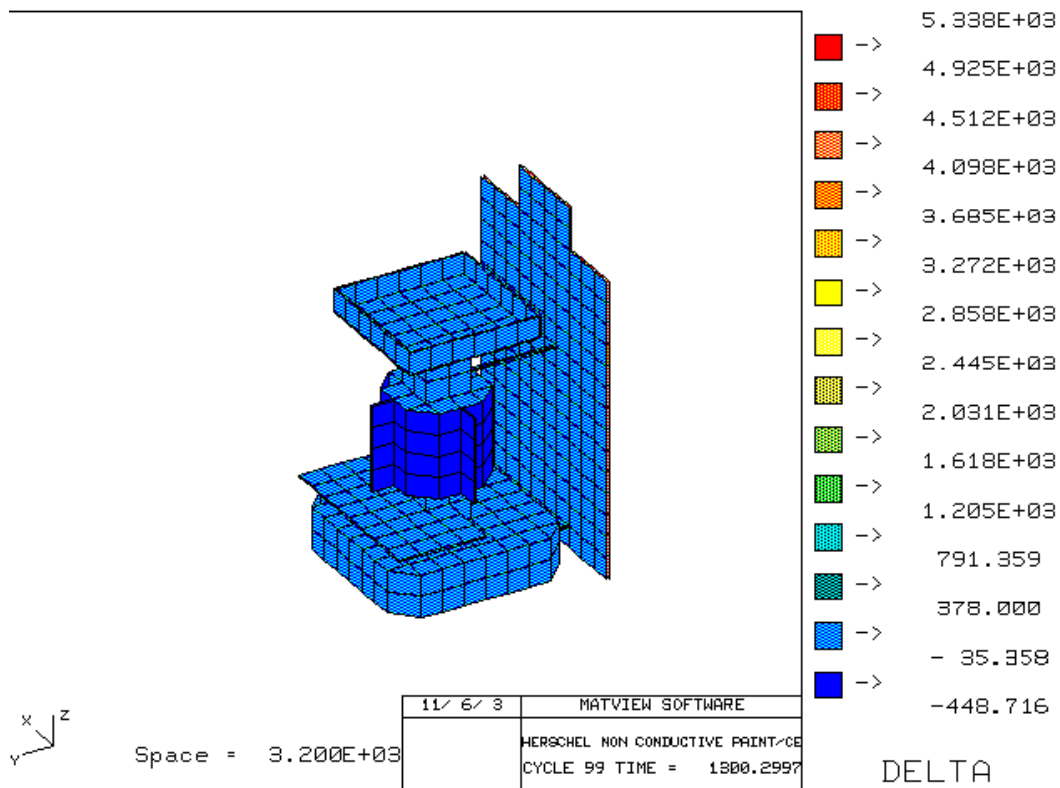


Figure 34. Distribution of differential potentials

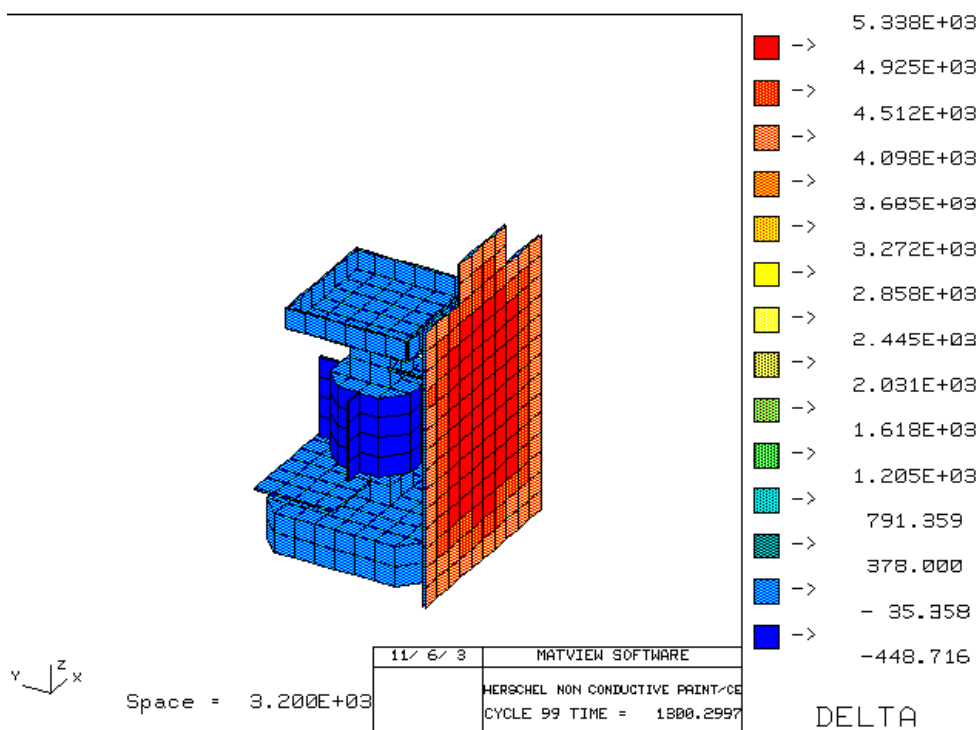


Figure 35. Distribution of differential potentials

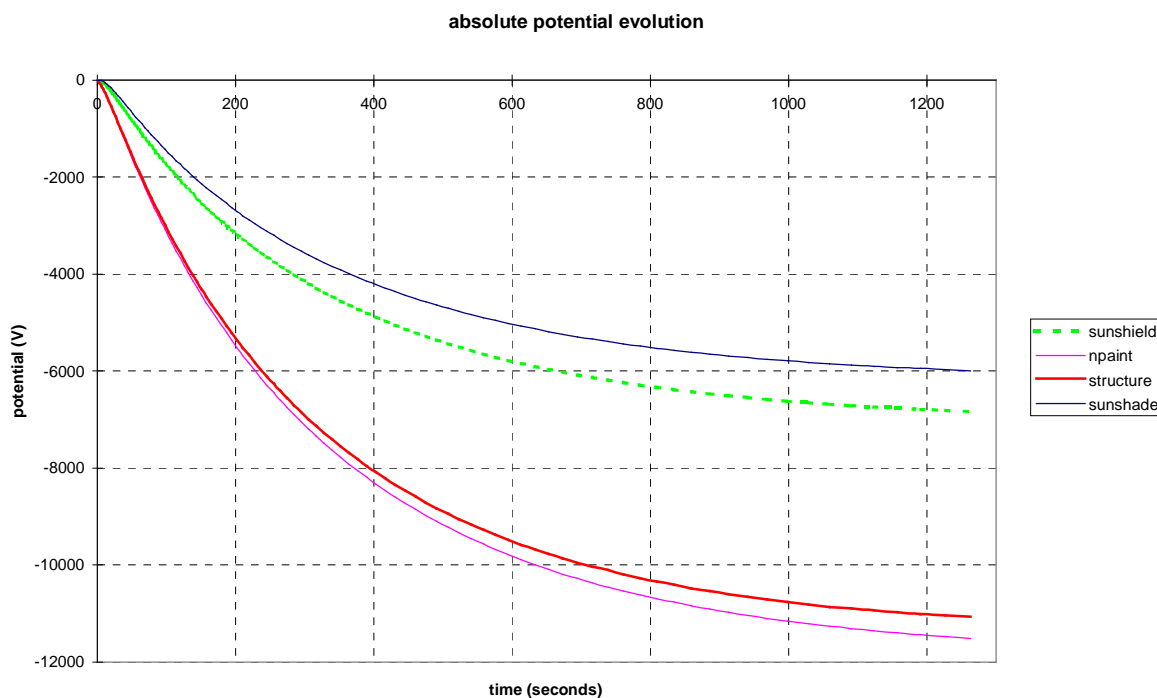


Figure 36. Evolution of absolute potentials during charging

## 4.1.3.2.2.4 CMX on the cells and non conductive OSR grounded

The Figures 37 and 38 show the differential potentials of Herschel spacecraft surfaces after 1300 s of charging.

The Figure 39 presents the evolution of the absolute potentials of some Herschel representative cells during charging.

The main results of NASCAP simulations are following :

- The final absolute potential of the structure is -1660 V.
- Negative differential potentials exist on the non conductive paint, -910 V.
- The positive differential potential reaches +760 V on the OSR and +670 V on the sunshield (CMX cells).

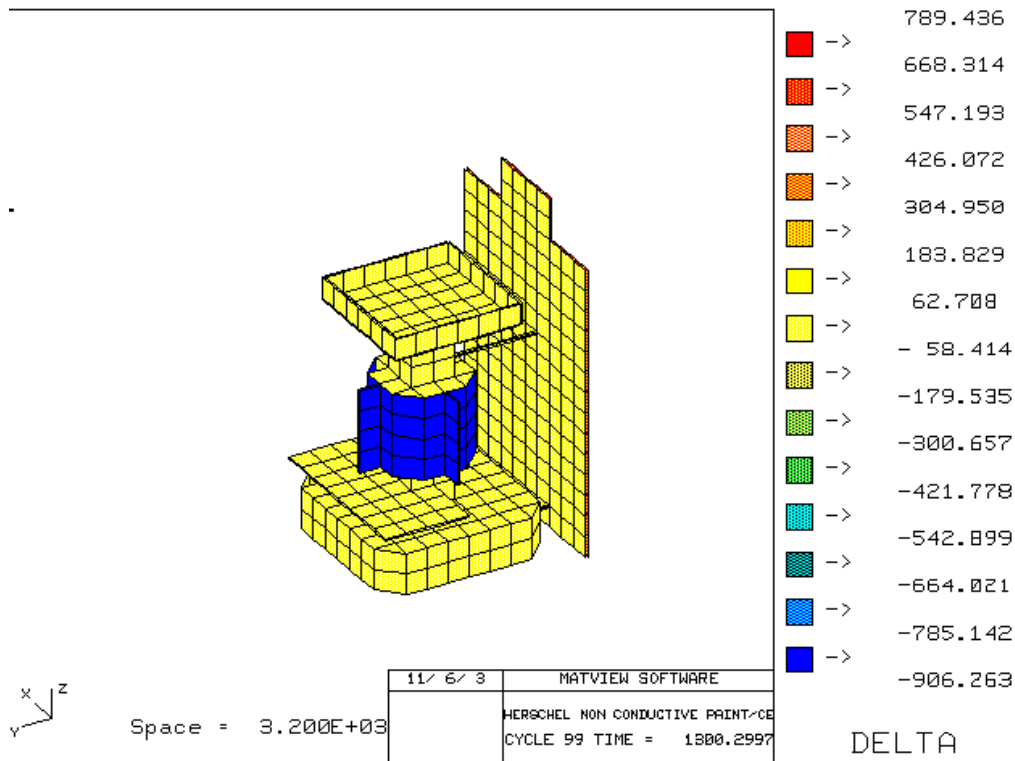


Figure 37. Distribution of differential potentials



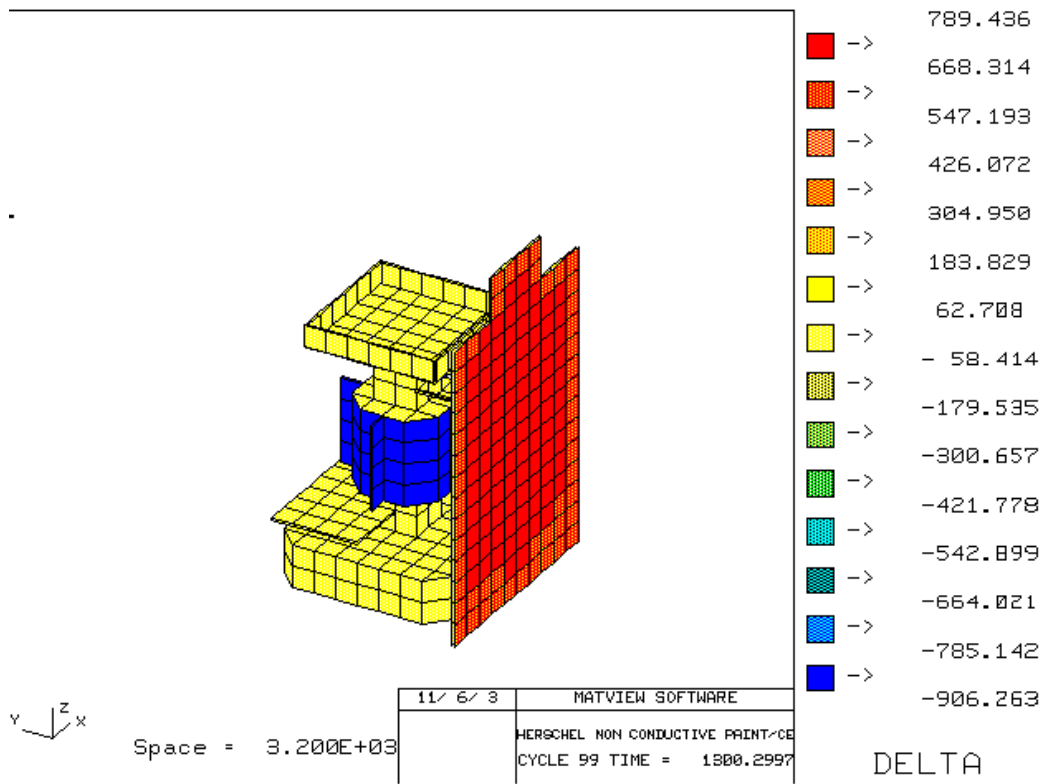


Figure 38. Distribution of differential potentials

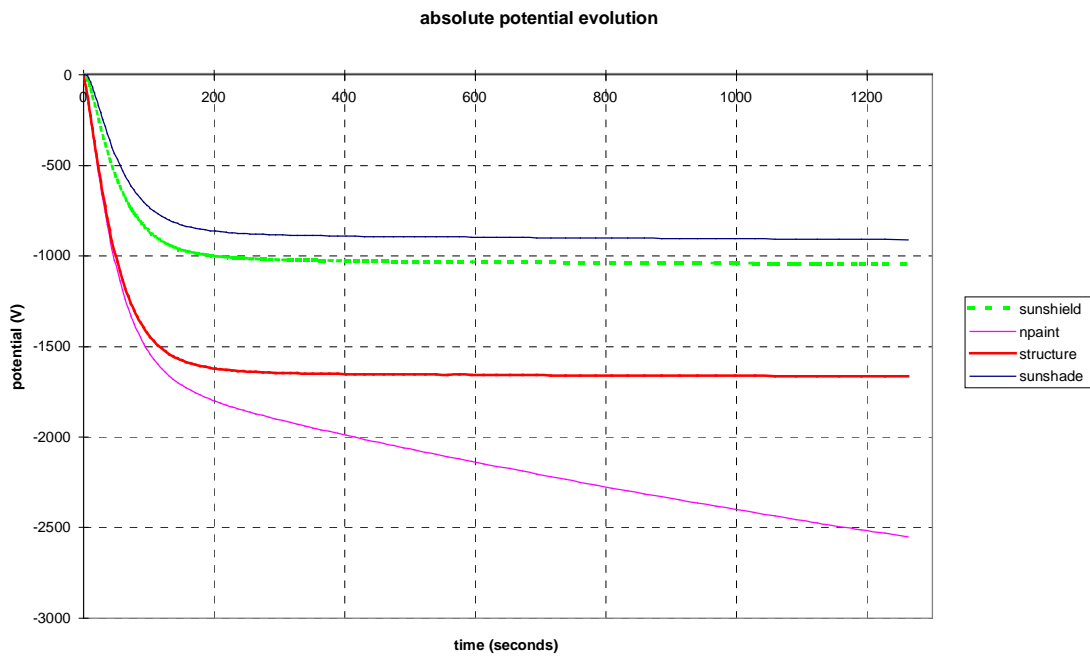


Figure 39. Evolution of absolute potentials during charging

### 4.1.3.2.3 Non conductive paint with a resistivity of $1.E+15$ W.m (configuration 4)

#### 4.1.3.2.3.1 CMO on the cells and non conductive OSR not grounded

The Figures 40 and 41 show the differential potentials of Herschel spacecraft surfaces after 1300 s of charging.

The main results of NASCAP simulations are following :

- The final absolute potential of the structure is -10660 V.
- Negative differential potentials exist on the non conductive paint, -510 V.
- The positive differential potential reaches +4000 V on the OSR (not grounded) and reaches the maximum value +5200 V on the sunshield (CMO cells).

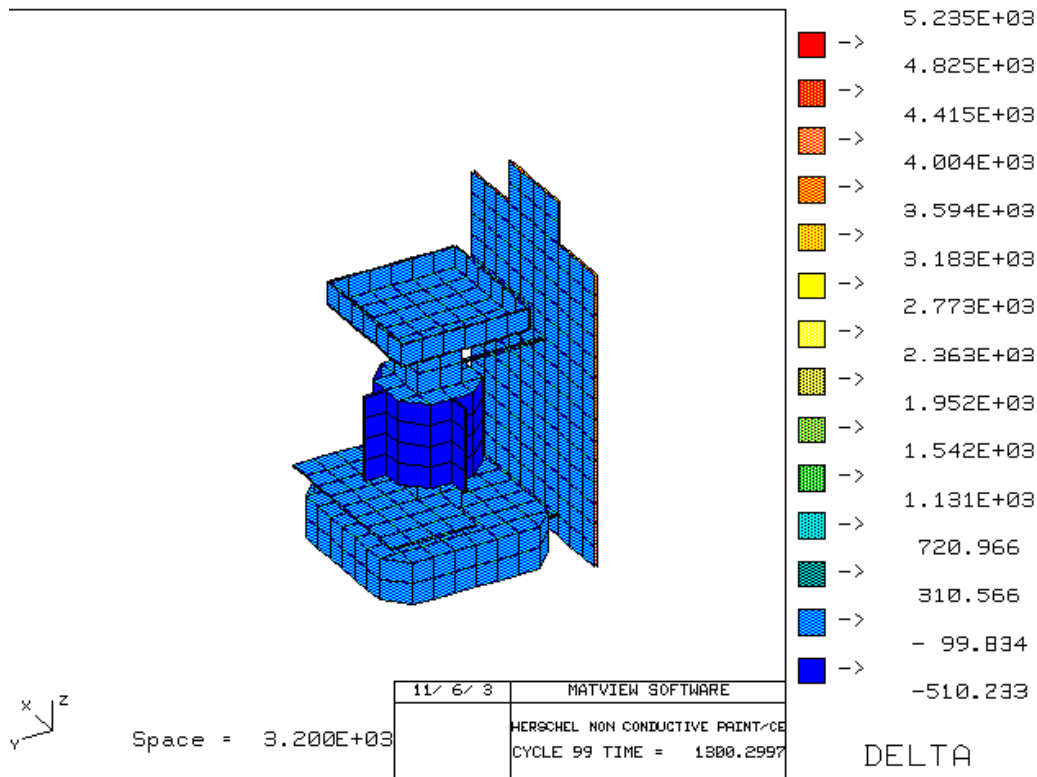


Figure 40. Distribution of differential potentials

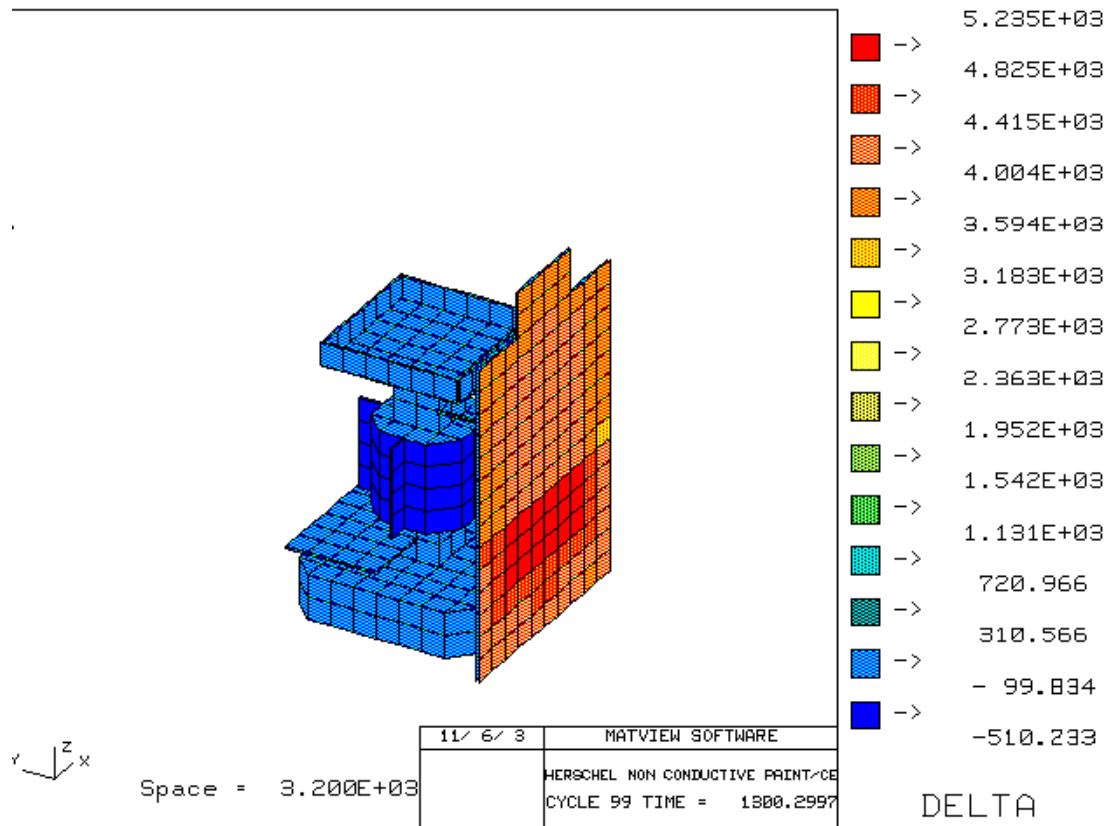


Figure 41. Distribution of differential potentials

### 4.1.3.2.3.2 CMX on the cells and non conductive OSR not grounded

The Figures 42 and 43 show the differential potentials of Herschel spacecraft surfaces after 1300 s of charging.

The main results of NASCAP simulations are following :

- The final absolute potential of the structure is -2450 V.
- Negative differential potentials exist on the non conductive paint, -1290 V.
- The positive differential potential reaches +3800 V on the OSR (not grounded) and +1075 V on the sunshield (CMX cells).

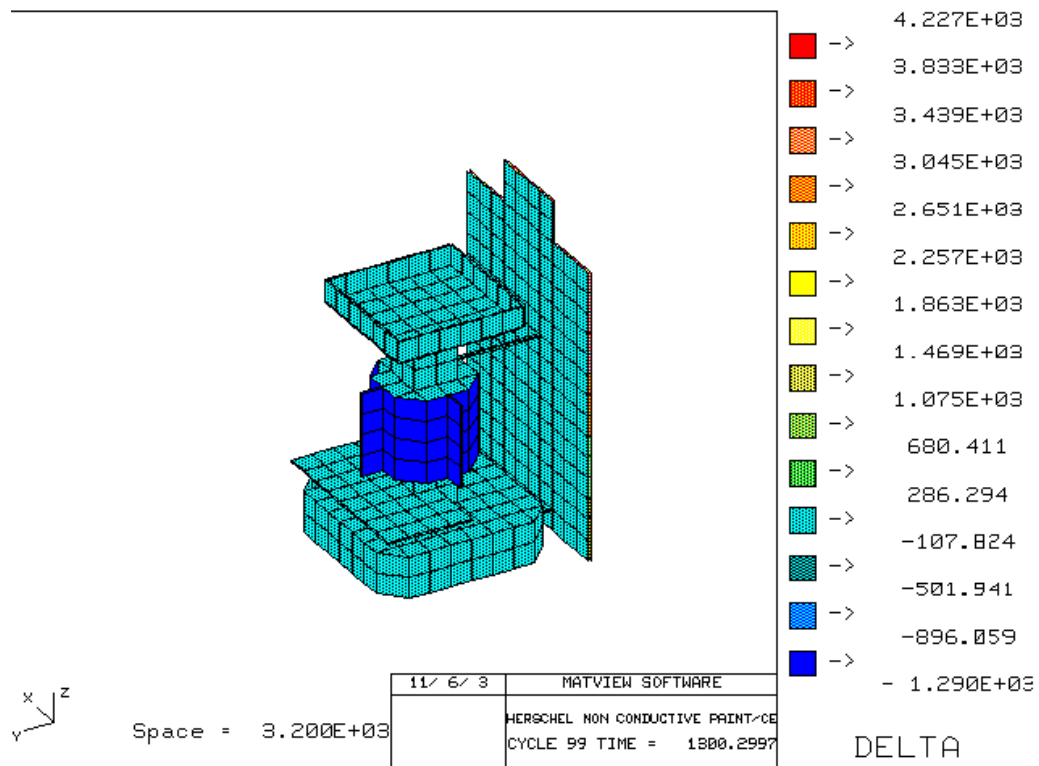


Figure 42. Distribution of differential potentials

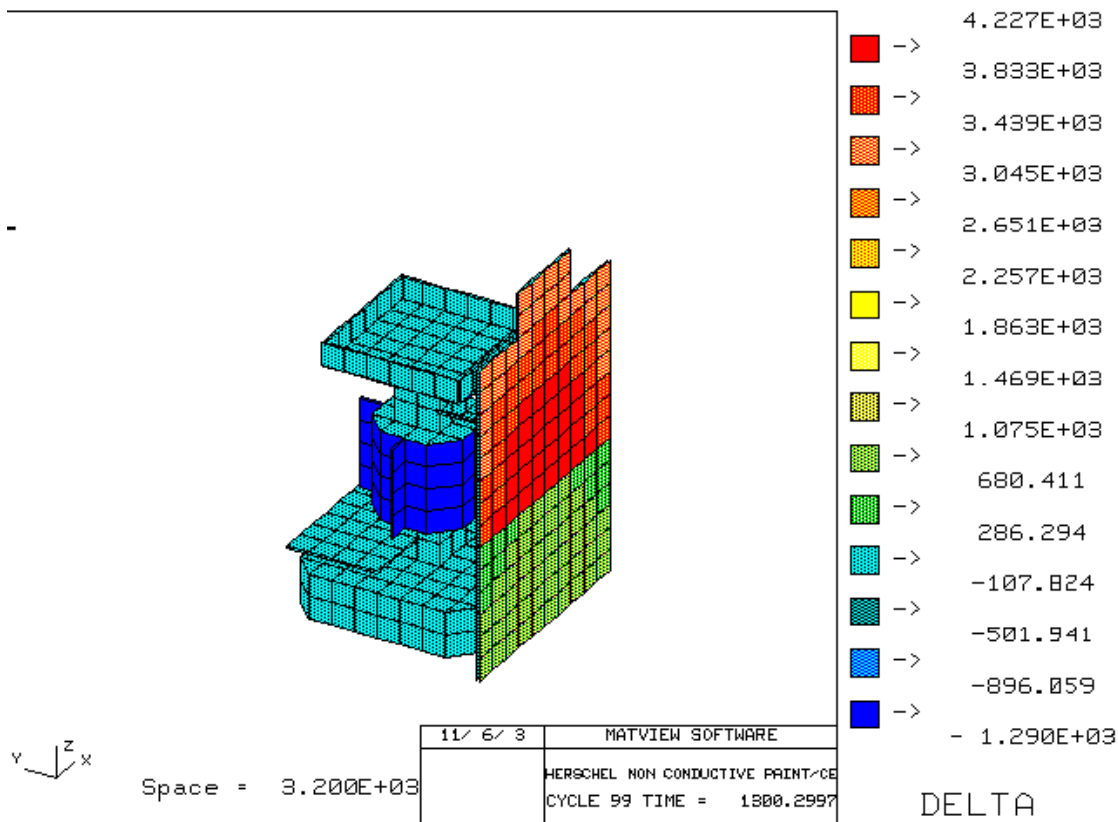


Figure 43. Distribution of differential potentials

### 4.1.3.2.3.3 CMO on the cells and non conductive OSR grounded

The Figures 44 and 45 show the differential potentials of Herschel spacecraft surfaces after 1300 s of charging.

The Figure 46 presents the evolution of the absolute potentials of some Herschel representative cells during charging.

The main results of NASCAP simulations are following :

- The final absolute potential of the structure is -11100 V.
- Negative differential potentials exist on the non conductive paint, -560 V.
- The positive differential potential reaches +5000 V on the OSR and +4600 V on the sunshield (CMO cells).

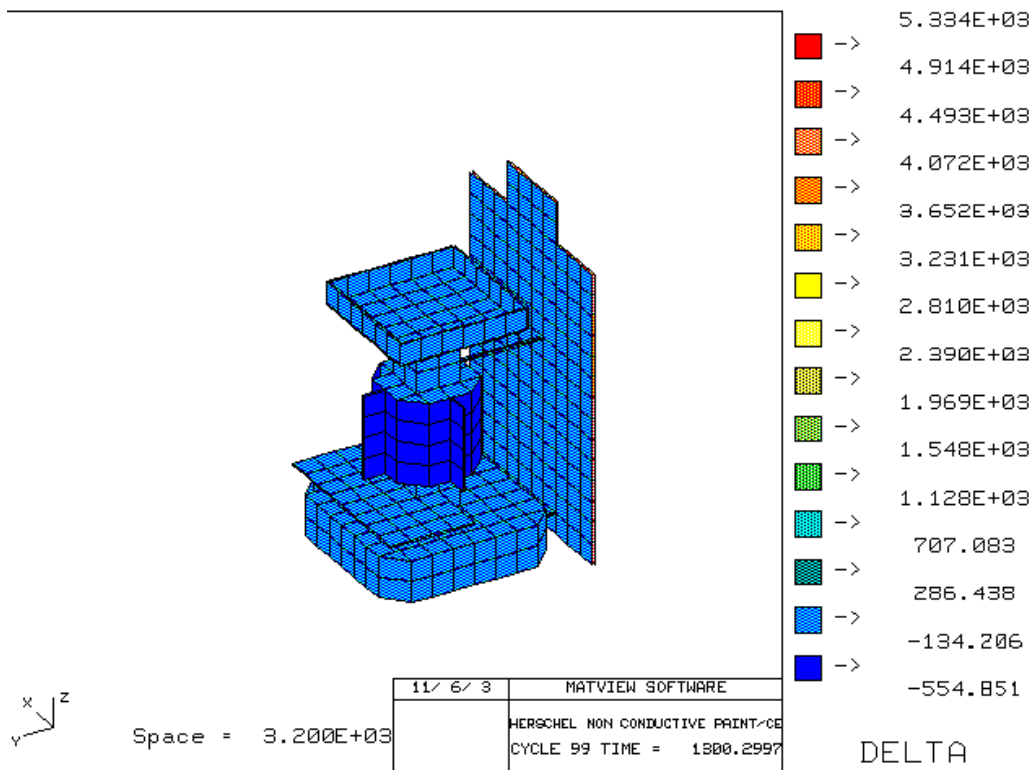


Figure 44. Distribution of differential potentials

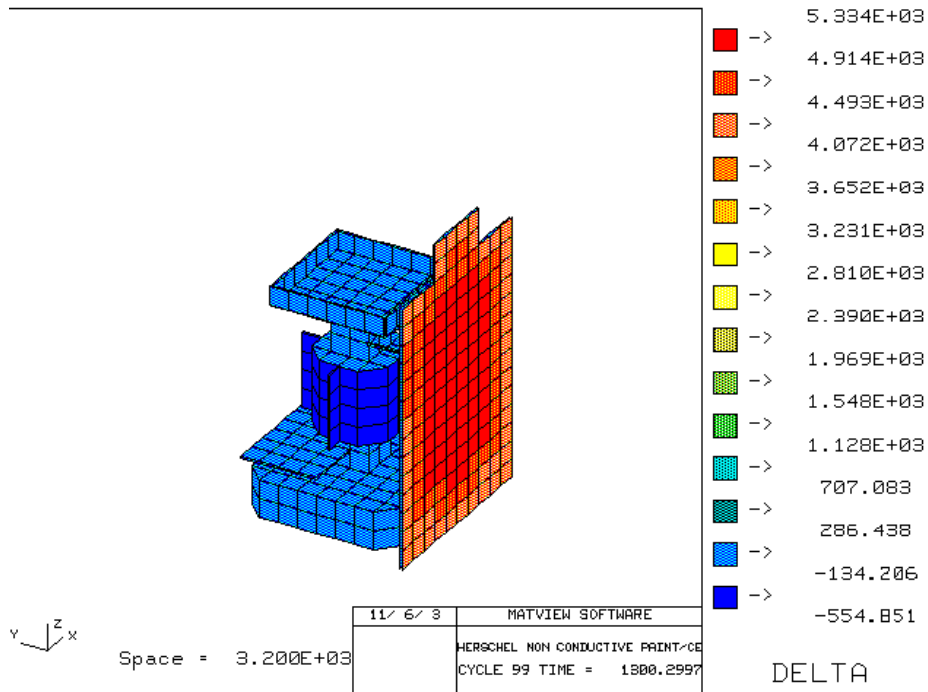


Figure 45. Distribution of differential potentials

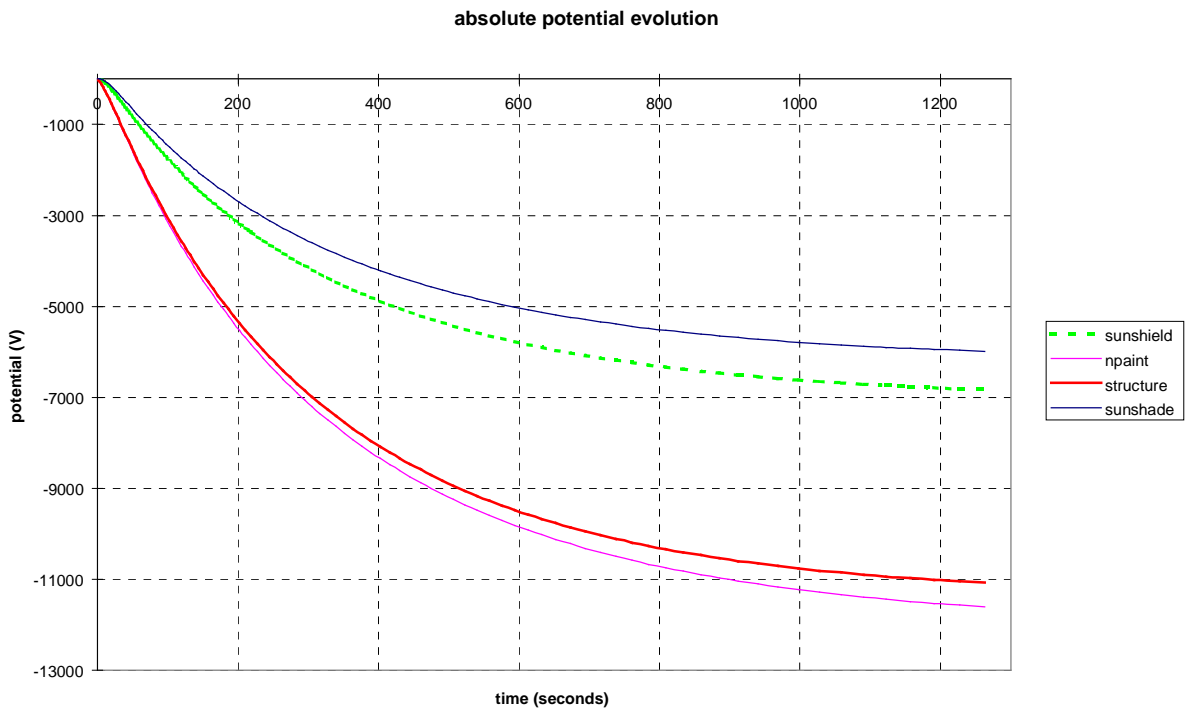


Figure 46. Evolution of absolute potentials during charging

### 4.1.3.2.3.4 CMX on the cells and non conductive OSR grounded

The Figures 47 and 48 show the differential potentials of Herschel spacecraft surfaces after 1300 s of charging.

The Figure 49 presents the evolution of the absolute potentials of some Herschel representative cells during charging.

The main results of NASCAP simulations are following :

- The final absolute potential of the structure is -670 V.
- Negative differential potentials exist on the non conductive paint, -1060 V.
- The positive differential potential reaches +760 V on the OSR and +670 V on the sunshield (CMX cells).

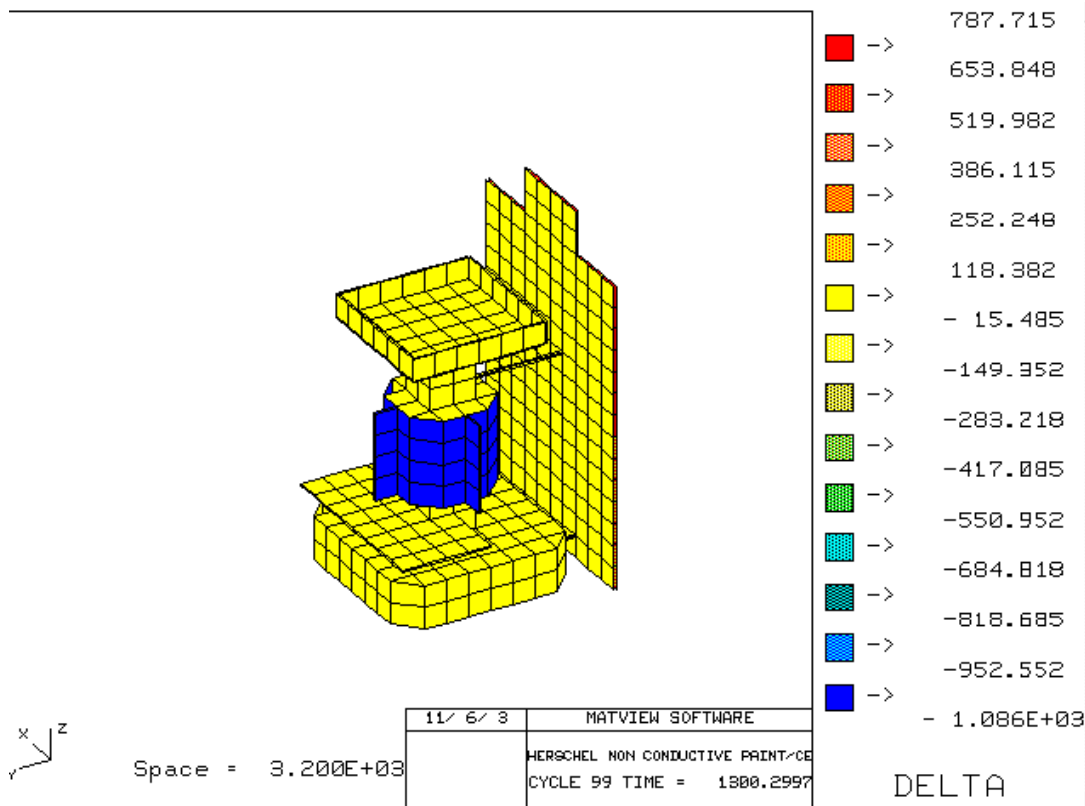


Figure 47. Distribution of differential potentials



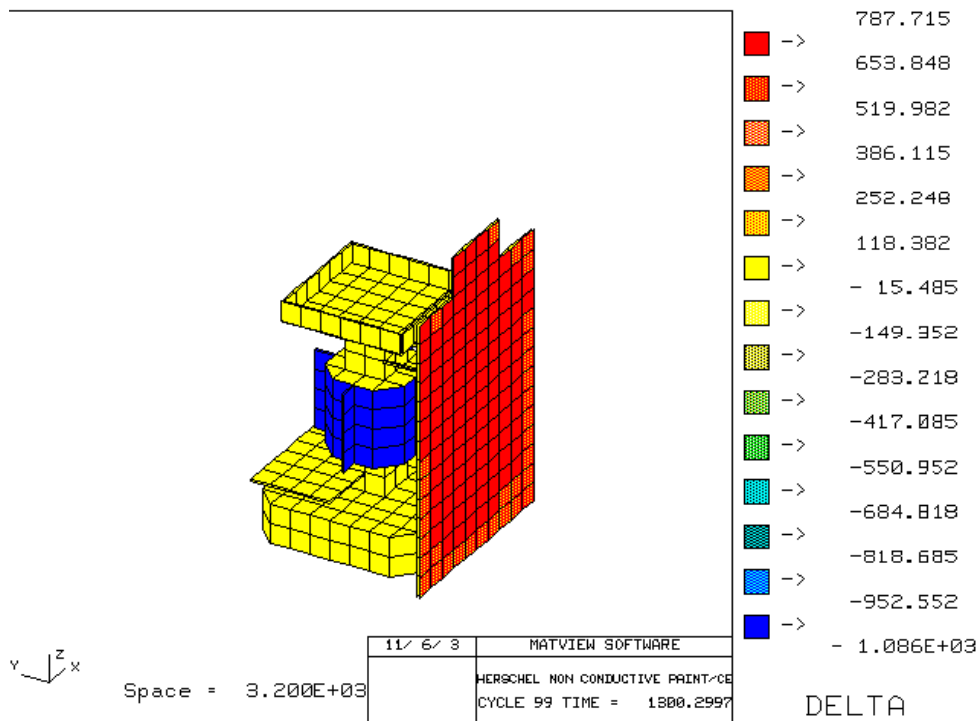


Figure 48. Distribution of differential potentials

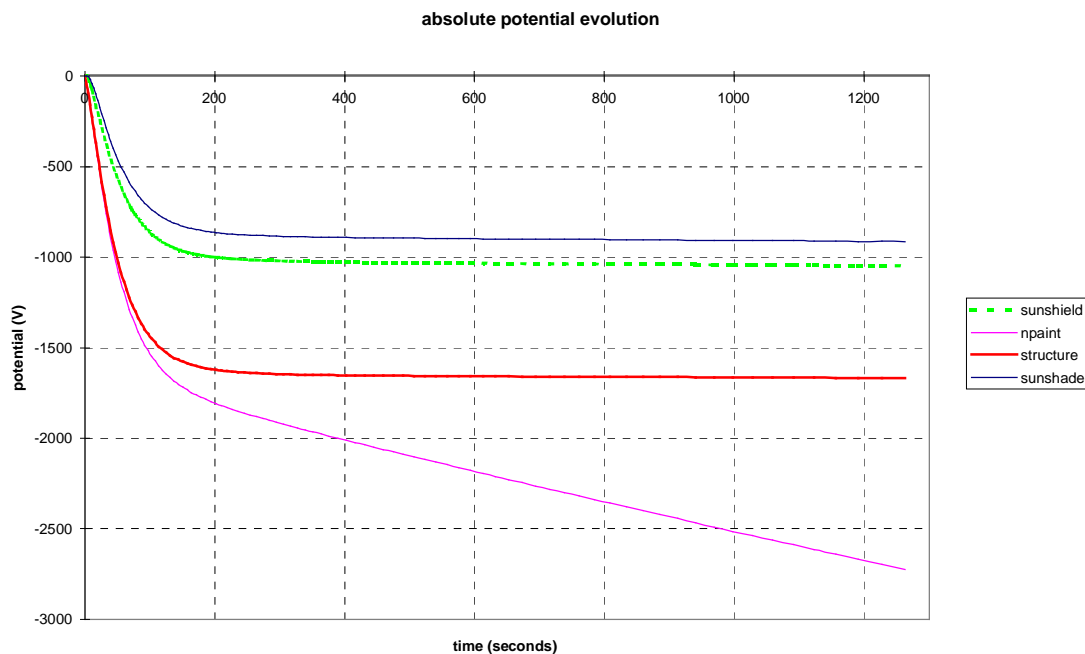


Figure 49. Evolution of absolute potentials during charging

## 4.1.4 Synthesis

The results of the simulations are summarized in the following table 2 :

Type of configuration			Absolute potential	Differential potential	
PPLM paint	Sunshade	Sunshield	Structure (V)	Coverglass (V)	Paint (V)
Anti-static paint 1.E+08 Ω.m	OSR not grounded	CMO	-10390	+4770	0
		CMX	-2280	+1530	0
	OSR grounded	CMO	-10420	+4300	0
		CMX	-1650	+680	0
Non conductive paint 1.E+13 Ω.m	OSR (CMX) not grounded	CMO	-10530	+5200	-110
		CMX	-2200	+600	-400
	OSR (CMX) grounded	CMO	-10660	+4400	-110
		CMX	-1650	+680	-270
	OSR with ITO	CMO	-15.5	+10	-310
Non conductive paint 1.E+14 Ω.m	OSR not grounded	CMO	-10660	+5240	-410
		CMX	-2320	+1100	-1230
	OSR grounded	CMO	-11100	+4600	-450
		CMX	-1660	+670	-910
Non conductive paint 1.E+15 Ω.m	OSR not grounded	CMO	-10660	+5200	-510
		CMX	-2450	+1075	-1290
	OSR grounded	CMO	-11100	+4600	-560
		CMX	-1670	+670	-1060

Table 1. Main results of NASCAP calculations

The satellite charging is strongly related to the coverglass bulk resistivity :

- If the coverglass resistivity is too high, the solar array differential charging comes rapidly above the +500 V threshold that leads to discharge. Nevertheless, primary discharges that could occur should be harmless to the solar array ought to the power system and solar array operating conditions (low solar array operational voltage, low section current), as addressed in section 3.2.4. The use of a non-conductive paint deteriorates the satellite charging level. If such paint should be used in conjunction with resistive coverglasses, even a moderate charging environment would lead to – harmless - discharges on the solar array.
- If the coverglass resistivity is low, the absolute charging level is moderate, although the solar array differential charging has strongly decreased, it remains above the 500V limit. More over, the equilibrium state can be reached quickly.
- The amount of negative differential charging of the non-conductive paint is not significant because the secondary electron emission parameters are currently unknown. The equilibrium state on the paint is not yet reached. But, large negative differential charging (some thousands of Volt) is generally possible without discharge. This should be verified by dedicated ground tests.

## 4.2 CDR BASELINE

### 4.2.1 Simulations parameters and configuration

The charging environment described in section 4.1.2 has not evolved.

NASCAP model of Herschel satellite has been updated in order to take into account aluminum on back side of the CVV (in front of Solar Array) except 5/12<sup>th</sup> of its surface covered with KAPTON.

After analysis of the various elements of the material trade off, the baseline configuration established for Herschel satellite is as follows :

- q Non conductive "paint" that covers the front side of the CVV which conductivity assumed to be  $1.E-15 \Omega^{-1}.m^{-1}$
- q CMO on the cells
- q Non conductive OSR not grounded

The selection of a Non conductive "paint" has been made essentially for thermal reasons. CMO has been preferred to CMX for power reasons : CMO is the type of coverglass especially adapted to the use of AsGa triple junction solar cells. The not grounded OSR option has been selected mainly for manufacturing purpose (process of grounding is difficult to put in place. All these solutions are clearly not optimum from a charging point of view (see Table 1) but, as stated in §4.1.4, they are acceptable in the context of Herschel : in case of geomagnetic substorms during the crossing of the Van Allen belts, electrostatic discharges will occur on the solar array, but will not propagate into a failure.

The external materials, used on Herschel satellite NASCAP model baseline, are shown on figures 50, 51, 52 and 53 (telescope back side).

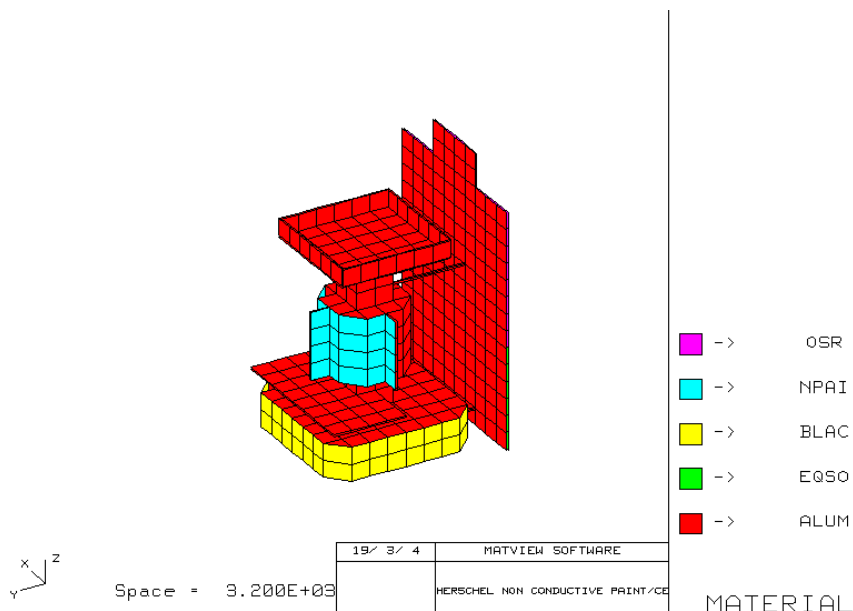


Figure 50. Materials of Herschel NASCAP baseline model

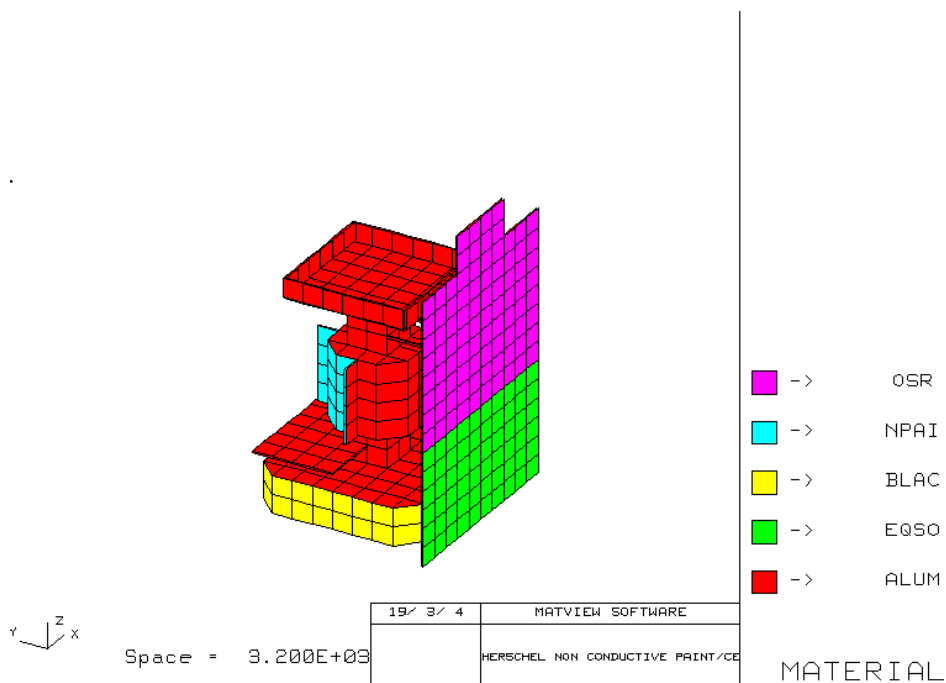


Figure 51. Materials of Herschel NASCAP baseline model

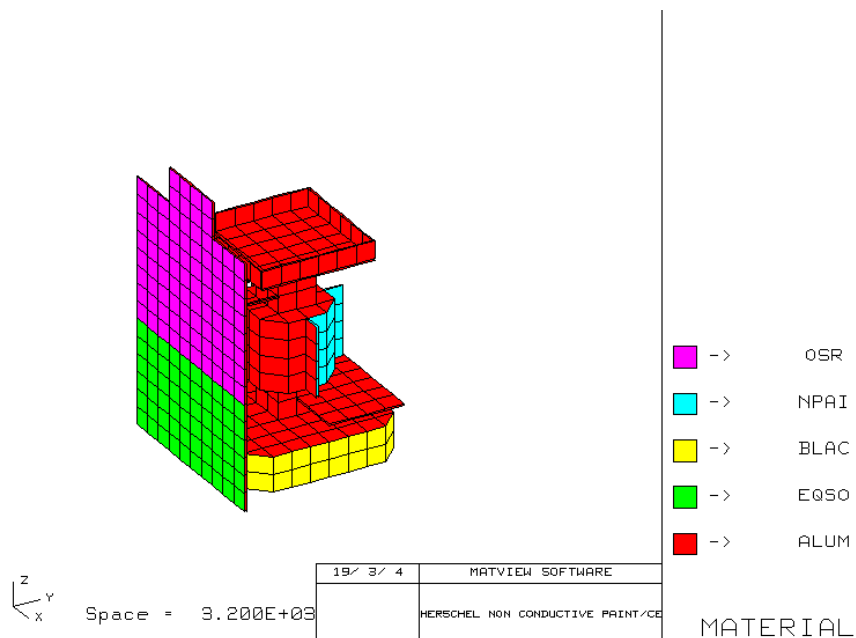


Figure 52. Materials of Herschel NASCAP baseline model

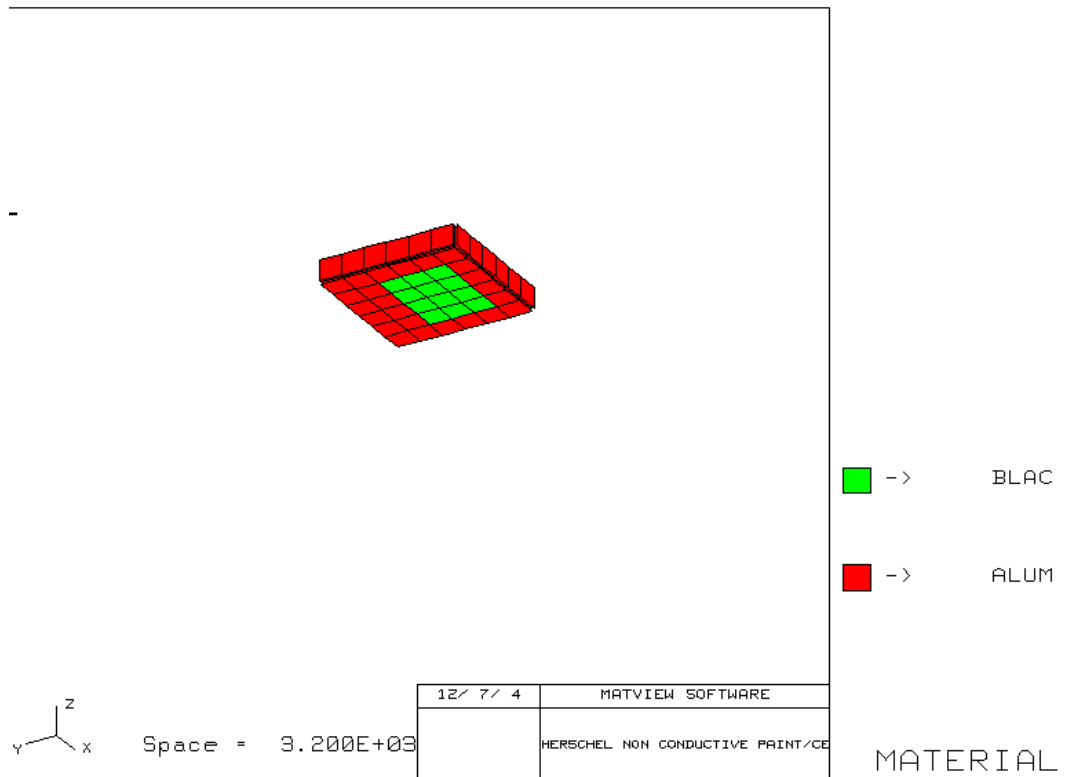


Figure 53 : Materials of Herschel Telescope NASCAP baseline model

#### 4.2.2 Results

The Figures 54 and 55 show the differential potentials of Herschel spacecraft surfaces after 1300 s of charging, while the Figure 56 shows the evolution of the absolute potentials over the time.

The main results of NASCAP simulations are following :

- The final absolute potential of the structure is -10630 V.
- Negative differential potentials exist on the non conductive paint, -500 V.
- The positive differential potential reaches +4700 V on the OSR (not grounded) and reaches the maximum value +4900 V on the sunshield (CMO cells).

These values confirm the statement made in §4.2.1.

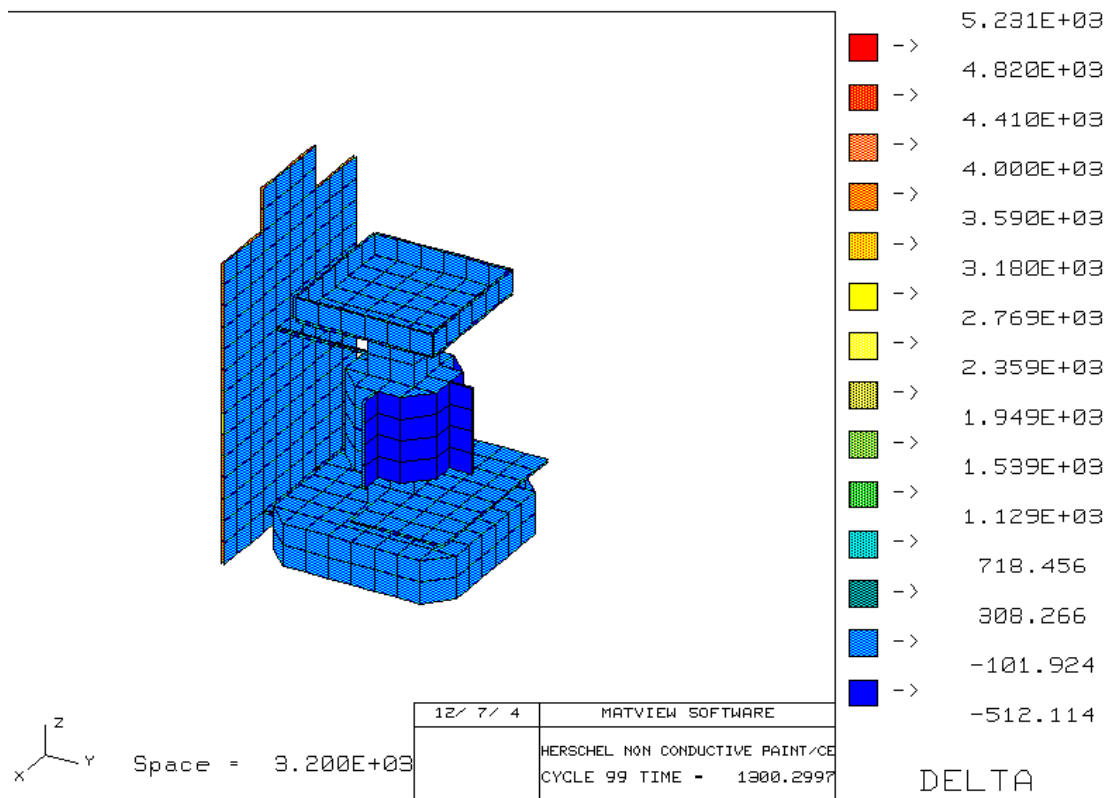


Figure 54 : Distribution of differential potentials

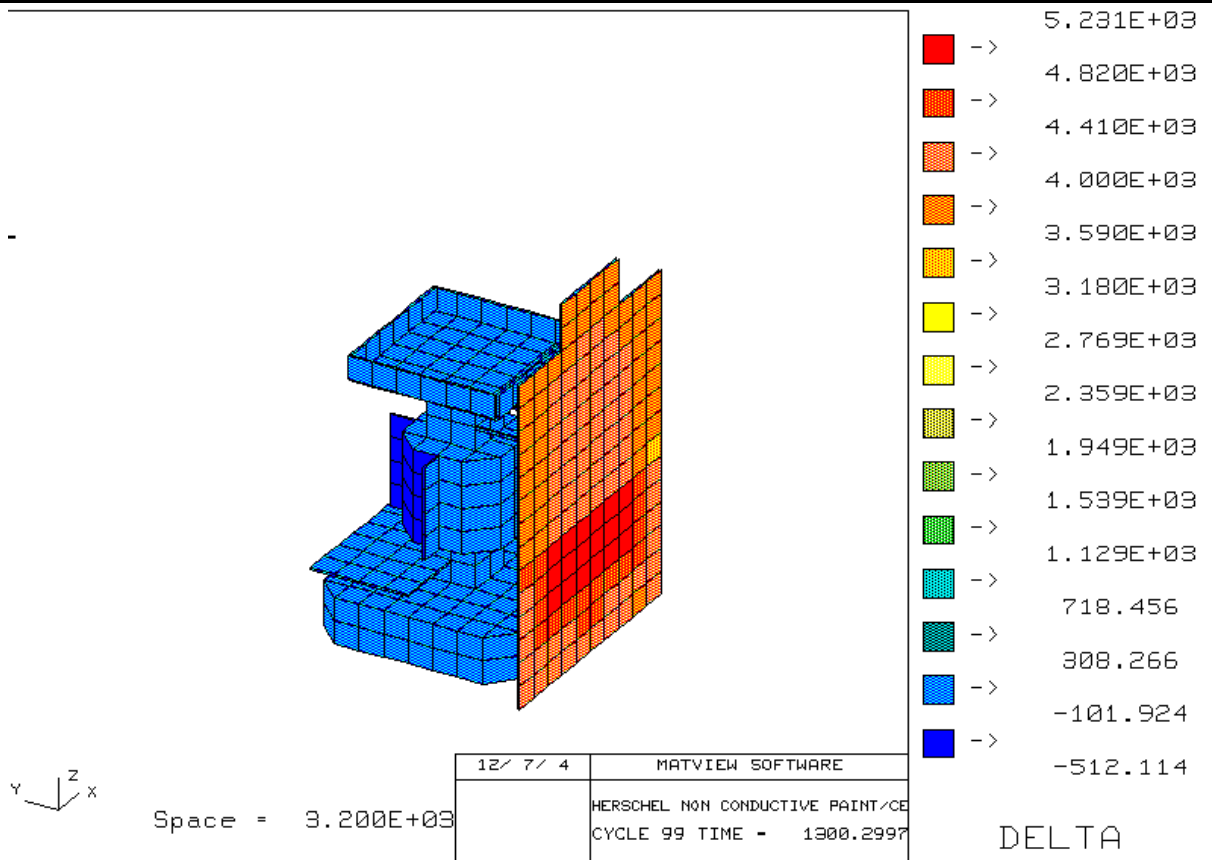


Figure 55 : Distribution of differential potentials

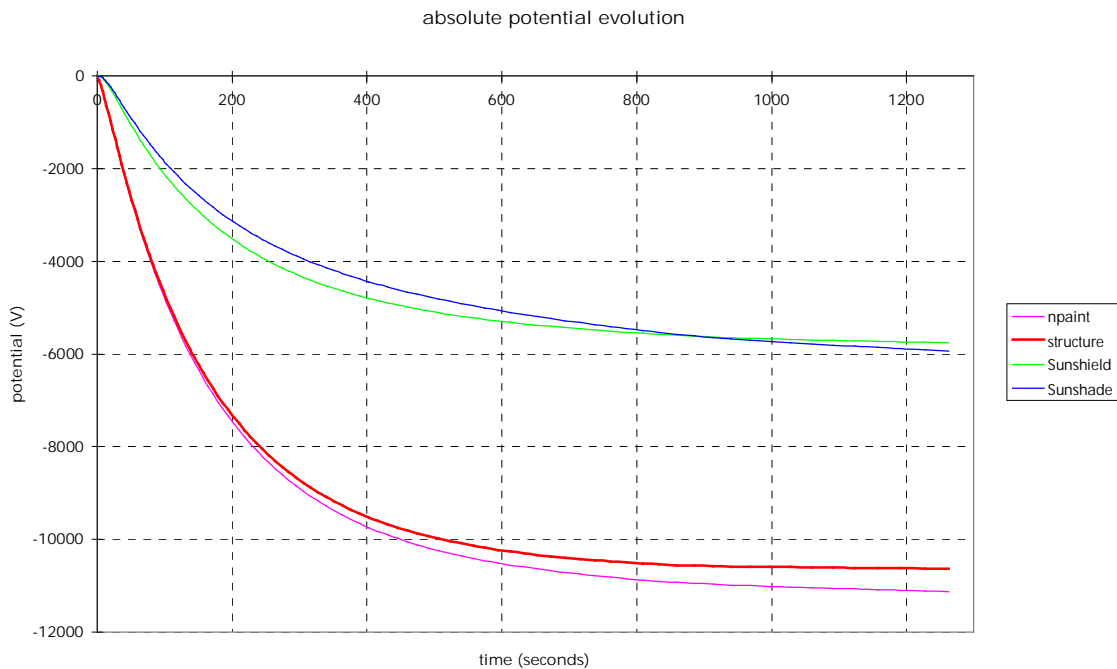


Figure 56 : absolute potentials evolution

## 5. PLANCK NASCAP ANALYSIS

### 5.1 TRADE-OFF

#### 5.1.1 Introduction

The present chapter presents the charging analyses of Planck satellite using the NASCAP software. NASCAP is a 3D finite element software, which enables the calculation of differential charging, by taking into account the electrostatic properties of materials and the effects of 3D electric fields.

An essentially thermally design driving configuration has been analyzed in order to quantify its impact from a charging point of view :

- the use of high resistivity paint on the Planck telescope baffle

The solution baselined for Herschel and potentially applicable to Planck (eg. the use of CMO coverglass on solar cells) have not been submitted to a trade off here : Herschel baseline has been adopted.

NASCAP software does not take into account the discharges occurring in the orbit but only the charging phenomenon. So, the predicted absolute potential values (especially for solar array) can be overestimated because natural discharges may occur with rather low differential charging (+500 V). NASCAP allows quantifying the sensitivity of the spacecraft to the electrostatic charging.

The simulations have been carried out considering a worse case for the charging environment and a very simplified geometry of Planck spacecraft in transfer orbit.

The section 5.1.2. describes the parameters used for NASCAP analysis, charging environment, spacecraft geometry and the property of surface materials (pessimistic values have been considered to ensure the worse charging prediction).

The section 5.1.3. presents the results of analysis for 2 different configurations which have been studied. In conclusion §5.1.4. summarizes the main results of this study.

#### 5.1.2 Simulation parameters

##### 5.1.2.1 Environment

The following charging environment for electrons and protons is a worse case in geostationary orbit recommended by NASA [1]. In practice, such severe environments would probably be encountered very rarely in a satellite lifetime. Moreover, for Planck satellite, this probability is to be applied to the very first part of the transfer to L2, at the crossing of the magnetosphere. The particle flux is modeled as a single Maxwellian function that is summarized in the following Table 1.

	Electrons	Protons
Density	1.12 cm-3	0.236 cm-3
Temperature	12 keV	29.5 keV

Table 2 : Charging environment description



## 5.1.2.2 Configurations

2 spacecraft configurations have been studied essentially to provide some inputs for the selection of the telescope baffle coating material :

- With an anti-static paint on the PPLM baffle
- With a non-conductive paint on the PPLM baffle

The satellite is always sunlit perpendicularly to the solar array.

The duration of simulation is between 600 s and 1300 s. This duration does not always allow to achieve a total equilibrium of the potentials but is largely sufficient to establish the probability of discharges on the solar array. If longer simulations were required, the stability of NASCAP algorithm is not guaranteed.

## 5.1.2.3 Satellite geometry

The model used in NASCAP represents a very simplified Planck geometry. This simplification is due to the calculation box of NASCAP (32x16x16 cells) and due to the elements of geometry used in the NASCAP tool, which are very simple. For example, the PPLM baffle is modeled by some rectangles. The NASCAP tool imposes to choose only one elementary mesh, that is 0.4 meter in our case. These inaccuracies about the geometrical representation are inherent to the NASCAP modeling.

With this elementary mesh size, the surfaces of the NASCAP model are as closed as possible to the real spacecraft surfaces. The ratio between the real surface and the model surface for all elements is less than 15 %.

Some examples are mentioned in the following list:

- |               |                                       |                                      |
|---------------|---------------------------------------|--------------------------------------|
| • SVM         | real surface = 9.11 m <sup>2</sup>    | model surface = 9.49 m <sup>2</sup>  |
| • Solar array | real surface = 13.85 m <sup>2</sup>   | model surface = 16.00 m <sup>2</sup> |
| • grooves     | real surface = 9.47 m <sup>2</sup>    | model surface = 10.24 m <sup>2</sup> |
| • PPLM baffle | radiative surface = 56 m <sup>2</sup> | model surface = 56.32 m <sup>2</sup> |

## 5.1.2.4 Spacecraft surface materials

The external materials, used on Planck satellite, are detailed below and are shown on the Figure 1, Figure 2, Figure 5, Figure 6. The material names of NASCAP are written in brackets.

- [CFPR] represents the carbon.
- [EQSO] represents the coverglass which covers the sunshield, always exposed to the sun. The coverglass resistivity is the driving parameter of the calculation and is very sensitive to the temperature. Planck solar array is "hot" (Tmin=106°C) and the coverglass resistivity decreases with temperature. 2 coverglass types have been originally studied : CMO and CMX MgF2 with both 100 μm thickness [8] [9] [10]. This analysis has been performed in the frame of the Herschel NASCAP analysis, and the result of the trade off are reported in section 4. As far as Planck analysis is concerned, only the baseline is considered comprising CMO 100μm coverglass., with a resistivity of 1.E+13 Ω.m as a conservative value.
- [BLAC] represents the black kapton MLI.
- [APAIN] represents an anti-static paint that covers the PPLM and the upper face of the 3<sup>rd</sup> groove. The paint resistivity is assumed to be 1.E+08 ohm.m.

- [NPAIN] represents a non conductive paint that could cover the PPLM and the upper face of the 3<sup>rd</sup> groove. The paint resistivity is assumed to be 1.E+15 ohm.m (high value).
- [ALUM] represents aluminum (back side of the solar array)

The electrical properties of the materials are extracted from the literature as from the NASCAP reference manual and from measurements performed at the ONERA-DESP.

As the black paint for the PPLM is not yet selected, its electrostatic parameters are unknown. They have been replaced by the values extracted from NASCAP reference "CPAI" [12], except for the resistivity.

## 5.1.3 Results

In this section, two kinds of potentials are presented which are explained below:

- 'delta' is defined as being the differential potential between the dielectric material and the underlying conductor
- 'potential' is defined as being the absolute potential. Indeed, a spacecraft material reaches a potential that is referred to the absolute potential of space, considered as being equal to zero.

The solar cells coverglass resistivity is assumed to be  $1E+13$  ohm.m

The orientation of Planck satellite – solar array in sunlit / satellite body in shadow – is a worse case for the satellite charging phenomenon. Indeed, sunlit dielectrics (as coverglass) are known to create a large differential charging area while sunlit conductive materials are wholesome to charging. The large satellite body in shadow collects many electrons and re-emits a few. This can lead to a fast decrease of the satellite absolute potential. A largely negative satellite absolute potential is not dangerous by its own, but unfortunately, the most negative absolute potential leads to the worst differential charging on the S/A.

### 5.1.3.1 Planck satellite charging with anti-static paint

The Figure 1 and the Figure 2 show the satellite surface materials used for the calculations.

The Figure 3 shows the differential potentials of Planck spacecraft surfaces after 1300 s of charging.

The Figure 4 presents the evolution of the absolute potentials of some Planck representative cells during charging.

The main results of NASCAP simulations are following:

- The final absolute potential of the structure is -6700 V. The equilibrium is reached after 500 s of simulation. The satellite charging is high.
- Ought to the anti-static paint and the use of black kapton, no negative differential potential exists.
- The positive differential potential reaches the maximum value + 3100 V on the solar array. The photoemission is responsible for this phenomenon. This value is above the threshold of primary discharge on solar array (+500 V). Some ESD could occur. This high level of differential charging is due to the high resistivity of the CMO coverglasses ( $\rho=1.E+13$  ohm.m,  $T=106^{\circ}\text{C}$ ).

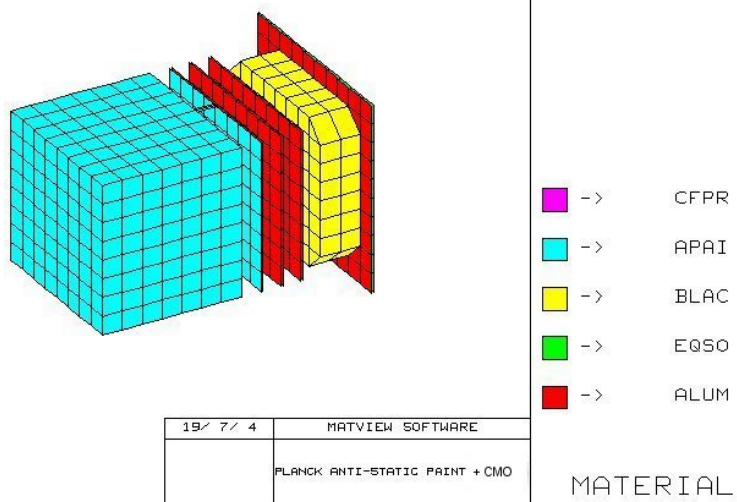


Figure 1: Planck Nascap model (Anti Sun face view)

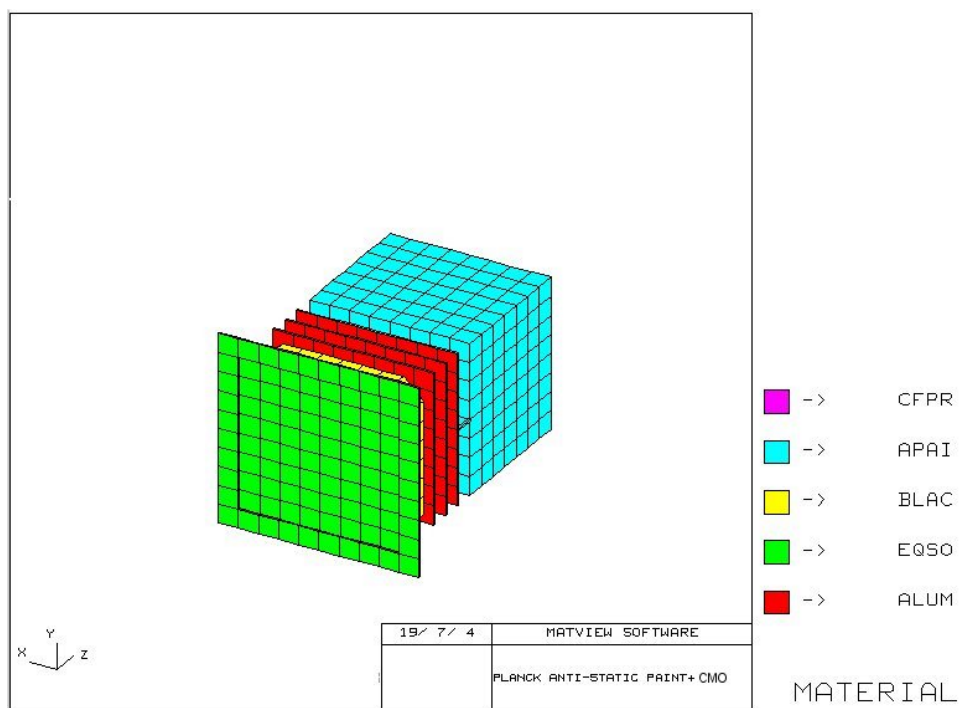


Figure 2: Planck Nascap model (Sun face view)

NB : the red triangles on the Figure 2 are due to a visualization error of ESABASE software

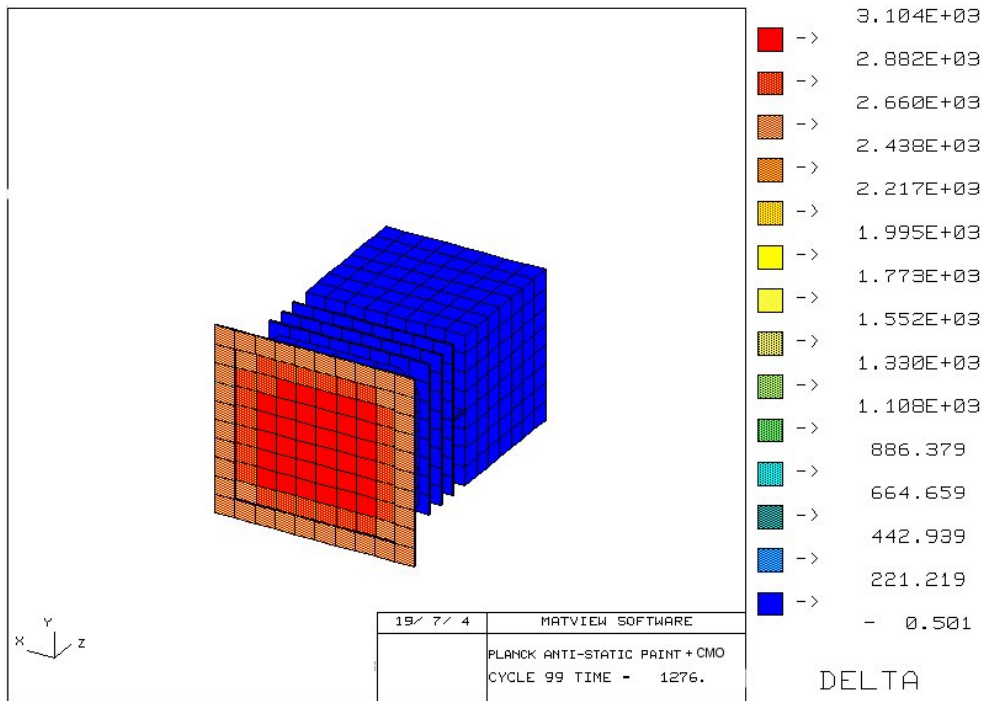


Figure 3 : Distribution of differential potentials (Sun side view)

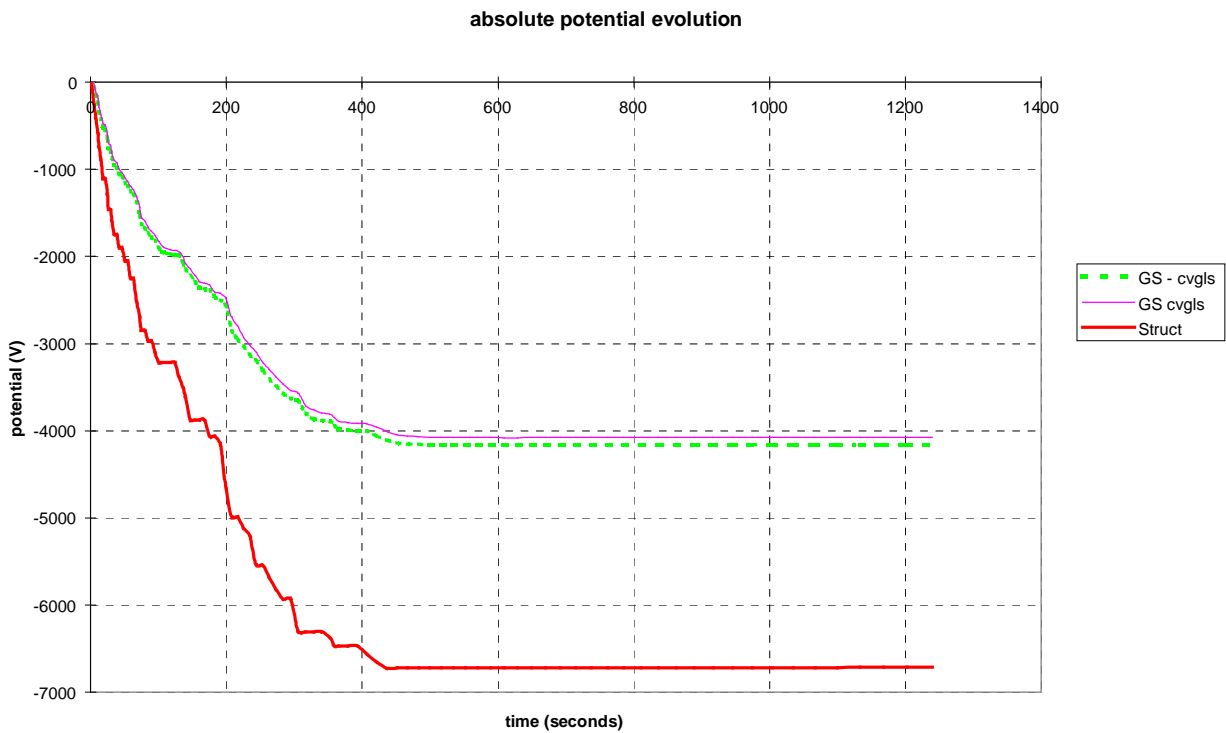


Figure 4.: Evolution of absolute potentials during charging

NB : the blue triangles on the Figure 6 are due to a visualization error of ESABASE software

## 5.1.3.2 Planck satellite charging with non conductive paint

The Figure 5 and the Figure 6 show the satellite surface materials used for the calculations.

The Figure 7 shows the differential potentials of Planck spacecraft surfaces after 630 s of charging.

The Figure 8 presents the evolution of the absolute potentials of some Planck representative cells during charging.

The main results of NASCAP simulations are following:

- The absolute potential of the structure is -10700 V at  $t=1300$  s.
- Negative differential potentials exist on the non-conductive paint, - 500 V at  $t=1300$  s. It is not possible to quantify exactly the level of negative differential charging. Indeed, this level depends on the secondary electron emission parameters that are unknown.
- The positive differential potential reaches the maximum value + 4870 V on the solar array. This value is above the threshold of primary discharge on solar array (+500 V). This high level of differential charging is due to the rather high resistivity of the CMO coverglasses ( $\rho=1.E+13$  ohm.m,  $T=106^{\circ}\text{C}$ ).

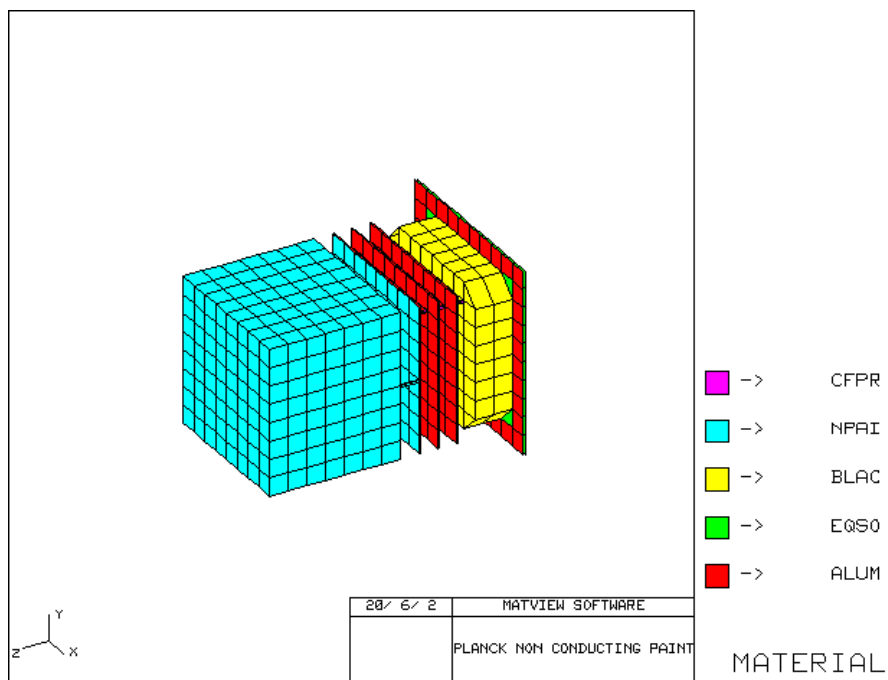


Figure 5.: Planck NASCAP model (Anti Sun face view)

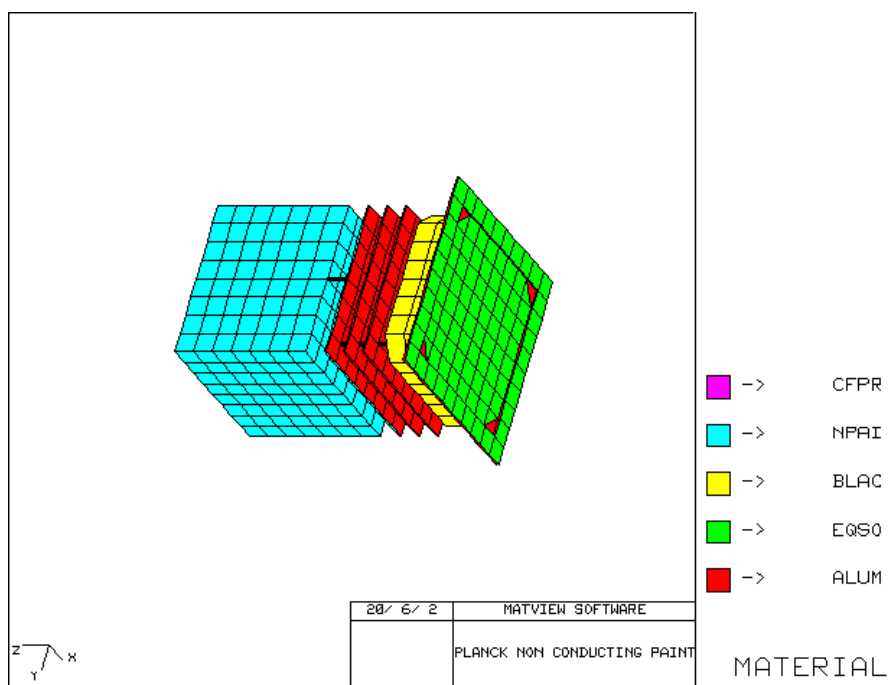


Figure 6.: Planck NASCAP model (Sun face view)

NB : the red triangles on the Figure 6 are due to a visualization error of ESABASE software

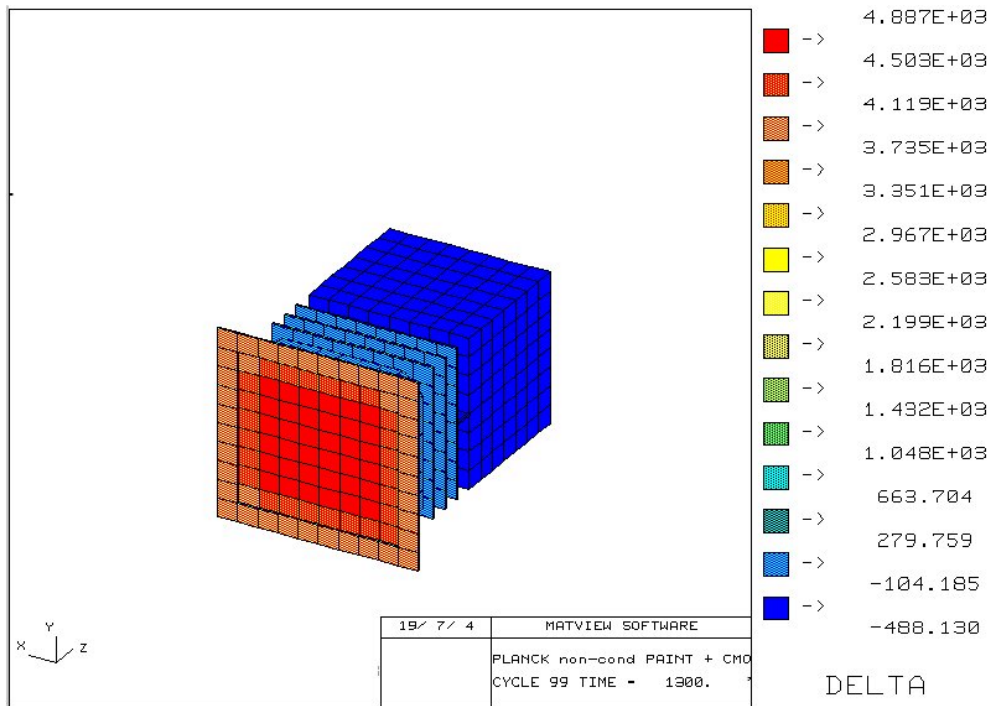


Figure 7.: Distribution of differential potentials (Sun side view)

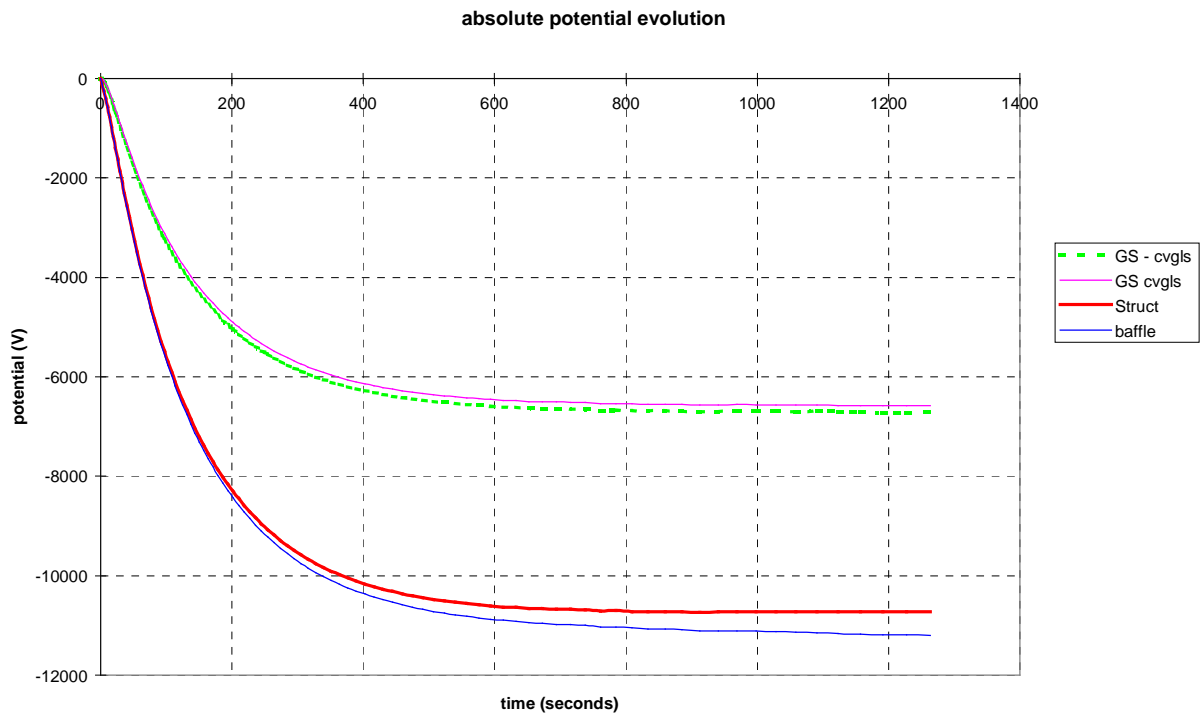


Figure 8.: Evolution of absolute potentials during charging

NB : the orange triangles on the Figure 7 are due to a visualization error of ESABASE software



## 5.1.4 Synthesis

Due to uncertainties of modeling and missing input data, the results shall not be considered as the exact picture of the satellite electrostatic state but only indicate trends.

The results of the simulations are summarized in the following table 2 :

Coverglass resistivity Ohm.m	PPLM paint	Absolute potential (V) (t=1300 s)			Differential potential (V) (t=1300 s)	
		Structure	Coverglass	Paint	Coverglass	paint
1.E+13	Anti-static	- 6700V	- 3600 V	- 6700 V	+ 3100 V	0 V
1.E+13	Non conduc.	- 10720 V	- 5850 V	- 11200 V	+4870 V	- 500 V

Table 2 : main results of NASCAP calculations

The satellite charging is strongly related to the coverglass bulk resistivity :

- When the coverglass resistivity is too high, the solar array differential charging rapidly comes above the +500 V threshold that leads to discharge. Nevertheless, primary discharges that could occur should be harmless to the solar array ought to the power system and solar array operating conditions (low solar array operational voltage, low current per section), as addressed in section 3.2.4.
- The use of a non-conductive paint deteriorates the satellite charging level. If such a paint is used in conjunction with resistive coverglasses, even a moderate charging environment would lead to – harmless - discharges on the solar array.
- The negative differential charging of the non-conductive paint is not significant because the secondary electron emission parameters are currently unknown. The equilibrium state on the paint is not yet reached. But, large negative differential charging (some thousands of Volt) is generally possible without discharge. This should be verified by dedicated ground tests.

## 5.2 CDR BASELINE

### 5.2.1 Simulations parameters and configuration

The charging environment described in section 5.1.2 has not evolved.

NASCAP model of Planck satellite has been updated in order to take into account that up to 30% of the Solar array surface is covered with Kapton. However the simulation has not been conclusive because of NASCAP convergence problems. Some qualitative statement can nevertheless be made : an important characteristics noticed for Kapton is that, when illuminated by the Sun which is always the case of Planck, it features a high UV emission such that it basically poorly charges. The consequence is that the amount of positive charging of the Solar array wrt Structure can only be smaller with Kapton on the array than without. To summarize, Kapton on Planck Solar array can only have a positive effect.

Finally, after analysis of the various elements of the material trade off, the baseline configuration established for Planck satellite is as follows :

- q Conductive paint on the Planck telescope baffle and upper face of 3<sup>rd</sup> groove. However because the conductivity parameters of the paint are not yet accurately known, a very conservative assumption with a conductivity =  $1.E-15 \Omega^{-1}.m^{-1}$  has been taken into account as baseline analysis.
- q CMO as solar cells coverglass
- q 30% Kapton on Solar Array

The selection of the paint has been made essentially for thermal reasons, however the electrical characteristics have also been taken into account: a paint with an a priori good conductivity has been selected. CMO has been preferred to CMX for power reasons, as for Herschel. Both solutions are clearly not optimum from a charging point of view (see Table 2) but, as stated in §5.1.4, they are acceptable in the context of Planck : in case of geomagnetic substorms during the crossing of the Van Allen belts, electrostatic discharges will occur on the solar array, but will not propagate into a failure.

## 6. CONCLUSION

The various electrostatic environments met by Planck & Herschel satellites imply different electrostatic interactions. The only risky part of the mission is the way through the internal magnetosphere around the geostationary orbit. The geomagnetic storms are known to create electrostatic charging and discharges that can lead to failures. This is why, even if the satellites will stay only a few minutes in this environment once in their life, the same precautions as for geostationary satellites, are be applied.

As far as Planck is concerned, if a geomagnetic substorm would occur during transfer, the satellite electrostatic charging should be highly negative and harmless electrostatic discharges are expected on the solar array. The use of a conductive paint on the PPLM should not lead to any significant negative differential charging. Should the conductivity parameter of the paint be worst than expected, negative differential charging could occur, difficult to quantify because of uncertainties on secondary electron emission parameters : probability of discharge remains limited.

On Herschel, if a geomagnetic substorm would occur during transfer, the satellite electrostatic charging should be highly negative and harmless electrostatic discharges are expected on the solar array. The use of a non-conductive coating on the CVV could lead to negative differential charging (difficult to quantify because of uncertainties on secondary electron emission parameters). Probability of discharge remains limited, however it remains desirable to quantify the discharge threshold of the selected coating by ground testing.

END OF DOCUMENT